Title
Markers and Regulators Defining the Development of Hematopoietic Stem Cells and their Niches

Author
Lee, Lydia Kyung-Min

Publication Date
2014

Peer reviewed|Thesis/dissertation

UNIVERSITY OF CALIFORNIA
Los Angeles

Markers and Regulators Defining the Development of Hematopoietic Stem Cells and their Niches

A dissertation submitted in partial satisfaction of the
requirements for the degree of

Doctor of Philosophy
in
Molecular, Cell and Developmental Biology

By

Lydia Kyung-Min Lee

2014

ABSTRACT OF THE DISSERTATION

Markers and Regulators Defining the Development
of Hematopoietic Stem Cells and their Niches

by

Lydia Kyung-Min Lee
Doctor of Philosophy in Molecular, Cell and Developmental Biology
University of California, Los Angeles, 2014
Professor Hanna A. Mikkola, Chair

The future of personalized regenerative cellular medicine depends on the ability to faithfully differentiate pluripotent cells to tissue stem cells, or reprogram them from other cellular sources. So far, the efforts to generate transplantable multi-potent hematopoietic stem cells (HSC) *in vitro* have yielded hematopoietic cells with only limited functional potential. Thus, improved understanding of *in vivo* programs that direct specification of hematopoietic stem versus progenitor cells during embryonic development holds immense clinical implication. However, characterization of the unique properties of these cell populations is currently hindered by the inability to distinguish them prospectively due to the absence of discriminating cell surface markers or genes.

Here, we uncovered lymphatic vessel endothelial receptor-1 (LYVE1) as a unique cell surface marker that identifies definitive hematopoietic stem and progenitor cells and their cellular precursor, the hemogenic endothelium, in the yolk

sac. Furthermore, we showed that *LYVE1-eGFP-hCre* knock-in mouse is a powerful tool to separate the primitive erythropoiesis from definitive, even after the cell admixture upon onset of embryonic circulation. Using this tool, we provide *in vivo* evidence that the earliest progenitors to seed the fetal liver derive from the yolk sac.

The mechanisms that establish multilineage differentiation potential in hemogenic endothelium are poorly understood. The vascular endothelial growth factor A (VEGF-A) is essential for endothelial development; however, its role in hemogenic endothelium has not been elucidated. Incorporating several unique mouse models of VEGF-A gene targeting, we document that proper VEGF-A dosage is critical for vascular remodeling and generating multipotent HS/PCs in embryonic hemogenic tissues. Our data support the fact that VEGF-A haploinsufficiency is able to establish primitive erythropoiesis and generate transient myelo-erythroid progenitors from the yolk sac. Moreover, we discover a new cellular source of VEGF-A in placental trophoblasts, and show that trophoblast VEGF-A is important for angiogenesis and hematopoiesis in distant hemogenic organs as well.

The dissertation of Lydia Kyung-Min Lee is approved

By

Luisa Iruela-Arispe

Gay Crooks

Atsushi Nakano

Hanna K.A. Mikkola, Committee Chair

University of California, Los Angeles

2014

To my patients,

TABLE OF CONTENTS

PRELIMINARY PAGES:

DISSERTATION RESEARCH

LIST OF FIGURES

ACKNOWLEDGEMENTS

Chapter 3 is a version of Ueno M, Lee L, Chhabra A, Kim Y, Sasidharan R, Van Handel B, Wang Y, Kamata M, Kamran P, Sereti K, Ardehali R, Jiang M, Mikkola HKA. C-Met-Dependent Multipotent Labyrinth Trophoblast Progenitors Establish Placental Exchange Interface. *Dev Cell* 2013 Nov 25;27(4):373-86

Appendix 1 is a version of Lee LK, Ueno M,Van Handel B, Mikkola H. Placenta as a newly identified source of hematopoietic stem cells, *Current Opinion in Hematology* 2010 Jul;17(4):313-8.

Appendix 2 is a version of Calvanese V, Lee LK, Mikkola HKA. Sex hormone drives blood stem cell reproduction. *EMBO* 2014 Feb: 33(6):534-5

This thesis is only the end of the beginning to a journey of transformation from a clinical to a translational investigator.

My mentor Dr. Hanna Mikkola gave me the wings to find scientific adventures, showed me how to rise above a funding freeze during a federal shutdown, and use the pride of our work to face personal challenges.

I had the privilege of racing for knowledge with driven coaches and fun-loving bench partners.

Dr. Yanling Wang for her unending support

Dr. Masaya Ueno for countless scientific discussions

Dr. Encarnación Montecino-Rodriguez for helpful discussions

Dr. Meisheng Jiang for technical support in lentiviral transfection of blastocysts

Jessica Scholes and Felicia Codrea at the FACS Core for technical support in cell sorting and flow cytometry analysis

Elias Sideris for his summer friendship and technical assistance

Dr. Gautam Chaudhuri for his visionary leadership

Dr. Louise Wilkins-Haug for opening the doors to the world of Maternal-Fetal Medicine

Dr. Masato Asai for showing me how to fill a lab with persistence and silent kindness

Dr. Joseph Majzoub and Dr. David Miller for changing my life

Special thanks to my committee members Dr. Luisa Iruela-Arispe, Dr. Gay Crooks and Dr. Atsushi Nakano for helpful discussions.

This work was supported by the NIH R01097766, CIRM New Faculty Award RN1-00557-1 and Leukemia & Lymphoma Society Scholar awards for H.K.A.M. L.K.L was supported by the Specialty Training and Advanced Research Fellowship at UCLA, TG2-01169 California Institute of Regenerative Medicine Type I Training Grant, and the American Association of Obstetricians and Gynecologists Foundation Scholarship.

BIOGRAPHICAL SKETCH

NAME	POSITION TITLE
Lee, Lydia Kyung-Min	Assistant Professor of Maternal Fetal Medicine, Department of Obstetrics and Gynecology UCLA (to begin in September 2014)
eRA COMMONS USER NAME (credential, e.g., agency login)	

EDUCATION/TRAINING *(Begin with baccalaureate or other initial professional education, such as nursing, include postdoctoral training and residency training if applicable.)*

INSTITUTION AND LOCATION	DEGREE *(if applicable)*	MM/YY	FIELD OF STUDY
University of Rochester, Rochester, NY	B.A.	06/1994	Biology, Spanish Literature
University of Rochester, Rochester, NY	M.D.	06/1998	Medicine
UT Southwestern Medical Center, Dallas, TX	Residency	06/2002	Obstetrics & Gynecology
Harvard Medical School, Boston, MA	Fellowship	06/2007	Maternal Fetal Medicine

A. Positions and Honors

Positions and Employment

2002-2003 Private practice, Obstetrics & Gynecology, Boston, MA
2003-2004 Clinical Instructor, Obstetrics and Gynecology, Brigham & Women's Hospital, Boston, MA
2007-2009 Staff Physician, Maternal-Fetal Medicine, Cedars-Sinai Medical Center, Los Angeles, CA
2008-2009 Perinatal Coordinator, General Clinical Research Center at Cedars-Sinai, Los Angeles, CA
2009-2014 Clinical Instructor, Maternal-Fetal Medicine, University of California, Los Angeles, CA
2014- Assistant Professor, Maternal-Fetal Medicine, University of California, Los Angeles, CA

Other Experience and Professional Memberships

2004 - Fellow, American College of Obstetrics and Gynecology
2009 - Fellow, Society of Maternal Fetal Medicine
2010 - Associate Member, International Society for Stem Cell Research

Honors

1994 Summa cum laude, University of Rochester
1994 Phi Beta Kappa, University of Rochester
2002 Resident Teaching Award, Parkland Memorial Hospital
2002 Best Research Presentation Award, Parkland Memorial Hospital

B. Selected publications

Lee LK, Montecino-Rodriguez E, Wang YL, Dorskind K, Mikkola HKA. LYVE1 identifies yolk sac definitive hemogenic endothelium (manuscript in preparation)

Anuwutnavin S, **Lee LK**, Satou G, Sklansky M. Fetal diagnosis of double aortic arch associated with D-transposition of the great arteries: case report and review of the literature. *J Ultrasound Med* 2014 July (in review)

Hoffman Y, **Lee LK**, Thomas AM, Benson C, Shipp TD. Fetal adrenal gland volume and prediction of preterm birth: a prospective third-trimester screening evaluation. *J Ultrasound Med* 2014 July (in review)

Anuwutnavin S, **Lee LK**, Silverman N, Sklansky M. Fetal cardiac manifestations of Marfan syndrome: case report and review of the literature. *J Ultrasound Med* 2014 March (in print)

Calvanese V, **Lee LK**, Mikkola HKA. Sex hormone drives blood stem cell reproduction. *EMBO* 2014 Feb: 33(6):534-5

Ueno M, **Lee LK**, Chhabra A, Kim YJ, Sasidharan R, Van Handel B, Wang Y, Kamata M, Kamran P, Sereti K-J, Ardehali R, Jiang M, Mikkola HKA. c-Met-dependent multipotent labyrinth trophoblast progenitors establish placental exchange interface. *Dev Cell* 2013 Nov 25;27(4):373-86.

Lee LK, Ueno M,Van Handel B, Mikkola H. Placenta as a newly identified source of hematopoietic stem cells, *Current Opinion in Hematology* 2010 Jul;17(4):313-8.

Lee LK, Robinson J, Norwitz E. Respiratory Complications, Manual of Obstetrics, edited by Arthur Evans, 7th ed, Philadelphia: Lippincott Williams & Wilkins, 2007.

Lee LK. Physiological Adaptations of Pregnancy Affecting the Nervous System, *Seminars in Neurology*, 27(5):405-10, Nov 2007.

C. Research Support
Ongoing Research Support

American Association of Obstetricians and Gynecologists Foundation Scholarship
07/01/2012- 06/30/2015
The Role of Vascular Endothelial Growth Factor in Placental Vascularization and Hematopoiesis.

INTRODUCTION

Healthy donors comprise the only source of transplantable hematopoietic stem cells (HSC) to date. However, the limited supply of HLA-matched donors remains as one of the most pressing bottlenecks for the treatment of many patients with hematopoietic malignancies and inherited blood and immune disorders. Hence, it becomes evident that the *in vitro* production of transplantable HSCs carries immense clinical implications. Furthermore, the high stake incentives to broaden regenerative medicine into other organ systems build upon the success of the pioneering HSC therapies.

The potential for *in vitro* generation of targeted cellular therapies was accelerated by recent discoveries in induced pluripotent stem cells. In order to ultimately offer personalized patient-specific cell replacement treatments, many stem cell biologists have centered on how to faithfully steer the induced pluripotent cell to differentiate into the specific cell of need. Unfortunately, directing cell reprogramming in the laboratory has remained elusive so far. In fact, while hematopoietic progenitor cells with restricted lineage and repopulating potential have been produced *in vitro*, multipotent, self-renewing HSCs have not yet, despite being the best characterized tissue stem cell. Therefore, understanding how HSC development and maintenance are regulated will not only advance efforts to satisfy the clinical demand for transplantable HSCs, but also provide insights to the shared tenets that define other tissue specific stem cells, namely, long-term engraftment ability, self-renewal capacity and multipotency.

DEVELOPMENTAL HEMATOPOIESIS

It is remarkable that the stem cells that are responsible for sustaining the production of all blood cell types in the lifespan of a human are generated exclusively during few days of embryogenesis. Hence, recapitulating this powerful developmental program stands out as one of the most compelling approaches to design protocols of HSC generation in the laboratory.

HSCs are not the first hematopoietic cells that are generated in the embryo: they are produced last, and only after two other waves of provisional progenitors that fulfill the immediate needs of the growing fetus by ensuring oxygen delivery and tissue remodeling and defense, have been formed. These earlier two waves are termed "primitive" and "transient-definitive" and emerge from the extra-embryonic yolk sac (Fig. 1). The HSC-forming wave is termed "definitive" hematopoiesis and

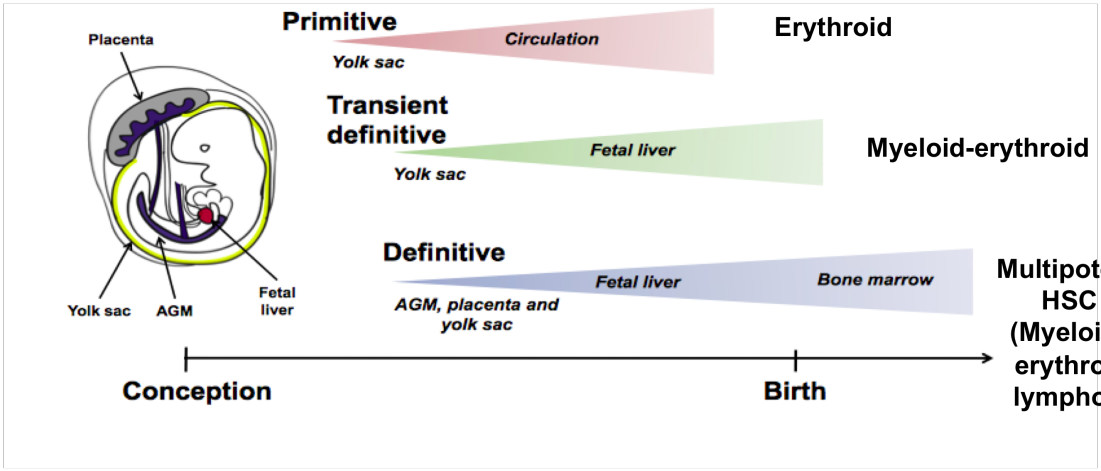

Figure 1. Waves of hematopoiesis during mammalian development

takes place In multiple sites: the aorta-gonad-mesonephros region, the umbilical and vitelline vessels, the placenta, and the yolk sac. Once generated, progeny from the transient-definitive and definitive waves seed the fetal liver for proliferation and maturation, before migrating to the bone marrow, their lifelong niche of residence.

While it was long recognized that the primitive progenitors arise from the fetal liver kinase 1 (Flk1) expressing mesoderm in the blood islands of the yolk sac, the cellular founder of the definitive waves was contested until recent imaging and lineage tracing studies nominated a rare subset of highly specialized endothelial cells, termed as "hemogenic endothelium", as the precursor of definitive cells. Real-time *in vivo* visualization of the dorsa aorta of *cmyb:eGFP;kdrl:memCherry* double-transgenic transparent zebrafish embryos showed that *kdrl:memCherry*$^{+}$ cells changed into *cmyb;eGFP*$^{+}$ cells (Bertrand et al., 2010). When mouse embryos with green fluorescent protein (GFP) expressed under the control of the *Ly-6A* (also known as *Sca1*) transcriptional elements were flushed with fluorochrome-conjugated endothelial cell-specific CD31 antibodies, sliced and then cultured directly under the confocal microscope for sequential time-lapsed imaging, rare GFP^{+} cells were noted to bud from GFP^{+}CD31^{+} endothelial cells lining the lumen of the aorta (Boisset et al., 2010). Lineage tracing studies using *kdrl:Cre;switch* DsRed reporter zebrafish and inducible VE-Cadherin Cre mouse line further demonstrated the endothelial origin of HSCs (Bertrand et al., 2010; Zovein et al., 2008).

The lineage tracing studies showed conclusively that HSCs emerge from endothelial cells; however, neither these nor the time-lapsed reports addressed the

origin of the transient-definitive wave. Given that endothelial cells display plasticity in adopting venous versus arterial identity, it is unknown whether the self-renewing, multipotent HSCs and the transient myelo-erythoid restricted progenitors emerge from a common or wave-specific hemogenic endothelium. The discovery of similar plasticity in hemogenic endothelium to stir its fate would provide an exciting avenue to elucidate why *ex vivo* attempts to produce HSCs have failed. However, how the hemogenic endothelium responsible for the transient-definitive wave differs from the one responsible for the definitive wave is poorly understood because of the lack of wave-specific cell markers. Therefore, identifying tools for prospective fractionation of the temporally and spatially overlapping products from the two definitive waves will be critical to dissect the regulatory programs that govern the diversity and fate of hemogenic endothelium.

ROLE OF VASCULAR ENDOTHELIAL GROWTH FACTOR A IN HEMATOPOIESIS

One critical signaling pathway acting on embryonic mesoderm and endothelium involves the Vascular Endothelial Growth Factor A (VEGF-A), a potent regulator of vasculogenesis and angiogenesis during development. VEGF is a secreted mitogen that binds with high affinity to two receptor tyrosine kinases, fms-related tyrosine kinase 1 (flt-1) and fetal liver kinase 1 (flk-1). Mouse embryos that are homozygous for these receptors or even simply heterozygous for the ligand die between embryonic day 8.5 and 9.5 and display concomitant vascular and hematopoietic defects. Blood islands of yolk sacs with disrupted Flk1 or Flt1 signaling appear devoid of primitive cells (Carmeliet et al., 1996; Ferrara et al., 1996; Fong et al., 1995; Shalaby et al., 1995).

In adult HSCs, colony forming potential was reduced when VEGF signaling was interrupted by a small-molecule inhibitor of VEGF receptor tyrosine kinase that acts intracellularly and was only mildly affected when a soluble Flt1, which blocks VEGF signaling extracellularly, was administered. This suggested that HSC survival is regulated by VEGF-A via an internal autocrine loop mechanism (Gerber et al., 2002).

In adults, endothelial cells have been shown to express VEGF. Despite intact levels of circulating VEGF-A protein or mRNA in whole organs, systemic endothelial apoptosis with neonatal demise can ensue when VEGF-A is inactivated specifically in VE-Cadherin-Cre expressing endothelial cells (Lee et al., 2007). This uncovered an autocrine VEGF-A signaling pathway that is required for adult endothelial cell

homeostasis and begs the question for a similar role of VEGF-A in hemogenic endothelium.

Because vascular and hematopoietic defects usually appear concurrently, it was difficult to exclude that defective hematopoiesis was a secondary effect of impaired or absent hemogenic endothelium. At least in *Xenopus* embryos, the VEGF-A requirement for HSC specification versus endothelial arterial formation appears to be VEGF-A isoform specific (Leung et al., 2013).

Taken together, a critical function of VEGF in embryonic hematopoiesis has been implied, but *in vivo* mammalian studies of VEGF deficiency during development are scarce. This might have been due to the experimental challenges posed by the lethality of the *VEGF-A* heterozygous embryos. However, new models of genetic manipulation are opening new avenues to readdress questions that could not be previously assessed.

PLACENTA AS A NOVEL NICHE FOR HEMATOPOIESIS

The chorioallantoic placenta contains cells of trophectoderm and mesoderm lineages, among others. The maternal-fetal exchange of gases, nutrients and waste products takes place between the fetal blood vessels lined by mesoderm-derived endothelial cells and the maternal blood spaces lined by trophectoderm-derived trophoblast cells (Cross et al., 1994; Georgiades et al., 2002). One class of trophoblast cells has very large cytoplasm and polyploid nuclei and is called trophoblast giant cells (TGC). These have been characterized into at least four different types depending on their location in the placenta and their endocrine/paracrine function (Simmons et al., 2007).

The placenta, more specifically, TGCs have been reported to express VEGF-A (Demir et al., 2004; Voss et al., 2000). The VEGF-A receptor flt1 is not only present in endothelial cells but also in the trophoblasts of the ectoplacental cone first and the spongiotrophoblast region later. However, chimeric placentas with inactivating $flt1^{lacZ/lacZ}$ trophoblasts and $flt1^{+/+}$ fetal endothelium do not display any defects in placental, vascular, or hematopoietic compartments (Hirashima et al., 2003). Alternatively, the VEGF-A receptor flk1 is robustly expressed in endothelial cells and hematopoietic progenitors but absent in trophoblasts. Of note, the placenta also secretes another member of the VEGF family, the placental-like growth factor, which binds to flt1, enhancing VEGF-A signaling through flk1 (Autiero et al., 2003).

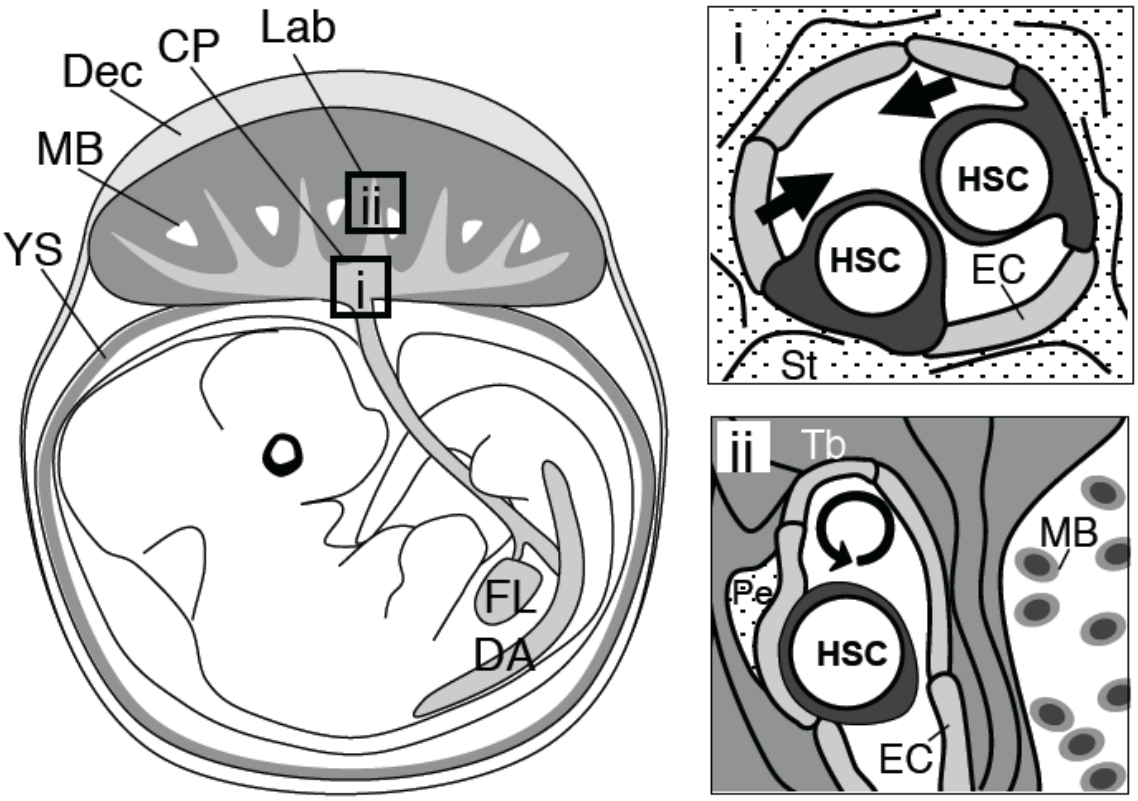

Figure 2. The hematopoietic niches in the placenta

While previously HSCs found in the placenta were disregarded as simply circulating, it is now accepted that they can emerge *de novo* from the placenta (Alvarez-Silva et al., 2003; Barcena et al., 2009; Rhodes et al., 2008; Robin et al., 2009). In fact, the murine placenta harbors 15-fold more HSCs than any other HSC-generating organ (Gekas et al., 2005). Two functionally distinct hematopoietic niches have been described: the large fetal blood vessels in the chorioallantoic mesenchyme for HSC generation and the small fetal blood vessels in the labyrinth for HSC proliferation (Rhodes et al., 2008) (Fig. 2; YS, yolk sac; MB, maternal blood; Dec, decidua; CP, chorionic plate; Lab, labyrinth; FL, fetal liver; DA, dorsal aorta; HSC, hematopoietic stem cell; EC, endothelial cell; Tb, trophoblast; Pe, pericyte). The placenta

constitutes a unique hematopoietic microenvironment that can support HSC expansion without promoting differentiation. (Ottersbach and Dzierzak, 2005). Our group recently expanded the repertoire of the trophoblast as an important niche cell that prevents premature differentiation of HS/PCs in the placental labyrinth vasculature via PDGF-B/PDGFRβ signaling (Chhabra et al., 2012). Many more cell types likely contribute to the placental niche and their differential regulation of the HSC-generating versus proliferating segregated niches awaits further investigation.

REFERENCES

Alvarez-Silva, M., Belo-Diabangouaya, P., Salaun, J. and Dieterlen-Lievre, F. (2003). Mouse placenta is a major hematopoietic organ. *Development* **130**, 5437-44.

Autiero, M., Waltenberger, J., Communi, D., Kranz, A., Moons, L., Lambrechts, D., Kroll, J., Plaisance, S., De Mol, M., Bono, F. et al. (2003). Role of PlGF in the intra- and intermolecular cross talk between the VEGF receptors Flt1 and Flk1. *Nat Med* **9**, 936-43.

Barcena, A., Kapidzic, M., Muench, M. O., Gormley, M., Scott, M. A., Weier, J. F., Ferlatte, C. and Fisher, S. J. (2009). The human placenta is a hematopoietic organ during the embryonic and fetal periods of development. *Dev Biol* **327**, 24-33.

Bertrand, J. Y., Chi, N. C., Santoso, B., Teng, S., Stainier, D. Y. and Traver, D. (2010). Haematopoietic stem cells derive directly from aortic endothelium during development. *Nature* **464**, 108-11.

Boisset, J. C., van Cappellen, W., Andrieu-Soler, C., Galjart, N., Dzierzak, E. and Robin, C. (2010). In vivo imaging of haematopoietic cells emerging from the mouse aortic endothelium. *Nature* **464**, 116-20.

Carmeliet, P., Ferreira, V., Breier, G., Pollefeyt, S., Kieckens, L., Gertsenstein, M., Fahrig, M., Vandenhoeck, A., Harpal, K., Eberhardt, C. et al. (1996). Abnormal blood vessel development and lethality in embryos lacking a single VEGF allele. *Nature* **380**, 435-9.

Chhabra, A., Lechner, A. J., Ueno, M., Acharya, A., Van Handel, B., Wang, Y., Iruela-Arispe, M. L., Tallquist, M. D. and Mikkola, H. K. (2012). Trophoblasts regulate the placental hematopoietic niche through PDGF-B signaling. *Dev Cell* **22**, 651-9.

Cross, J. C., Werb, Z. and Fisher, S. J. (1994). Implantation and the placenta: key pieces of the development puzzle. *Science* **266**, 1508-18.

Demir, R., Kayisli, U. A., Seval, Y., Celik-Ozenci, C., Korgun, E. T., Demir-Weusten, A. Y. and Huppertz, B. (2004). Sequential expression of VEGF and its receptors in human placental villi during very early pregnancy: differences between placental vasculogenesis and angiogenesis. *Placenta* **25**, 560-72.

Ferrara, N., Carver-Moore, K., Chen, H., Dowd, M., Lu, L., O'Shea, K. S., Powell-Braxton, L., Hillan, K. J. and Moore, M. W. (1996). Heterozygous embryonic lethality induced by targeted inactivation of the VEGF gene. *Nature* **380**, 439-42.

Fong, G. H., Rossant, J., Gertsenstein, M. and Breitman, M. L. (1995). Role of the Flt-1 receptor tyrosine kinase in regulating the assembly of vascular endothelium. *Nature* **376**, 66-70.

Gekas, C., Dieterlen-Lievre, F., Orkin, S. H. and Mikkola, H. K. (2005). The placenta is a niche for hematopoietic stem cells. *Dev Cell* **8**, 365-75.

Georgiades, P., Ferguson-Smith, A. C. and Burton, G. J. (2002). Comparative developmental anatomy of the murine and human definitive placentae. *Placenta* **23**, 3-19.

Gerber, H. P., Malik, A. K., Solar, G. P., Sherman, D., Liang, X. H., Meng, G., Hong, K., Marsters, J. C. and Ferrara, N. (2002). VEGF regulates haematopoietic stem cell survival by an internal autocrine loop mechanism. *Nature* **417**, 954-8.

Hirashima, M., Lu, Y., Byers, L. and Rossant, J. (2003). Trophoblast expression of fms-like tyrosine kinase 1 is not required for the establishment of the maternal-fetal interface in the mouse placenta. *Proc Natl Acad Sci U S A* **100**, 15637-42.

Lee, S., Chen, T. T., Barber, C. L., Jordan, M. C., Murdock, J., Desai, S., Ferrara, N., Nagy, A., Roos, K. P. and Iruela-Arispe, M. L. (2007). Autocrine VEGF signaling is required for vascular homeostasis. *Cell* **130**, 691-703.

Leung, A., Ciau-Uitz, A., Pinheiro, P., Monteiro, R., Zuo, J., Vyas, P., Patient, R. and Porcher, C. (2013). Uncoupling VEGFA functions in arteriogenesis and hematopoietic stem cell specification. *Dev Cell* **24**, 144-58.

Ottersbach, K. and Dzierzak, E. (2005). The murine placenta contains hematopoietic stem cells within the vascular labyrinth region. *Dev Cell* **8**, 377-87.

Rhodes, K. E., Gekas, C., Wang, Y., Lux, C. T., Francis, C. S., Chan, D. N., Conway, S., Orkin, S. H., Yoder, M. C. and Mikkola, H. K. (2008). The emergence of hematopoietic stem cells is initiated in the placental vasculature in the absence of circulation. *Cell Stem Cell* **2**, 252-63.

Robin, C., Bollerot, K., Mendes, S., Haak, E., Crisan, M., Cerisoli, F., Lauw, I., Kaimakis, P., Jorna, R., Vermeulen, M. et al. (2009). Human placenta is a potent hematopoietic niche containing hematopoietic stem and progenitor cells throughout development. *Cell Stem Cell* **5**, 385-95.

Shalaby, F., Rossant, J., Yamaguchi, T. P., Gertsenstein, M., Wu, X. F., Breitman, M. L. and Schuh, A. C. (1995). Failure of blood-island formation and vasculogenesis in Flk-1-deficient mice. *Nature* **376**, 62-6.

Simmons, D. G., Fortier, A. L. and Cross, J. C. (2007). Diverse subtypes and developmental origins of trophoblast giant cells in the mouse placenta. *Dev Biol* **304**, 567-78.

Voss, A. K., Thomas, T. and Gruss, P. (2000). Mice lacking HSP90beta fail to develop a placental labyrinth. *Development* **127**, 1-11.

Zovein, A. C., Hofmann, J. J., Lynch, M., French, W. J., Turlo, K. A., Yang, Y., Becker, M. S., Zanetta, L., Dejana, E., Gasson, J. C. et al. (2008). Fate tracing reveals the endothelial origin of hematopoietic stem cells. *Cell Stem Cell* **3**, 625-36.

CHAPTER 2

LYVE1 identifies yolk sac definitive hemogenic endothelium

INTRODUCTION

Embryonic survival depends on orchestrated developmental programs that can rapidly produce differentiated blood cells and concomitantly generate a pool of undifferentiated hematopoietic stem cells (HSC) within a narrow window of time. This developmental challenge is met by segregating hematopoiesis into multiple functional waves. The earliest wave (called "primitive") appears in the extra-embryonic yolk sac and predominantly generates erythroid cells that express unique embryonic globins to meet the immediate metabolic needs of the developing embryo. The final wave (called "definitive") introduces the enduring HSCs that hold the lifelong capacity to replenish all blood cell types --namely, the myeloid, erythroid and lymphoid lineages. These multipotent hematopoietic cells emerge from the specialized hemogenic endothelium in several anatomical sites: the para-aortic splanchnopleural/aorta-gonad-mesonephros region (pSP/AGM), the yolk sac, the placenta, and the vitelline and umbilical vessels that connect the dorsal aorta to the yolk sac and placenta, respectively (Medvinsky and Dzierzak, 1996; Muller et al., 1994; Palis et al., 1999; Rhodes et al., 2008; Zeigler et al., 2006). Flanking these two waves, an intermediate wave (called "transient-definitive") consisting of provisional progenitors with predominantly myelo-erythroid potential emerges from the yolk sac (Mikkola and Orkin, 2006). The red cells made from these progenitors express "definitive" adult type globins; however, these progenitors lack self-renewal ability and the robust lymphoid potential characteristics of HSCs. Although the characterization of the hematopoietic waves and organs that give rise to them is gradually improving, the contribution of each wave to fetal hematopoiesis remains poorly defined

due to the lack of wave-specific cell markers hindering the prospective isolation of these temporally and spatially overlapping products. Currently, our toolbox of cell surface antigens to prospectively isolate developing hematopoietic stem and progenitor cells (HS/PCs) includes CD41, ckit, CD45, CD150, Sca1, Mac1 (Ferkowicz et al., 2003; Gazit et al., 2014; Mikkola et al., 2003a; Morrison et al., 1995). However, none of these markers can segregate the myelo-erythroid restricted progenitors from the multipotent stem cells.

One strategy to discriminate cells from individual waves is to characterize them at the time of their specification before they intermix in circulation. The mesoderm-derived blood islands in the yolk sac have been recognized as the origin of the primitive erythroid cells (Haar and Ackerman, 1971), but the precise precursor for the latter two waves had remained contested for decades, as they emerge at the time or after circulation is already established. Time-lapsed imaging of *in vitro* and *in vivo* HS/PC emergence as well as lineage tracing experiments provided long-awaited evidence that a subset of highly specialized endothelial cells was capable of generating definitive hematopoietic cells (Bertrand et al.; Boisset et al.; Chen et al., 2009; Eilken et al., 2009; Lancrin et al., 2009; Zovein et al., 2008). However, like the HS/PC markers, most antigens/genes known to be expressed in hemogenic endothelium --such as, flk1, CD31, VE-Cadherin and Tie2-- are not specific to individual waves or anatomical sites. Moreover, although many of these markers are developmentally regulated (McKinney-Freeman et al., 2009), none of them are wave-specific. Thus, there are no robust methods to prospectively identify or genetically target only one of the hematopoietic waves or organs, while sparing others.

Here we identify surface expression of the lymphatic vessel endothelial hyaluronan receptor-1 (LYVE1) as a unique marker that distinguishes hemogenic endothelium and definitive HS/PCs in the yolk sac from the primitive erythroid lineage, as well as from the hemogenic endothelium and HS/PCs in other anatomical sites. Moreover, we used the *LYVE1-eGFP-hCre* knock-in mouse to mark the molecular divergence between the primitive and definitive hematopoietic programs in the yolk sac. While a fraction of definitive HSCs also become labeled, the majority of the HSC compartment was unaffected. As the primitive wave originating from the yolk sac and the HSC waves arising from the placenta and AGM are completely and partially spared, respectively, from LYVE1-Cre mediated excision, this tool now enables the tracing and genetic manipulation of hemogenic endothelium that gives rise to the yolk sac definitive hematopoietic waves.

RESULTS

LYVE1 protein is expressed exclusively in yolk sac hematopoietic stem and progenitor cells and hemogenic endothelium

Our objective was to identify a novel hemogenic endothelial cell surface marker that could illuminate the divergence of the hematopoietic waves. Our laboratory had previously screened for differentially expressed hematovascular genes in yolk sac endothelium lacking the Stem Cell Leukemia (*Scl/Tal1*) gene, which encodes a transcription factor that is critical for the establishment of hemogenic identity in endothelium (Lancrin et al., 2009; Van Handel et al., 2012). We reasoned that endothelial genes that are down-regulated upon Scl inactivation could potentially serve as markers that highlight the hemogenic endothelium, or distinct subsets of it. We selected the LYVE1 as a candidate because it is extensively expressed in the early yolk sac vasculature but largely absent from the dorsal aorta (Banerji et al., 1999; Gordon et al., 2008), and thereby potentially provide a tissue specific marker for hemogenic endothelium.

We first assessed the expression of LYVE1 protein in hemogenic tissues by immunostaining. Screening of E10.5 hemogenic tissues demonstrated that LYVE1 protein was robustly expressed in the yolk sac and vitelline vessels, but highly restricted in the embryo proper and undetectable in the placenta and umbilical vessels (Fig. 1A). Using flow cytometry analysis, LYVE1 protein could be detected in the yolk sac as early as at the 8 somite-pair embryonic stage (E8.5) (Fig. 1B).

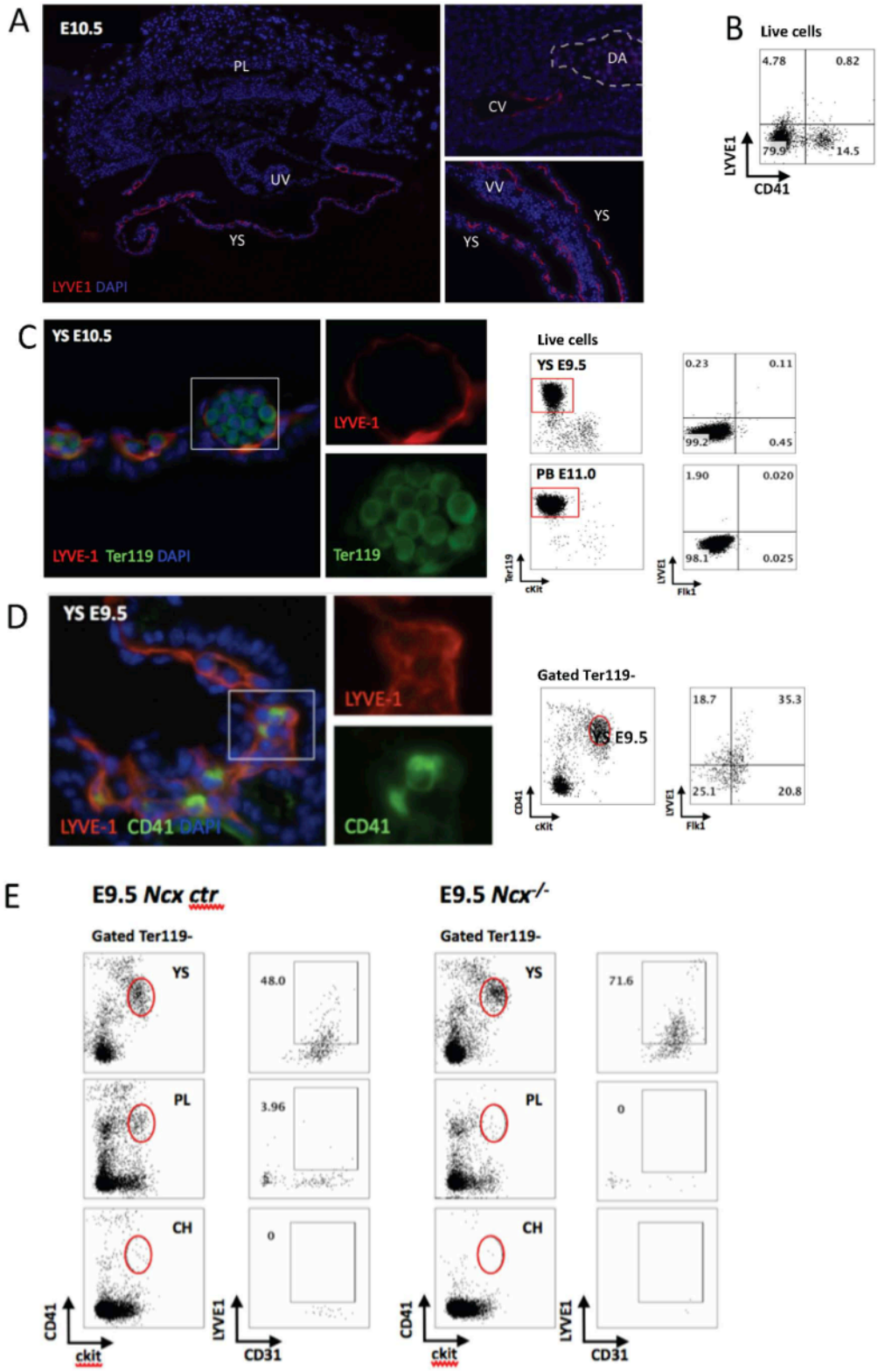

Figure 1. LYVE1 protein expression in hemogenic organs and hematopoietic compartments. (A) Immunofluorescence (IF) staining of tissues at E10.5. PL, placenta; UV, umbilical vessels; YS, yolk sac; DA, dorsal aorta; CV, cardinal vein; VV, vitelline vessels. (B) Flow cytometry analysis (FACS) of yolk sac at E8.5. (C) IF of yolk sac at E10.5 and FACS plot of primitive erythroid population in yolk sac at E9.5 and peripheral blood at E11.0. The right column shows the gated erythroid population from the corresponding left column. (D) IF and FACS plot of HS/PC fraction in yolk sac at E9.5. (E) FACS plot of HS/PCs from YS, PL and CH, caudal half from Ncx control and null littermate embryos at E9.5.

During early gestation, the yolk sac is primarily populated by Ter119^{+} primitive erythroid cells. Immunofluorescence and flow cytometry analysis revealed that primitive erythroid cells were devoid of LYVE1 protein expression both immediately after their emergence in the yolk sac at E9.5, and upon their maturation in the peripheral blood at E11.0 (Fig. 1C). In contrast, LYVE1 was expressed in 49.6% (± 15.9%) of CD41^{+} cKit^{+} nascent HS/PCs in E9.5 yolk sac (Fig. 1D)

Given that HS/PCs arise from hemogenic endothelium, we surveyed the vasculature for LYVE1 expression in all hemogenic organs. As previously reported (Gordon et al., 2008), immunostaining confirmed that LYVE1 was expressed almost ubiquitously in CD31^{+} endothelial cells of the E10.5 yolk sac. LYVE1 expression continued along the vitelline artery, which has been shown to give rise to hematopoietic clusters beginning at E10.0 (Zovein et al., 2010). Within intra-embryonic tissues, LYVE1 expression was confined to the cardinal vein and spared from the dorsal aorta (Fig. 1A). Flow cytometry analysis further highlighted the striking contrast of LYVE1^{+} fraction in the Flk1^{+}CD41^{-} endothelial compartment between the distinct hemogenic organs at E9.5: 89.0% ± 2.9% in the yolk sac versus 3.2% ± 1.9% and 5.0% ± 2.6% in the placenta and embryonic caudal half, respectively (Fig. S1). Altogether, these data show that the yolk sac is the predominant site that contains the putative hemogenic endothelium with LYVE1 protein expression during the window of HS/PC emergence.

To verify whether the yolk sac is the only source of LYVE1^{+} HS/PCs, we assessed LYVE1 surface expression in HS/PC populations in the different hemogenic tissues of *Ncx1*$^{-/-}$ embryos that are heartbeat-deficient and hence lack circulation (Koushik et al., 2001). Flow cytometry of *Ncx1*$^{-/-}$ tissues showed co-expression of LYVE1 with

$CD41^+cKit^+$ HS/PCs specifically in the yolk sac, but not in the placenta or embryo proper, which harbored some $LYVE^+$ HS/PCs in control littermates with intact circulation (Fig. 1E and Suppl. 2). These data nominated the yolk sac as a sole source of $LYVE1^+$ HS/PCs, and suggested that during normal cardiac function, the HS/PC pool in the placenta and embryo is infused with $LYVE1^+$ HS/PCs circulating from the yolk sac (Fig. 1E).

LYVE1Cre lineage tracing bypasses the primitive erythroid lineage but labels yolk sac definitive myelo-erythroid progenitors

To define the fate of $LYVE1^+$ candidate hemogenic endothelial cells, we performed lineage-tracing analysis by interbreeding *LYVE1-eGFP-hCre* knock-in mice (referred as "LYVE1Cre" hereafter) with the *R26-stop-YFP* reporter line (referred as "YFP"). Cells with Cre recombinase activity driven by the *LYVE1* promoter underwent excision of the floxed transcriptional stop preceding the YFP sequence in the Rosa26 locus, permanently labeling them and all their daughter cells with YFP expression (Fig. 2 A).

Flow cytometry analysis of E9.0 *LYVE1Cre;YFP* yolk sacs showed that the $Ter119^+$ primitive red blood cells were not labeled (Fig. 2A). The absence of reporter activity in E9.0 yolk sac erythroid cells was not due to *YFP* gene silencing as they were 90% labeled when crossed with the hemato-endothelial cell specific *Tie2/Tek Cre* strain, in which Cre is activated after gastrulation in hemato-vascular precursors and 100% labeled when mated with the germ cell specific *VasaCre* mouse, in which Cre is active

during fertilization resulting in labeling of all cells of the conceptus (Fig. 2B). This demonstrated that primitive erythropoiesis does not arise from the LYVE1-lineage. Consistent with previous studies, we also found that YFP expression from the Rosa26 locus is silenced in primitive erythroid cells as these cells mature in circulation irrespective of the Cre that was used for activating YFP expression (Fig. S3).

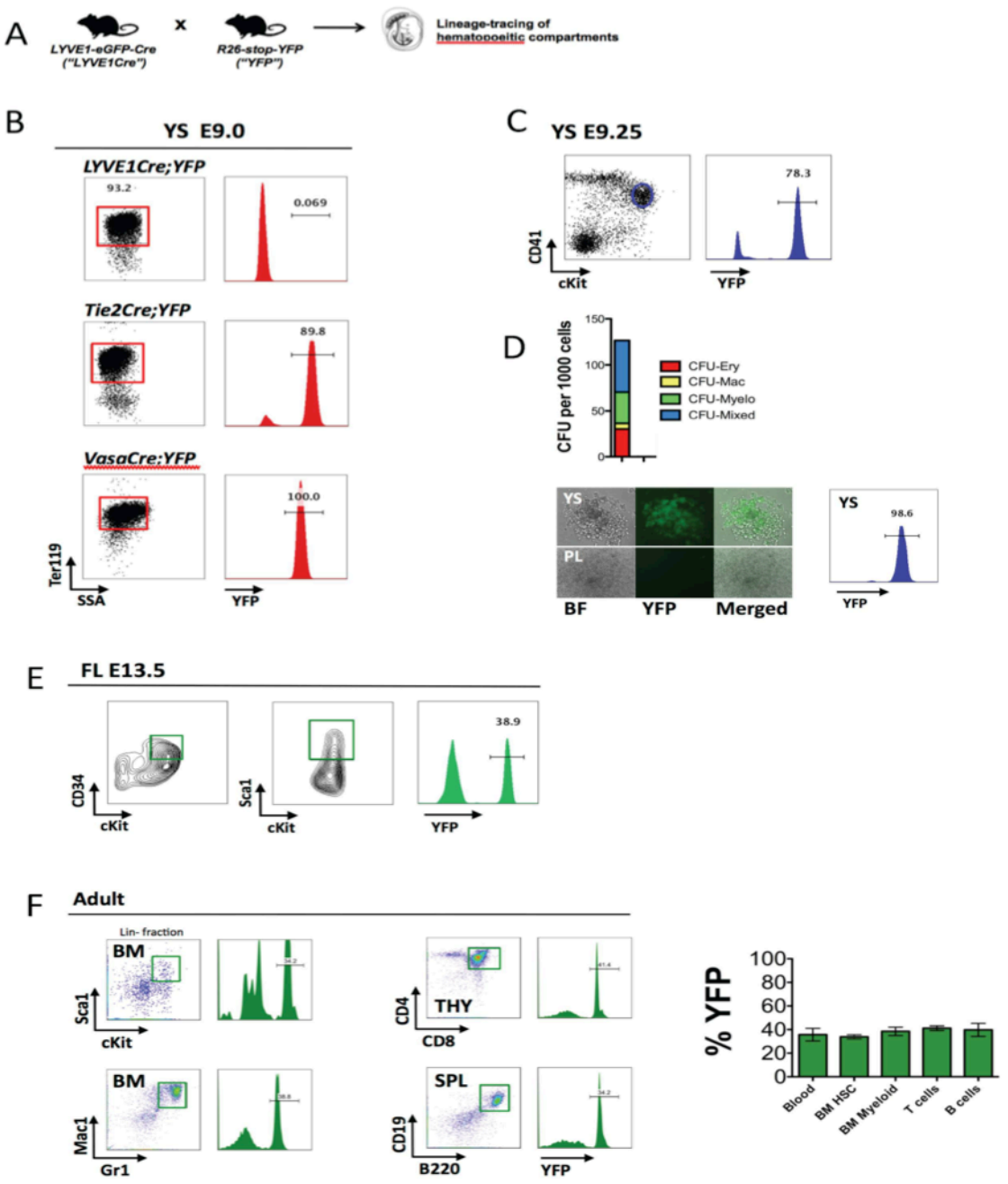

Figure 2. LYVE1Cre lineage tracing of hematopoietic waves. (A) Cartoon of mouse model for lineage tracing. (B) FACS plots of yolk sac erythroid population at E9.0. The right column show representative YFP marking fractions. (C) FACS plot of yolk sac HS/PC and its YFP marking at E9.25. (D) Methylcellulose assay of E9.5 yolk sac and direct visualization of yellow fluorescent protein expressing colony via inverted fluorescence microscope. (E) FACS plot of HS/PC fraction in fetal liver at E13.5 (F) FACS plot of blood cell types in adult tissues, such as, BM, bone marrow, TM, thymus and SPL, spleen.

In contrast to the primitive erythroid cells that were not lineage-traced by LYVE1-Cre, 74% (± 3.7% SEM) of $CD41^{+}cKit^{+}$ HS/PCs from E9.25 *LYVE1Cre;YFP* yolk sac were marked by YFP. Furthermore, 100% of myelo-erythroid hematopoietic colonies that were formed from yolk sac single cell suspension were labeled with YFP (Fig. 2C and 2D). These data are in concordance with the observed surface expression for LYVE1 protein, and suggest that the majority of yolk sac HS/PCs, at least the myelo-erythroid progenitors that constitute the transient definitive hematopoietic wave, emerge from LYVE1-lineage traced hemogenic endothelium

LYVE1 lineage traced cells contribute to a subset of fetal and adult HSCs and their progeny

We next assessed the contribution of LYVE1 lineage traced cells to the definitive HSC compartment in the fetal liver and adult bone marrow. In E13.5 fetal liver, the $Lin^{-}Sca1^{+}cKit^{+}CD34^{+}$ HSC pool was 38.9% YFP marked (Fig. 2E). Moreover, in the adult, similar fractions of YFP labeled cells were found in the $Lin^{-}Sca1^{+}cKit^{+}$ HSC compartment of the bone marrow (33.8 ±1.7%), $Mac1^{+}Gr1^{+}$ myeloid cells of the bone marrow (38.5 ±3.5%), $CD4^{+}CD8^{+}$ T lymphocytes in the thymus (41.1 ±1.9%), $CD19^{+}B220^{+}$ B lymphocytes in the spleen (39.75 ±5.5%), and $CD45^{+}$ cells in the peripheral blood (35.73 ±5.3%) (Fig. 2F). These data establish that a subgroup of long-term populating, self-renewing HSCs stem emerge from the LYVE1 lineage while the majority of them arise from precursors not marked by LYVE1 lineage trace.

LYVE1Cre lineage tracing robustly labels HS/PCs in the yolk sac but also shows some ectopic labeling in the placenta and AGM

As 44.0% and 42.9% of $CD41^{+}cKit^{+}$ HS/PC populations in E9.5 placenta and caudal half, respectively, were also labeled by YFP despite the lack of LYVE1 protein expression in these tissues in the absence of circulation, we compared YFP labeling in *Ncx1*$^{-/-}$ versus control littermates to investigate for the contribution of HS/PCs migrating through circulation. At E9.5, only 0.7% of HS/PCs residing in the *Ncx1*$^{-/-}$ placenta showed YFP labeling. The *Ncx1*$^{-/-}$ embryonic HS/PCs could not be assessed due to insufficient number of cells (Fig. 3A). To evaluate the labeling in myeloerythroid progenitors, *Ncx1*$^{-/-}$ and control hemogenic organ explants underwent co-culture in OP9-DL1 stroma for 5 days and then colonies were allowed to grow in methylcellulose for 7-10 days (Fig. 3B). When examined under fluorescence microscope, 92%, 65% and 77% of colonies derived from the *Ncx1* control yolk sac, placenta and embryonic caudal half showed green fluorescence. In contrast to the concepti with circulating cells, 95%, 10% and none of the colonies derived from circulation deficient *Ncx1*$^{-/-}$ yolk sac, placenta and embryo, respectively, were YFP+ (Fig. 3C). These data further support the notion that the LYVE1Cre is a useful tool for labeling definitive HS/PCs originating from the yolk sac.

To further outline the source of LYVE1-traced HS/PCs, we next focused on the endothelial cells, which release HS/PCs into circulation via endothelium-to-hematopoietic cell transition. Within the $Ter119^{-}CD41^{-}CD31^{+}$ endothelial compartment at E9.5, 85.6 ±0.1% in the yolk sac versus 4.7 ±2.4% and 4.2 ±1.2% in the placenta and

caudal half, respectively, were YFP marked (Fig. 3D). Of note, although the LYVE1 protein could not be visualized by immunofluorescence staining of the E10.5 placenta and only low level of LYVE1 protein could be discerned by flow analysis in 0.13% of endothelial cells, anti-YFP immunostaining was detected in some cells in placental

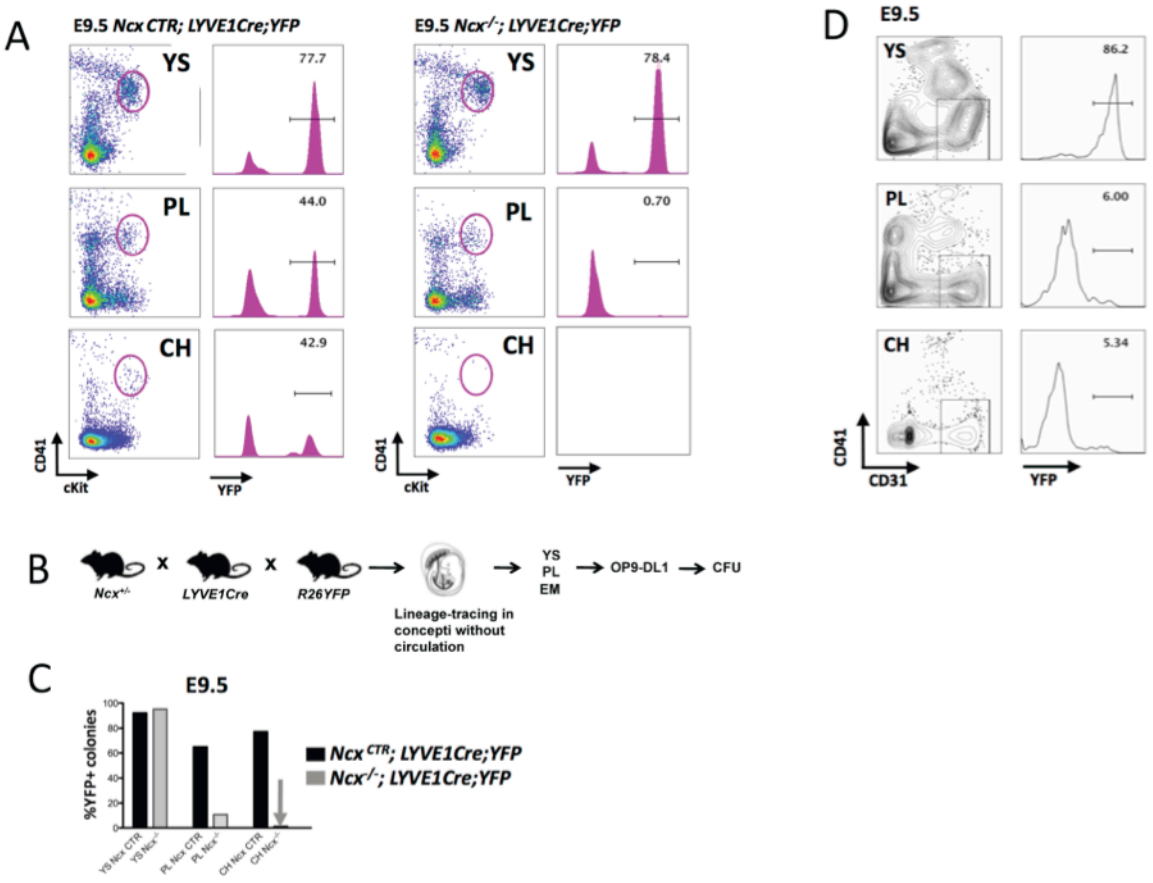

Figure 3. LYVE1Cre lineage tracing of yolk sac definitive hematopoiesis. (A) FACS plots of HS/PC from hemogenic tissues of Ncx control and null littermates at E9.5. (B) Cartoon diagram of experimental method. (C) Frequency of YFP$^+$ colonies. (D) FACS plot of vascular marking in wild type organs at E9.5

vascular walls. In the embryo proper, anti-LYVE1 immunostaining had localized the protein expression to the cardinal vein but not the aorta. However, anti-YFP staining was present in both vascular structures, indicating a discordant expression between LYVE1 protein and LYVE1-lineage traced YFP protein (Fig S4). In contrast to the hematopoietic cells, the fractions of endothelial cells with marking were not significantly changed in the *Ncx1*$^{-/-}$ tissues lacking circulation (84.4 ±0.1% in yolk sac, 4.5 ±2.2% in placenta, and 2.8 ±0.4% in caudal half) (Fig. S5). These data imply that LYVE1-Cre shows promiscuous activation in a subset of endothelial cells in the placenta and embryo proper in the absence of protein expression.

LYVE1Cre is a unique tool for molecular targeting of yolk sac definitive hematopoiesis and early fetal liver colonization

In addition to serving as a site for HSC expansion during late midgestation, the fetal liver has a critical role in supporting definitive erythropoiesis through most of fetal life. In contrast to the primitive erythroid cells that mature at their site of origin, namely the yolk sac, the progenitors for the definitive erythroid cells must transit through the fetal liver to mature. However, although postulated to also originate from the yolk sac, the anatomical origin of the precursors that first colonize the fetal liver and jump-start fetal definitive erythropoiesis has not been experimentally proven. FACS analysis of E13.5 fetal liver from *LYVE1Cre;YFP* mice showed that 87%±1.5% of the CD71^{+}Ter119^{low} proerythroblast compartment had derived from the LYVE1-lineage (Fig.

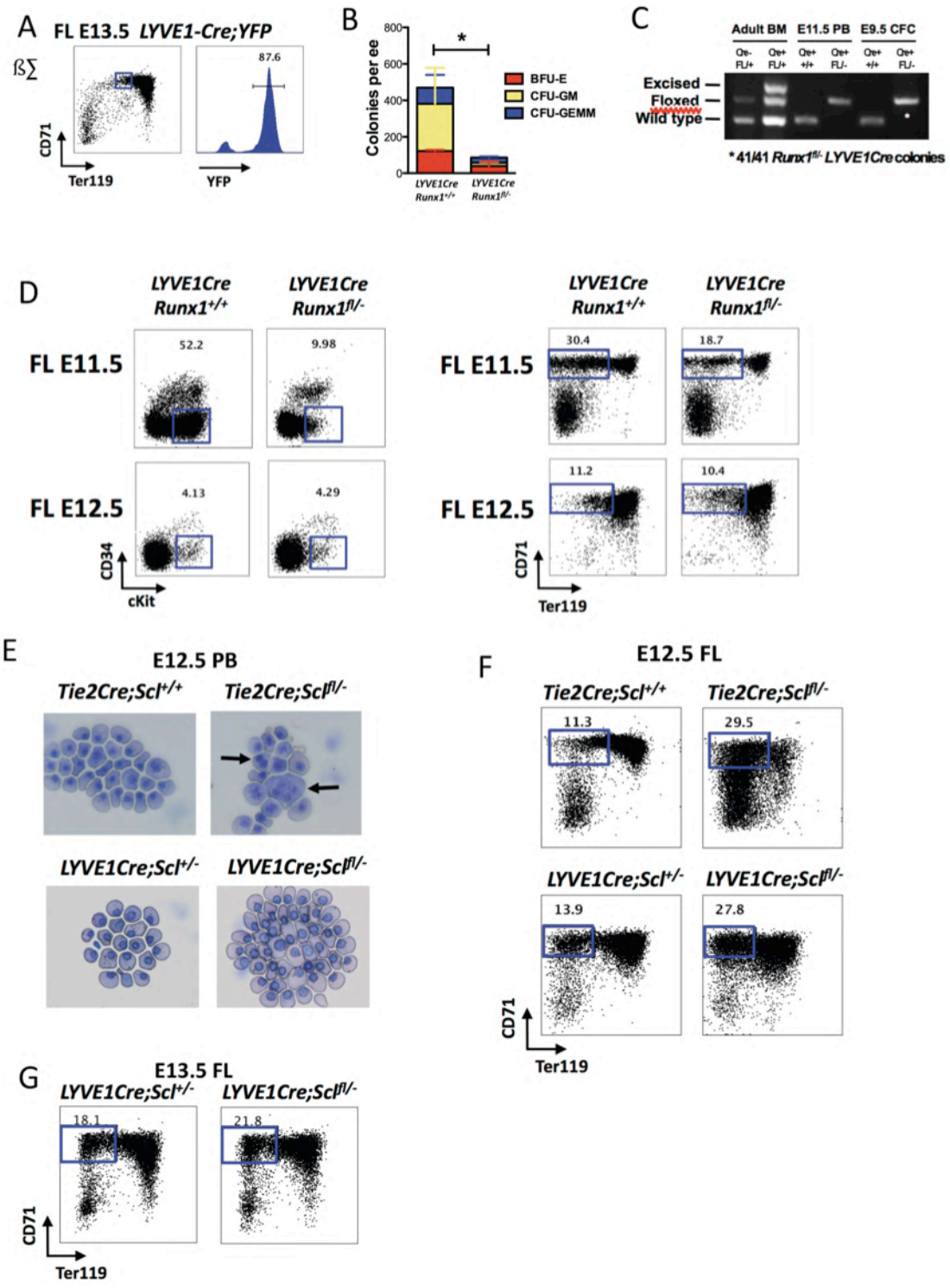

Figure 4. LYVE1Cre as a novel tool to study transient-definitive hematopoiesis. (A) FACS plot of YFP marking in fetal liver at E13.5. (B) Colony forming units from the E9.5 yolk sac of LYVE1Cre-specific Runx1 deletion. (C) Representative PCR genotyping of each colony. (D) FACS plot of definitive cKit$^+$ progenitors and immature proerythroblasts in fetal liver at E11.5 and E12.5 of LYVE1Cre-specific Runx1 null embryos. (E) May-Grünwald-Giemsa stain of peripheral blood from Tie2Cre versus LYVE1Cre specific Scl deletion. (F) FACS plot of immature proerythroblast fraction in fetal liver of Tie2Cre versus LYVE1Cre specific Scl null embryos. (G) FACS plot of immature proerythroblast fraction in fetal liver of LYVE1Cre-specific Scl deletion.

4A). As only a minimal subset of the HS/PCs originating in the early placenta and the embryo exhibit YFP marking, these data suggest that the progenitors that are responsible for initiating fetal liver definitive erythropoiesis are of yolk sac origin.

As the primitive erythroid lineage from the yolk sac and the majority of the definite HSC pool originating from the embryo and the placenta is not excised by the LYVE1Cre, we reasoned that the LYVE1Cre would provide a unique model to study the impact of yolk sac definitive hematopoiesis specifically on fetal hematopoiesis and survival. Runt-related transcription factor 1 (Runx1) is required for the generation of both the transient definitive hematopoietic progenitors in the yolk sac and HSCs in all hemogenic tissues.

At E9.5, LYVE1Cre-mediated Runx1 inactivation exhibited a dramatic reduction of myeloerythroid colonies from the yolk sac (from 469.5 in control to 85.5 total CFUs in *LYVE1Cre;Runx1*$^{fl/-}$) (Fig. 4B). As anticipated from the known requirement of Runx1 in hemogenic endothelium (Chen et al., 2009), genotyping of colonies confirmed that only cells that had escaped LYVE1Cre-mediated Runx1 deletion were able to grow (Fig. 4C). We then examined the fetal liver at E11.5 as it is where HS/PCs from all organs converge for maturation and expansion. Analysis of E11.5 *LYVE1Cre;Runx1*$^{fl/-}$ mutants revealed a marked reduction in both fetal liver cKit^{+}CD34^{-} erythroid enriched progenitors and CD71^{+}Ter119^{low} proerythroblasts. However, by E12.5, these population fractions did recover to numbers comparable to control littermates (Fig. 4D), suggesting that another source of undeleted precursors can sustain definitive erythropoiesis after midgestation. These data implied that the deletion of Runx1 from LYVE1Cre expressing hemogenic

endothelium allows depletion of transient definitive erythroid progenitors that initiate fetal liver definitive erythropoiesis.

To further investigate the impact of yolk sac definitive progenitors on definitive erythropoiesis, we utilized the LYVE1Cre to delete the transcription factor Scl. Scl is essential for the specification of hemogenic endothelium (Porcher et al., 1996; Van Handel et al., 2012), and later is required for the differentiation of both primitive and definitive red cells (Schlaeger et al., 2005), while being dispensable for HSC maintenance (Mikkola et al., 2003b). As shown in prior publications, deletion of *Scl* by Tie2Cre resulted in defects in both primitive and definitive erythropoiesis. May-Grunwald Giemsa stain of the E12.5 peripheral blood displayed erythroid cells that were binucleated and with larger nucleus to cytoplasm ratio. In contrast, an intact morphology of circulating erythroblasts was evident when LYVE1Cre had excised the *Scl* gene, indicating that primitive erythropoiesis had been spared (Fig. 4E). On the other hand, like the *Tie2Cre;Scl*$^{fl/fl}$ embryos, FACS analysis of the corresponding *LYVE1Cre;Scl*$^{fl/fl}$ fetal livers showed abnormal accumulation of the CD71^{+}Ter119^{low} immature erythroblasts (Fig. 4F). This defect was ameliorated one day later, possibly because HSC-derived erythroid cells replenished the fetal liver proerythroblast pool (Fig. 4G). This verified that LYVE1-Cre deletes Scl specifically from the transient-definitive erythroid cells but not primitive erythroid cells, enabling studies addressing the impact of the different erythroid waves on embryonic development and survival.

DISCUSSION

The inability to prospectively identify the rare multipotent hematopoietic stem cells from a pool of lineage-restricted progenitors has hindered the road to elucidate on one hand the regulatory mechanisms that confer stemness in developing HSCs, and on the other hand the impact of the transient progenitor waves in embryonic development and survival. Here, we have provided evidence to nominate LYVE1Cre knockin mouse as a novel tool to dissect the waves of developmental hematopoiesis, in particular, to target the transient-definitive progenitor wave.

Our data indicate that the LYVE1^{+} hemogenic endothelium compartment does not give rise to primitive erythroid cells. The absolute absence of LYVE1 protein expression and LYVE1Cre;YFP marking in these cells implies that they emerge from a mesodermal precursor that either is independent from the LYVE1 lineage, or gives rise to the primitive erythroid precursors before LYVE1Cre activation.

In sharp contrast, both LYVE1 expression and lineage-tracing were robust in the definitive HS/PC population arising from the hemogenic endothelium of the yolk sac. Such dichotomy offers a powerful tool to separate the primitive from definitive erythropoiesis even after circulatory admixture. In fact, using the LYVE1Cre-mediated recombination, we were able to uncouple the defective differentiation events in primitive and definitive erythroid cells caused by Tie2Cre-specific Scl deletion (Schlaeger et al., 2005). This selective inactivation of Scl in the definitive wave only allows now to study

the requirement of Scl in fetal liver erythropoiesis without confounding effects of early embryonic lethality --as in the germline Scl null (Porcher et al., 1996)-- or primitive erythroid defects --as in the *Tie2Cre;Scl*$^{fl/fl}$. Furthermore, we show *in vivo* evidence that the earliest progenitors to seed the fetal liver are products of the yolk sac; however, the deletion of Runx1 from these cells causes only temporary effect on fetal liver hematopoiesis without compromising blood development during late gestation.

The promiscuous activation of LYVE1Cre transgene in the placental vasculature and dorsal aorta in the absence of LYVE1 protein expression during the window of HSC specification precludes strong statements of the yolk sac as the sole source of LYVE1-lineage traced adult hematopoietic cells. Hence, to what extent adult hematopoiesis emerges *de novo* from the yolk sac awaits further studies.

MATERIALS AND METHODS

Mouse models. LYVE1-eGFP-hCre mice (Pham et al., 2010) were intercrossed with the reporter line carrying the YFP preceded by a floxed transcriptional stop in the Rosa26 locus (Srinivas et al., 2001). Similar breeding strategies were used for *Tie2Cre;YFP* and *VasaCre;YFP* concepti. *Ncx1* heterozygous mice for knockout experiments were obtained from (Koushik et al., 2001). Timed matings were performed and the noon of the day of vaginal plug was recorded as embryonic day 0.5 (E0.5). Mice were maintained according to protocols of Animal Research Committee at the University of California, Los Angeles.

Preparation of tissue sections. After isoflurane-induced anesthesia, mice were sacrificed by cervical dislocation. Fetal hematopoietic organs were dissected and fixed in 4% paraformaldehyde at 4° C for 4-6 hours, followed by 30% sucrose in PBS solution overnight, 1:1 30% sucrose:OCT (Tissue-Tek, Electron Microscopy Sciences) for 1 hour at 4° C, and finally embedded and frozen in 100% OCT. Frozen sections were cut at 5-7 μm with a Leica CM3050 S cryostat. For paraffin-embedded blocks, tissues were fixed in 4% paraformaldehyde at 4° C overnight and processed by standard protocol at the Tissue Procurement and Histology Core Laboratory of the Pathology and Laboratory Medicine at UCLA. Paraffin sections were cut at 5 μm.

Immunostaining. Fixed frozen and paraffin-embedded sections were prepared and immunostained as described elsewhere (Rhodes et al., 2008) but using the following

antibodies: LYVE1 conjugated to APC (1:200; BD Pharmingen), Ter119 (1:500, BD Pharmingen), CD41 (1:100; eBiosciences), and GFP (1:500; Abcam). Biotinylated secondary antibodies (1:500; Vector) and Tyramide Signal Amplification kit (PerkinElmer) were used as directed by manufacturer's protocol. Immunofluorescent images were obtained on a Zeiss Axio Imager.A1 with a Zeiss Axiocam MRm camera or a Zeiss LSM 510 microscope equipped with 405 nm, 488 nm, 543 nm, and 633 nm lasers.

Flow cytometry. Tissues were dissociated with collagenase (Worthington), DNase (Qiagen) and dispase (Invitrogen) at 37° C for 20 minutes. Cells were stained with rat anti-mouse monoclonal antibodies against Ter119, CD71, CD41, cKit, Sca1, CD31, flk1, and LYVE1 (all from BD Biosciences or eBiosciences). Dead cells were excluded with DAPI. Cells were assayed on a Becton Dickinson Biosciences LSRII or Fortessa flow cytometer and data was analyzed with FlowJo software (Tree Star Inc.).

Clonogenic progenitor assay. Methylcellulose colony-forming assays were performed as described previously (Chhabra et al., 2012). Briefly, single cell suspension was plated in MethoCult 3434 (Stem Cell Technologies) supplemented with TPO (PeproTech) and colonies were enumerated in 5-7 days. Clustering of 30 or more cells were defined as one colony. Colonies were imaged using a Canon PowerShot G6 camera connected to Zeiss Axiovert 40 CFL microscope. Individual LYVE1Cre;$Runx1^{fl/-}$ colonies were genotyped by PCR.

Cytospin. Peripheral blood cells were mounted on frosted microscope glass slides (Fisherbrand) using a Shandon Cytospin 4 (Thermo Electron). Air dried slides were stained MGG stain (Sigma Aldrich). Images were taken using an Olympus BX51 microscope with a DP72 camera.

Statistical analysis.

Mathematical analysis and statistics were performed using GraphPad Prism Software. P values and data reported as mean ± SEM were calculated using the Student's unpaired two-tailed t tests.

ACKNOWLEDGMENTS

We thank Encarnación Montecino-Rodriguez,and Vincenzo Calvanese for scientific discussions and advice. We thank Felicia Codrea and Jessica Scholes at the Flow Cytometry Core Laboratory at the Broad Center of Regenerative Medicine and Stem Cell Research at UCLA for flow cytometry, and the UCLA Translational Pathology Core Laboratory for preparing the paraffin tissue sections.

This work was supported by the following funding: NIH R01 HL097766-01 and Eli and Edythe Broad Center of Regenerative Medicine and Stem Cell Research at UCLA Innovation Award to H.K.A.M and TG2-01169 CIRM Type I Training Grant, the American Association of Obstetricians and Gynecologists Foundation Scholarship and the Specialty Training and Advanced Research (STAR) Training Fellowship at UCLA to L.K.L.

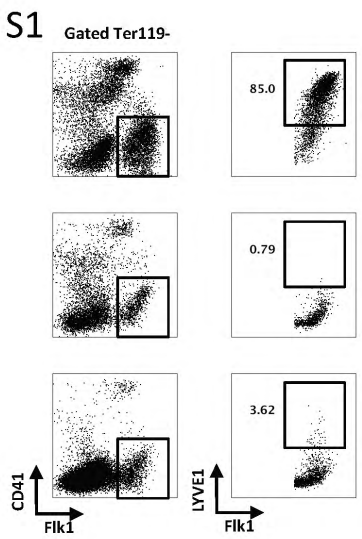

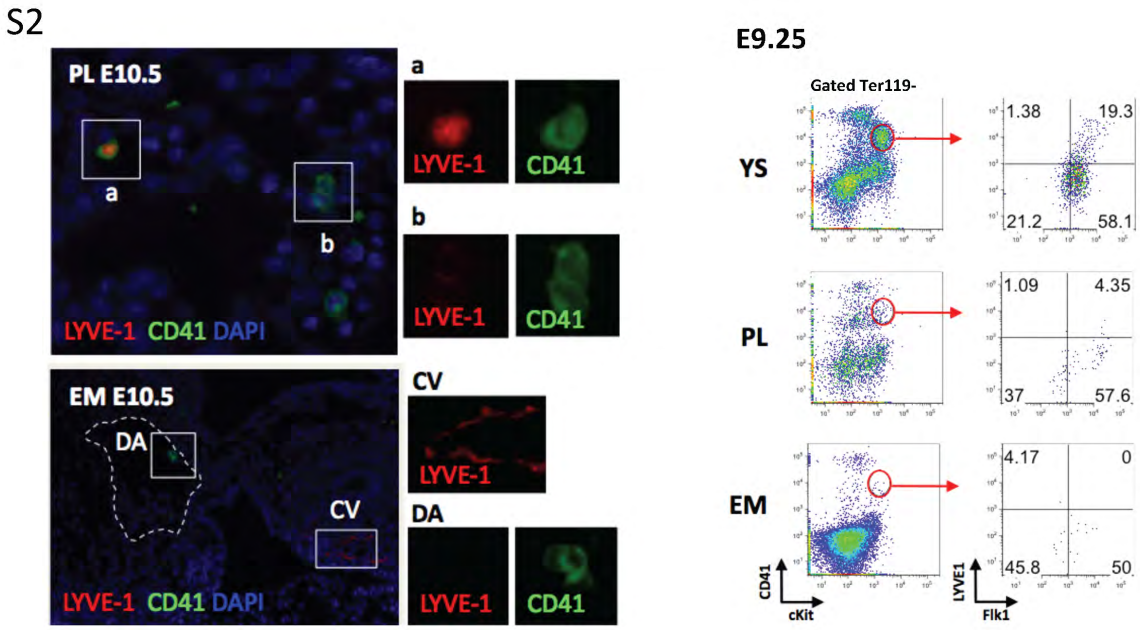

Figure S1. LYVE1 protein expression in the CD41^{-} Flk1^{+} endothelial compartment in the YS, PL and CH.

Figure S2. IF staining of CD41^{+} progenitors with and without co-expression of LYVE1 protein in placenta and dorsal aorta (DA). FACS plot of LYVE1 protein in HS/PC populations in the YS, PL and EM. Cardinal vein, CV.

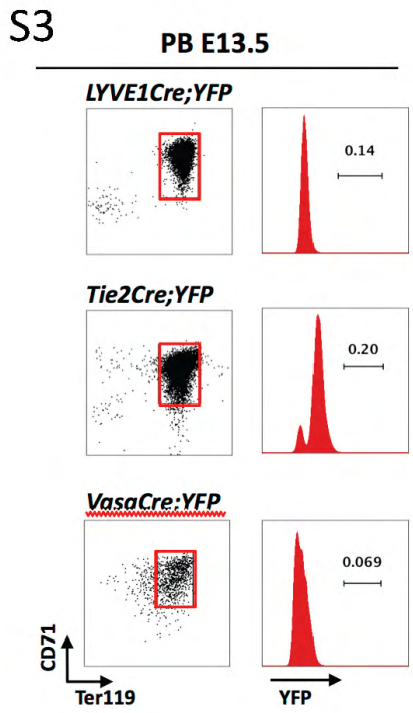

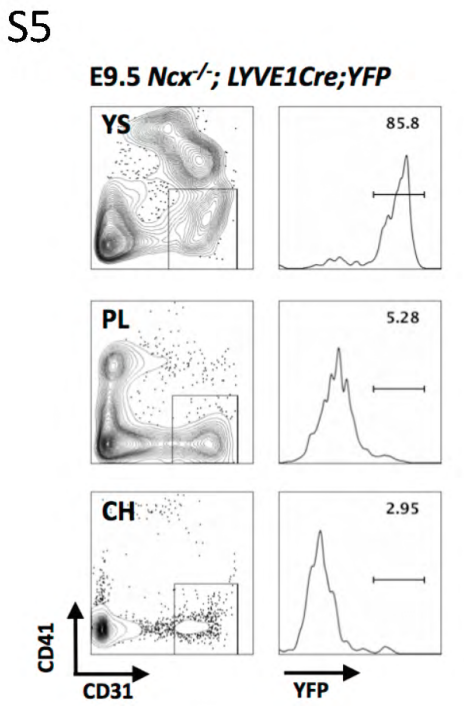

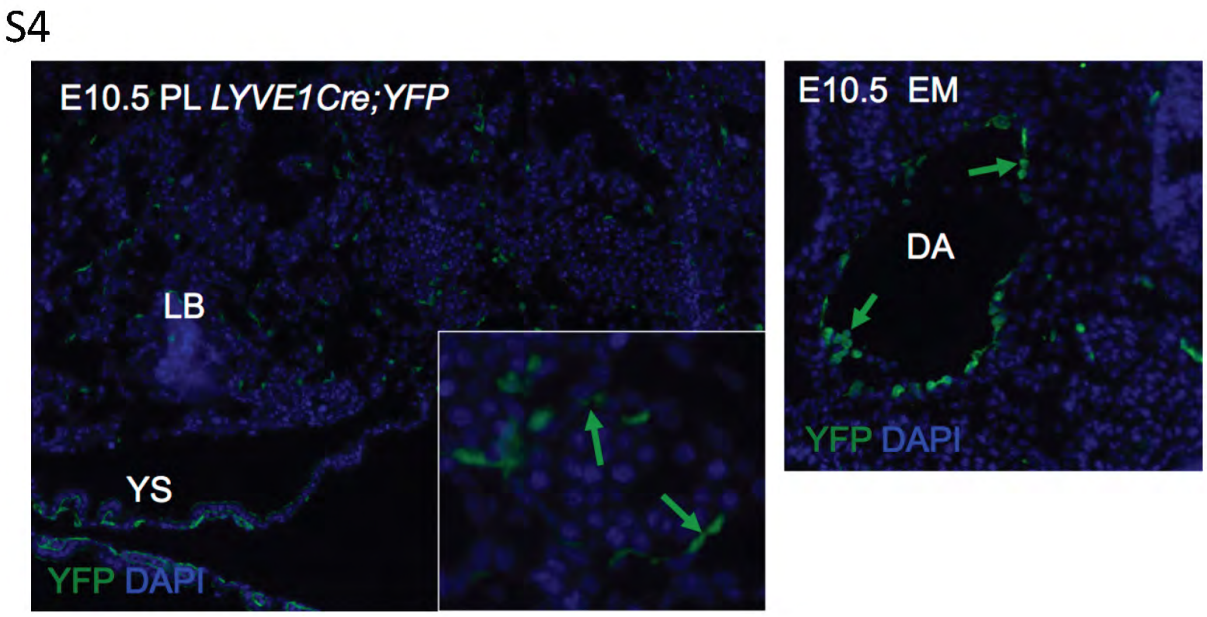

Figure S3. Silencing of YFP$^+$ marking from mature primitive erythroid cells in peripheral blood

Figure S4. Ectopic IF staining of YFP$^+$ cells lining the blood vessels in placenta and dorsal aorta at E10.5

Figure S5. LYVE1 protein expression in the CD41$^-$ Flk1$^+$ endothelial compartment in the Ncx null YS, PL and CH.

REFERENCES

Banerji, S., Ni, J., Wang, S. X., Clasper, S., Su, J., Tammi, R., Jones, M. and Jackson, D. G. (1999). LYVE-1, a new homologue of the CD44 glycoprotein, is a lymph-specific receptor for hyaluronan. *J Cell Biol* **144**, 789-801.

Bertrand, J. Y., Chi, N. C., Santoso, B., Teng, S., Stainier, D. Y. and Traver, D. Haematopoietic stem cells derive directly from aortic endothelium during development. *Nature* **464**, 108-11.

Boisset, J. C., van Cappellen, W., Andrieu-Soler, C., Galjart, N., Dzierzak, E. and Robin, C. In vivo imaging of haematopoietic cells emerging from the mouse aortic endothelium. *Nature* **464**, 116-20.

Chen, M. J., Yokomizo, T., Zeigler, B. M., Dzierzak, E. and Speck, N. A. (2009). Runx1 is required for the endothelial to haematopoietic cell transition but not thereafter. *Nature* **457**, 887-91.

Eilken, H. M., Nishikawa, S. and Schroeder, T. (2009). Continuous single-cell imaging of blood generation from haemogenic endothelium. *Nature* **457**, 896-900.

Ferkowicz, M. J., Starr, M., Xie, X., Li, W., Johnson, S. A., Shelley, W. C., Morrison, P. R. and Yoder, M. C. (2003). CD41 expression defines the onset of primitive and definitive hematopoiesis in the murine embryo. *Development* **130**, 4393-403.

Gazit, R., Mandal, P. K., Ebina, W., Ben-Zvi, A., Nombela-Arrieta, C., Silberstein, L. E. and Rossi, D. J. (2014). Fgd5 identifies hematopoietic stem cells in the murine bone marrow. *J Exp Med* **211**, 1315-31.

Gordon, E. J., Gale, N. W. and Harvey, N. L. (2008). Expression of the hyaluronan receptor LYVE-1 is not restricted to the lymphatic vasculature; LYVE-1 is also expressed on embryonic blood vessels. *Dev Dyn* **237**, 1901-9.

Haar, J. L. and Ackerman, G. A. (1971). A phase and electron microscopic study of vasculogenesis and erythropoiesis in the yolk sac of the mouse. *Anat Rec* **170**, 199-223.

Koushik, S. V., Wang, J., Rogers, R., Moskophidis, D., Lambert, N. A., Creazzo, T. L. and Conway, S. J. (2001). Targeted inactivation of the sodium-calcium exchanger (Ncx1) results in the lack of a heartbeat and abnormal myofibrillar organization. *FASEB J* **15**, 1209-11.

Lancrin, C., Sroczynska, P., Stephenson, C., Allen, T., Kouskoff, V. and Lacaud, G. (2009). The haemangioblast generates haematopoietic cells through a haemogenic endothelium stage. *Nature* **457**, 892-5.

McKinney-Freeman, S. L., Naveiras, O., Yates, F., Loewer, S., Philitas, M., Curran, M., Park, P. J. and Daley, G. Q. (2009). Surface antigen phenotypes of hematopoietic stem cells from embryos and murine embryonic stem cells. *Blood* **114**, 268-78.

Medvinsky, A. and Dzierzak, E. (1996). Definitive hematopoiesis is autonomously initiated by the AGM region. *Cell* **86**, 897-906.

Mikkola, H. K., Fujiwara, Y., Schlaeger, T. M., Traver, D. and Orkin, S. H. (2003a). Expression of CD41 marks the initiation of definitive hematopoiesis in the mouse embryo. *Blood* **101**, 508-16.

Mikkola, H. K., Klintman, J., Yang, H., Hock, H., Schlaeger, T. M., Fujiwara, Y. and Orkin, S. H. (2003b). Haematopoietic stem cells retain long-term repopulating activity and multipotency in the absence of stem-cell leukaemia SCL/tal-1 gene. *Nature* **421**, 547-51.

Mikkola, H. K. and Orkin, S. H. (2006). The journey of developing hematopoietic stem cells. *Development* **133**, 3733-44.

Montecino-Rodriguez, E. and Dorshkind, K. (2006). New perspectives in B-1 B cell development and function. *Trends Immunol* **27**, 428-33.

Morrison, S. J., Hemmati, H. D., Wandycz, A. M. and Weissman, I. L. (1995). The purification and characterization of fetal liver hematopoietic stem cells. *Proc Natl Acad Sci U S A* **92**, 10302-6.

Muller, A. M., Medvinsky, A., Strouboulis, J., Grosveld, F. and Dzierzak, E. (1994). Development of hematopoietic stem cell activity in the mouse embryo. *Immunity* **1**, 291-301.

Palis, J., Robertson, S., Kennedy, M., Wall, C. and Keller, G. (1999). Development of erythroid and myeloid progenitors in the yolk sac and embryo proper of the mouse. *Development* **126**, 5073-84.

Pham, T. H., Baluk, P., Xu, Y., Grigorova, I., Bankovich, A. J., Pappu, R., Coughlin, S. R., McDonald, D. M., Schwab, S. R. and Cyster, J. G. (2010). Lymphatic

endothelial cell sphingosine kinase activity is required for lymphocyte egress and lymphatic patterning. *J Exp Med* **207**, 17-27.

Porcher, C., Swat, W., Rockwell, K., Fujiwara, Y., Alt, F. W. and Orkin, S. H. (1996). The T cell leukemia oncoprotein SCL/tal-1 is essential for development of all hematopoietic lineages. *Cell* **86**, 47-57.

Rhodes, K. E., Gekas, C., Wang, Y., Lux, C. T., Francis, C. S., Chan, D. N., Conway, S., Orkin, S. H., Yoder, M. C. and Mikkola, H. K. (2008). The emergence of hematopoietic stem cells is initiated in the placental vasculature in the absence of circulation. *Cell Stem Cell* **2**, 252-63.

Schlaeger, T. M., Mikkola, H. K., Gekas, C., Helgadottir, H. B. and Orkin, S. H. (2005). Tie2Cre-mediated gene ablation defines the stem-cell leukemia gene (SCL/tal1)-dependent window during hematopoietic stem-cell development. *Blood* **105**, 3871-4.

Srinivas, S., Watanabe, T., Lin, C. S., William, C. M., Tanabe, Y., Jessell, T. M. and Costantini, F. (2001). Cre reporter strains produced by targeted insertion of EYFP and ECFP into the ROSA26 locus. *BMC Dev Biol* **1**, 4.

Van Handel, B., Montel-Hagen, A., Sasidharan, R., Nakano, H., Ferrari, R., Boogerd, C. J., Schredelseker, J., Wang, Y., Hunter, S., Org, T. et al. (2012). Scl represses cardiomyogenesis in prospective hemogenic endothelium and endocardium. *Cell* **150**, 590-605.

Zeigler, B. M., Sugiyama, D., Chen, M., Guo, Y., Downs, K. M. and Speck, N. A. (2006). The allantois and chorion, when isolated before circulation or chorio-allantoic fusion, have hematopoietic potential. *Development* **133**, 4183-92.

Zovein, A. C., Hofmann, J. J., Lynch, M., French, W. J., Turlo, K. A., Yang, Y., Becker, M. S., Zanetta, L., Dejana, E., Gasson, J. C. et al. (2008). Fate tracing reveals the endothelial origin of hematopoietic stem cells. *Cell Stem Cell* **3**, 625-36.

Zovein, A. C., Turlo, K. A., Ponec, R. M., Lynch, M. R., Chen, K. C., Hofmann, J. J., Cox, T. C., Gasson, J. C. and Iruela-Arispe, M. L. (2010). Vascular remodeling of the vitelline artery initiates extravascular emergence of hematopoietic clusters. *Blood* **116**, 3435-44.

CHAPTER 3

Dosage of Vascular Endothelial Growth Factor-A Is Critical for Multipotent Hematopoiesis

INTRODUCTION

Multipotent, self-renewing hematopoietic stem cells (HSCs) bestow bone marrow transplantations with their life-saving regenerative capacity. However, the quest to generate HSCs *in vitro* from induced pluripotent stem cells has so far yielded the production of progenitors with only restricted lineage potential. Hence, to overcome this hurdle, it will be critical to elucidate molecular mechanisms that distinguish the normal developmental programs that generate multipotent, hematopoietic cells from those that result in the lineage restricted hematopoietic counterparts.

During mammalian development, blood cells emerge in three distinct functional waves from segregated anatomical sites. The earliest embryonic hematopoietic cells arise from the yolk sac in a process called primitive hematopoiesis, which consists of the rapid production of mature hematopoietic cells (mainly erythroid cells that express unique embryonic globin chains) that can fulfill the immediate metabolic needs of the developing embryo (Mikkola and Orkin, 2006; Palis, 2008). Then follows a wave of progenitors with potential to differentiate into the myeloid and erythroid but not the lymphoid lineages. This wave is referred as transient-definitive hematopoiesis as the erythroid cells that emerge from these precursors are definitive, adult type; but incapable of self-renewal or repopulation of the recipient hematopoietic system upon transplantation. It is the subsequent and last wave, called definitive hematopoiesis, that arises from the placenta, the yolk sac

and the aorta-gonads-mesonephros (AGM) region in the embryonic caudal half and is responsible for the generation of the lifelong reservoir of HSCs in the bone marrow (Alvarez-Silva et al., 2003; de Bruijn et al., 2000; Gekas et al., 2005; Medvinsky and Dzierzak, 1996; Rhodes et al., 2008; Robin et al., 2009).

To understand how the hematopoietic waves diverge, it will be critical to pinpoint the precursors that give rise to the various cell types. The cellular origin of hematopoietic stem and progenitor cells (HS/PCs) had remained controversial for decades. However, recent studies using lineage tracing experiments as well as time-lapsed imaging of *in vivo* and *in vitro* hematopoietic emergence in mouse and zebrafish embryos demonstrated that a rare subset of highly specialized endothelial cells --now referred as hemogenic endothelium-- generates HS/PCs (Bertrand et al., 2010; Chen et al., 2009; Eilken et al., 2009; Lancrin et al., 2009; Zovein et al., 2008). Now, attention has turned to elucidate the molecular, cellular and developmental profiles of the hemogenic endothelium. Our group presented evidence that the stem cell leukemia (Scl/tal1) gene encodes for a critical transcription factor that provides hemogenic competence to endothelium by activating a broad hemato-vascular transcriptional program while repressing a competing cardiac fate (Van Handel et al., 2012). However, the mechanisms that establish multilineage differentiation ability in hemogenic endothelium and HSCs remain largely unknown.

Because the vascular endothelial growth factor-A (VEGF-A) plays a critical role in endothelial cell development and differentiation during the period when definitive hematopoiesis is established, we hypothesized that VEGF-A participates in

the specification and function of the hemogenic endothelium. VEGF-A is a potent secreted mitogen that binds with high affinity to two receptor tyrosine kinases, fms-related tyrosine kinase 1 (flt-1) and fetal liver kinase 1 (flk-1). VEGF-A signaling is critical for vasculogenesis and angiogenesis in embryonic and extra-embryonic tissues (Ferrara et al., 2003). Earlier reports revealed that genetic ablation of both or even a single *VEGF-A* allele caused marked vascular disruption in the dorsal aorta and yolk sac, resulting in embryonic lethality during midgestation (Carmeliet et al., 1996; Ferrara et al., 1996). These reports also suggested severely compromised hematopoiesis in the yolk sac, as the blood islands of *VEGF-A* deficient yolk sacs appeared devoid of primitive erythroblasts. However, developmental studies using *in vivo* mammalian models of VEGF-A deficiency have been far and few between because embryonic lethality posed significant methodological challenges. Embryonic lethality of the heterozygote required aggregation of *VEGF-A* mutant embryonic stem cells with wild-type tetraploid embryos in order to create embryos that were affected by a reduction in VEGF-A levels (Carmeliet et al., 1996; Ferrara et al., 1996). Hence, detailed *in vivo* studies of the hematopoietic perturbations during development have not been conducted.

Incorporating several unique mouse models of VEGF-A gene targeting, we document that proper VEGF-A dosage is critical for vascular remodeling and generating multipotent HS/PCs in embryonic hemogenic tissues. Our data support the fact that VEGF-A haploinsufficiency is able to establish primitive erythropoiesis and generate transient myelo-erythroid progenitors from the yolk sac. Moreover,

we discover a new cellular source of VEGF-A in placental trophoblasts that is important for angiogenesis and hematopoiesis in distant hemogenic organs as well.

RESULTS

Vasa-Cre intercross with *VEGF-A*$^{fl/wt}$ mice is a robust model for VEGF-A haploinsufficiency

To overcome the previously encountered experimental hurdles of generating *VEGF-A* heterozygous embryos, we established a robust *in vivo* model of global *VEGF-A* haploinsufficiency by interbreeding *VEGF-A*$^{fl/wt}$ mice with a germline *Cre* deleter. The germ cell specific Vasa-Cre is active in the egg at the time of fertilization, enabling germline excision of the *VEGF-A* gene and generation of concepti with *VEGF* heterozygocity in all cells (Gallardo et al., 2007). *Vasa-Cre;VEGF*$^{fl/wt}$ mutants displayed marked embryonic growth restriction and developmental delay at embryonic day 9.5 (E9.5), and lethality followed within a day (Fig. 1A). Of note, hypocellularity preceded gross findings, in particular, in the embryonic caudal half (Fig. 1B). Vascular disruptions were prominent in both embryonic and extra-embryonic tissues. The embryo had pericardiac effusion and the umbilical vessels appeared congested, while the yolk sac lacked well-defined red
cell-filled vascular branches (Fig. 1C). Whole mount staining of E9.5 embryo and yolk sac with anti-PECAM1 showed enlarged vessels and persistent plexuses,

consistent with immature vascular remodeling (Fig. 1D). In the placenta, the intricate intertwining of fetal blood vessels with maternal blood spaces was absent in the heterozygous mutants, giving the appearance of trophoblast crowding. Such appearance could be contributed in part by the severe reduction in fetal blood vessels as shown by immunohistochemistry with anti-PECAM1 (Fig. 1E). Taken together, the findings of the *Vasa-Cre;VEGF*$^{fl/wt}$ mutants mirrored characteristics of previously published models of VEGF-A haploinsufficiency.

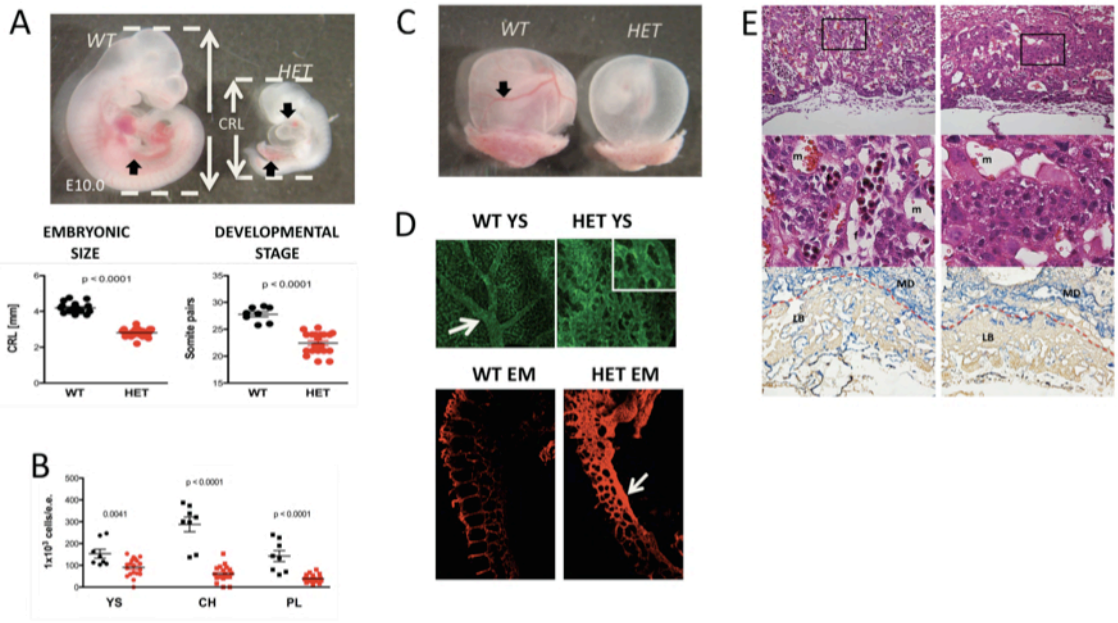

Figure 1. *VasaCre;VEGF*$^{fl/wt}$ heterozygote, a novel model for *VEGF-A* haploinsufficiency
(A) Gross morphology, size and developmental stage of heterozygous versus control embryos. CRL, crown-rump-length (B) Cellularity of each hemogenic organ at E9.25. (C) Gross morphology of yolk sac at E10.0. (D) Whole mount staining of yolk sac and embryo against pan-vascular marker PECAM1. (E) H&E stain and immunohistochemistry analysis of PECAM1 in placenta at E10.0.

VEGF-A haploinsufficiency does not disrupt primitive erythropoiesis

Prior studies had reported that hematopoiesis in *VEGF* heterozygous yolk sacs was markedly impaired (Carmeliet et al., 1996; Ferrara et al., 1996). *Vasa-Cre;VEGF$^{fl/wt}$* yolk sacs at E10.5 appeared pale on gross morphology and contained only rare hematopoietic cells on histologic screening (Fig. 1C, 2A). However, we observed nucleated cells with hematopoietic morphology in the corresponding placenta. To identify these cells, we performed immunofluorescence (IF) staining, which confirmed the presence of Ter119^{+} and βH1 globin expressing primitive erythroid cells in the VEGF-A haploinsufficient placenta (Fig. 2A). Flow cytometry analysis indicated that both the mutant yolk sac and placenta at E9.25 contained Ter119^{+} primitive erythroid cells, albeit at reduced levels. (Fig 2B)

To determine whether the production of primitive erythroid precursors was compromised in the yolk sac, we assayed the clonogenic potential of the yolk sac at E7.5 and E8.5, which comprise the developmental period when the primitive erythroid precursors can be found in the conceptus (Haar and Ackerman, 1971; Palis et al., 1999). VEGF-A haploinsufficiency did not affect the potential of the yolk sac to form primitive erythroid colonies (EryP-CFC) (Fig. 2C). Next, given the accumulation of primitive erythroblasts in the mutant placenta, we evaluated whether the placenta was capable of ectopic generation of primitive erythroid progenitors. We submitted the allantois --which eventually gives rise to the vasculature of the placenta-- to the colony-forming assay prior to the chorioallantoic

fusion. EryP-CFC colonies could not be obtained from either wild-type or mutant allantois, providing evidence that the primitive erythroid progenitors found in the placenta are not ectopically generated.

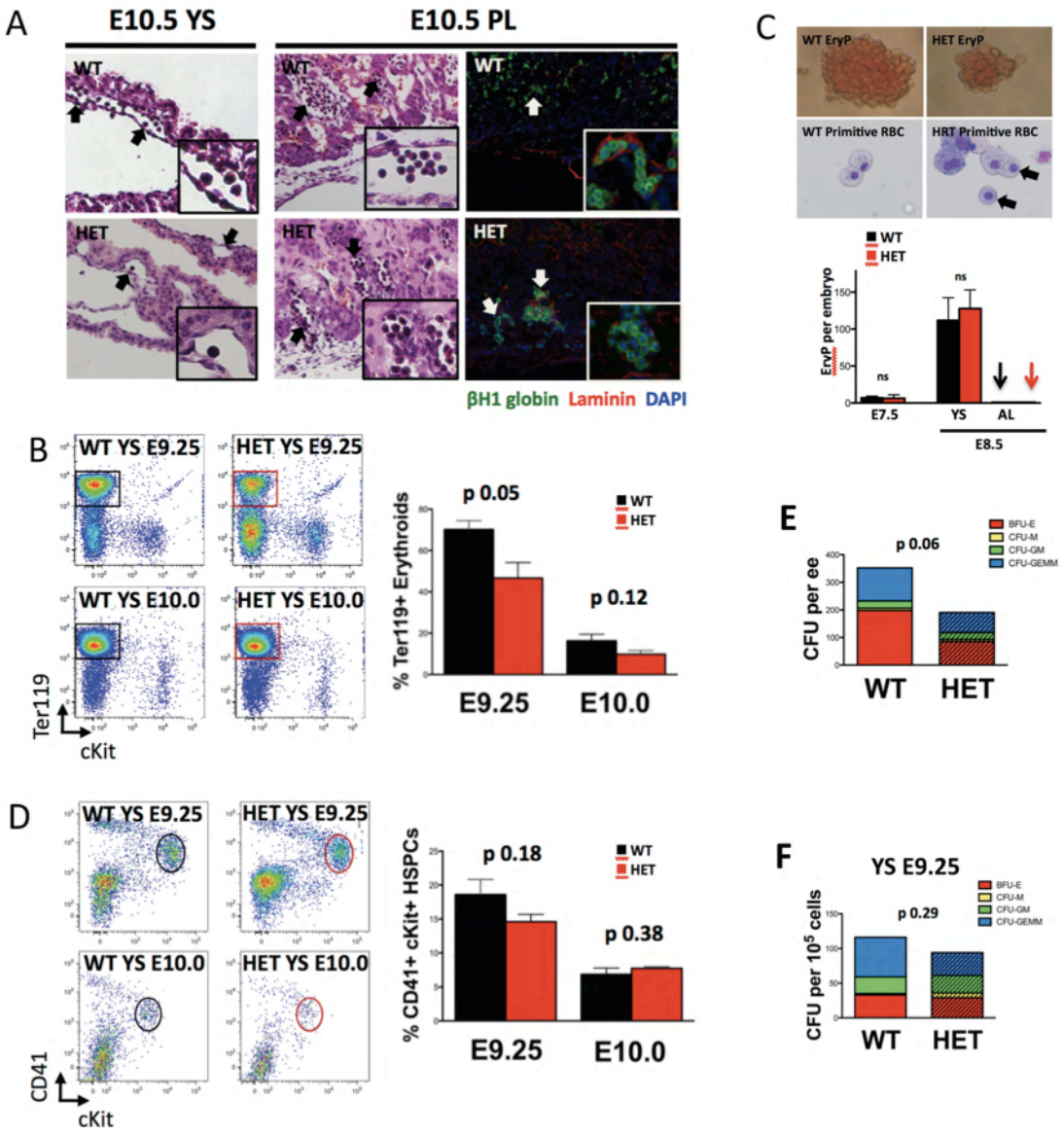

Figure 2. Effects of VEGF-A haploinsufficiency in hematopoietic waves
(A) H&E histology of wild-type and heterozygous yolk sac and placenta at E10.5. IF staining of βH1 globin expressing primitive erythroid cells in placenta. All arrows point to the erythroid cells. (B) FACS plot and quantification of primitive erythroid population in yolk sac at E9.25 and at E10.0. (C) EryP colony and corresponding May-Grünwald-Giemsa stain of primitive erythroid cells (see arrow). Quantification of EryP colonies from entire conceptus at E7.5 and from yolk sac versus allantois (AL). (D) FACS plot and quantification of of definitive HS/PCs in yolk sac at E9.25 and E10.0 (E) Yolk sac's clonogenic potential counted per embryo equivalent (ee). CFU, colony forming units (F) Yolk sac's clonogenic potential counted per number of cells seeded.

VEGF-A haploinsufficiency does not perturb the generation of transient myeloerythroid progenitors in the yolk sac

We next evaluated the requirement of VEGF-A in transient-definitive hematopoiesis. In the yolk sac, the fractions of CD41 and cKit expressing nascent HS/PCs were not significantly decreased either before or after gross abnormalities became evident, that is, at E9.25 and E10.0, respectively (Fig 2D). There was a slight reduction in the number of myeloerythroid colonies formed per embryo-equivalent by E9.5 heterozygous yolk sac (116 ± 16.7 total wild-type CFUs to 95.3 ± 10.5 total mutant CFUs) (Fig. 2E). However, comparable numbers and types of progenitor colonies were counted when the same number of dissociated cells was seeded (Fig 2F). These data provided evidence that *VEGF-A* heterozygocity is sufficient to support the formation of transient myeloerythroid progenitors in the yolk sac.

Dosage of VEGF-A is critical for establishing HS/PCs with lymphoid lineage differentiation capacity

We evaluated the requirement of VEGF-A for hematopoiesis in the placenta and the embryonic caudal half, which are sites of *de novo* generation of multipotent HS/PCs (Barcena et al., 2009; Rhodes et al., 2008; Zeigler et al., 2006). FACS analysis of $CD41^{+}cKit^{+}$ HS/PC fractions did not reveal a significant decrease of this subpopulation in these organs at E9.25 and E10.0. However, unlike the yolk sac, the placenta did show a significant reduction in the number of colonies (from 33 ± 13

total wild-type CFUs to 2 ± 1.4 total heterozygous CFUs) even when equivalent number of cells had been plated (Fig. 2G). This defective placental hematopoiesis was not due to a delay in development as the heterozygotes and controls were indistinguishable in somite-pair count and gross morphology. Only few colonies were able to grow from the caudal halves of both mutant and wild-type littermates at E9.25.

Because progenitors with restricted myeloerythroid potential and multipotent HSCs cannot be separated at this stage based on known cell surface markers or colony-forming ability, we used the OP9 and OP9-DL1 *in vitro* lymphoid assays to help distinguish the two waves of definitive hematopoiesis (Schmitt et al., 2004). In contrast to the tissues with intact VEGF-A levels, haploinsufficient E10.5 yolk sac, placenta and caudal half could not produce any $CD19^{+}B220^{+}$ B lymphoid cells on OP9 stroma co-culture. Likewise, generation of $CD4^{+}CD8^{+}$ T lymphoid cells in OP9-DL1 stroma was completely abolished in VEGF-A haploinsufficient E9.5 hemogenic tissues (Fig. 2H). These results imply that *VEGF-A* heterozygous tissues cannot specify HS/PCs with full myelo-lymphoid differentiation ability, a key property of definitive HSCs.

Hemogenic tissues have multiple cellular sources of VEGF during development

As VEGF-A/Flk1 signaling is crucial for vascular development during embryogenesis, others have previously described the patterns of VEGF-A expression

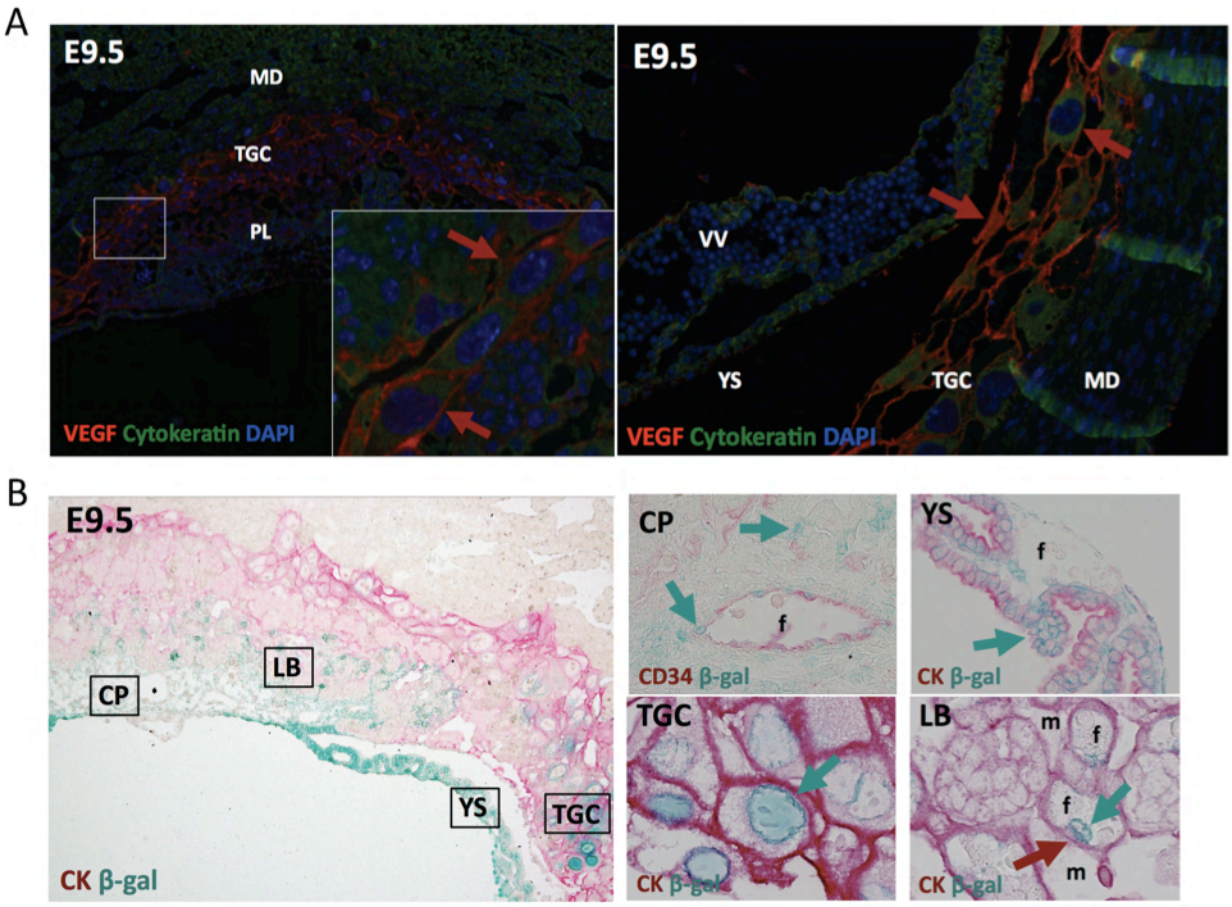

Figure 3. Localization of VEGF protein and VEGF-A/LacZ
(A) IF staining of wild-type E9.5 placenta against VEGF-A. MD, maternal decidua; TGC, trophoblast giant cell; PL, placenta; VV, vitelline vessels. (B) β-gal costained with trophoblast marker cytokeratin (CK). CP, chorionic plate; LB, labyrinth; YS, yolk sac. In the inset, the arrows point to cells expressing β-gal.

in the AGM region and the yolk sac . However, the precise cellular source for the VEGF-A ligand required for hemato-vascular development has not been verified at the molecular level. Moreover, despite the fact that the placenta is now recognized as being capable of generating and expanding multipotent HS/PCs, which cells supply the VEGF-A ligand to the Flk1^{+} hemogenic endothelium in the placenta remain poorly characterized. To delineate the cellular sources of VEGF-A in the placenta, we first screened E9.5 wild-type placentas for VEGF-A protein expression using immunofluorescence. As previously reported, VEGF-A activity was observed in the yolk sac visceral endoderm as well as the parietal trophoblast giant cells (TGC) that wrap the yolk sac during midgestation. The TGC cells located between the spongiotrophoblast layer and the maternal decidua also robustly expressed VEGF (Fig. 3A).

To verify that *VEGF-A* gene regulatory regions are active in the cells where the VEGF-A protein is found, we performed beta-galactosidase (β-gal) staining in hemogenic organs of *VEGF-LacZ* knockin mice (Miquerol et al., 1999). Within E9.25 hemogenic tissues, β-gal activity could be appreciated in three distinct extraembryonic hemogenic niches: the chorionic plate and the labyrinth in the placenta, as well as the yolk sac (Fig 3B). Credited to host the potential to generate HSCs *de novo* from its large fetal blood vessels (Rhodes et al., 2008), the chorionic plate contained chorioallantoic mesenchymal cells that stained for β-gal. On the other hand, β-gal activity could be appreciated in the trophoblasts surrounding the small fetal vessels within the labyrinth, which harbor highly proliferative HS/PCs. As

previously reported, β-gal staining was detected in the yolk sac's visceral endoderm and mesoderm. These cells are adjacent to the yolk sac's hemogenic endothelium.

Autocrine VEGF-A signaling in hemato-vascular cells is not critical for HSC development

Postnatal endothelial cells express VEGF and their autocrine VEGF signaling in VE-Cadherin expressing endothelial cells is required for vascular homeostasis in adult life (Lee et al., 2007). To examine whether an autocrine mechanism is also required for specification or function of the hemogenic endothelium during development, we ablated VEGF exclusively from the vascular endothelial cells and their progeny (including hematopoietic cells) by crossing *Tie2-Cre* transgenic males with $VEGF^{fl/fl}$ females. As the *Tie2-Cre;*$VEGF^{fl/wt}$ heterozygous offsprings survived to adulthood, we further interbred *Tie2-Cre;*$VEGF^{fl/wt}$ with $VEGF^{fl/fl}$ and generated conditional null concepti (Fig 4A). These hemato-vascular cell specific VEGF-A mutants also survived to 6 months of age without obvious differences in their peripheral red blood cell, white blood cell and platelet count profiles (Fig. 4B).

To assess for the presence of a transient hemato-vascular deficiency that could have resolved prior to birth, we evaluated the midgestation concepti. No gross abnormalities in the yolk sac or embryo were evident (Fig. 4C). IF co-staining for endothelial cell marker CD34 and trophoblast cell marker cytokeratin did not show perturbations in the overall architecture of the *Tie2-Cre;*$VEGF^{fl/fl}$ null placenta at

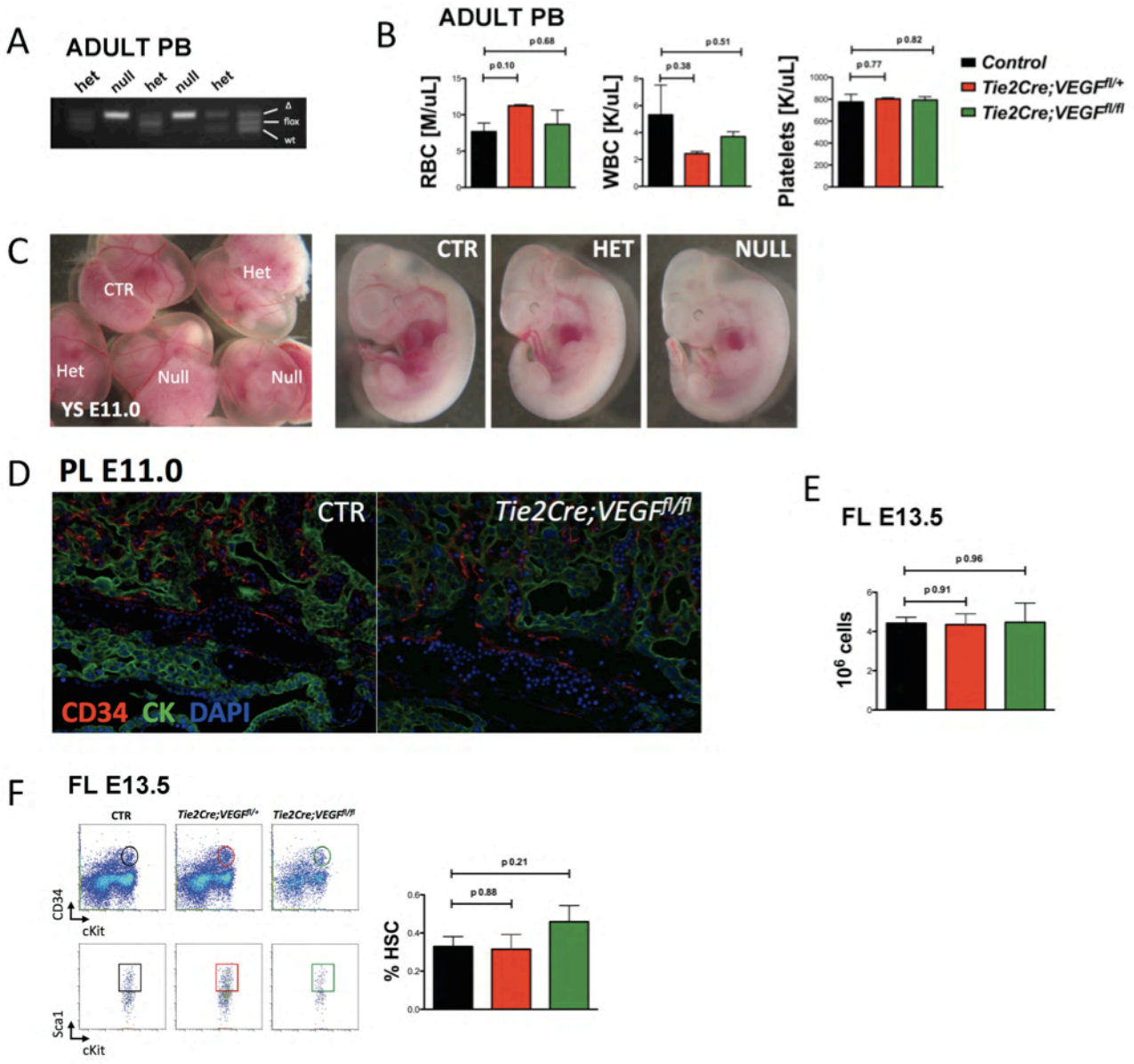

Figure 4. Requirement of hemato-vascular source of VEGF-A

(A) PCR genotyping of peripheral blood from mutant adults. (B) Complete blood count of adult peripheral blood. RBC, red blood cells; WBC, white blood cells. (C) Gross morphology of yolk sac and embryos at E11.0. (D) IF staining for placental vasculature. (E) Fetal liver cellularity at E13.5. (F) FACS plot and quantification of HS/PC population in E13.5 fetal liver.

E11.0 (Fig. 4D). Fetal liver cellularity at E13.5 was comparable between the genotypes ($4x10^6 \pm 2.6x10^6$ cells in null, $3.4\ x10^6 \pm 0.3x10^6$ cells in heterozygous, and $1.7\ x10^6 \pm 1.9x10^6$ cells in wild-type controls) (Fig. 4E). The $Sca1^+cKit^+CD34^+$ HSC compartment in the fetal liver was also unaffected at this stage (Fig. 4F). These findings indicated that autocrine VEGF signaling in Tie2-Cre expressing cells and their progeny is not required during development.

Mesodermal VEGF-A has minimal function in hemato-vascular development during embryogenesis

Since β-gal staining analysis demonstrated *VEGF-lacZ* activity in the allantois as well as the chorioallantoic mesenchyme, we asked whether VEGF-A generated in early mesodermal cells and their derivatives regulated specification of the hemogenic endothelium and thus HS/PC development. Hence, we intercrossed $VEGF^{fl/wt}$ with *Mesp1-Cre* mice and deleted one *VEGF* allele from Mesp1-expressing mesoderm. *Mesp1-Cre* becomes active during early gastrulation and can excise the floxed sequence earlier and in a broader spectrum of mesoderm-derived tissues than *Tie2-Cre* (Saga et al., 1999). By E10.5, the *Mesp1-Cre;*$VEGF^{fl/wt}$ mutants demonstrated no obvious abnormalities in embryonic growth and development, gross morphology or vascular remodeling in the yolk sac (Fig. 5A). FACS analysis did not reveal any defect in the $Ter119^+$ erythroid cell or $CD41^+cKit^+$ HS/PC fractions in any of the hematopoietic tissues (Fig. 5B). Myeloerythroid clonogenic potential was also unaffected in all organs at E9.5 (Fig. 5C). Finally, *Mesp1-Cre;*$VEGF^{fl/wt}$ tissues

could produce $CD4^+CD8^+$ T cells after 21 days of OP9-DL1 co-culture, albeit at lower percentages than the control littermates for the placenta (Fig. 5D). Taken together, this data indicated that reduction of mesoderm-derived VEGF-A to half doses does not compromise embryonic hematopoiesis or vasculogenesis. However, whether it reduces the efficiency to generate multipotent HS/PCs in the placenta requires further investigation.

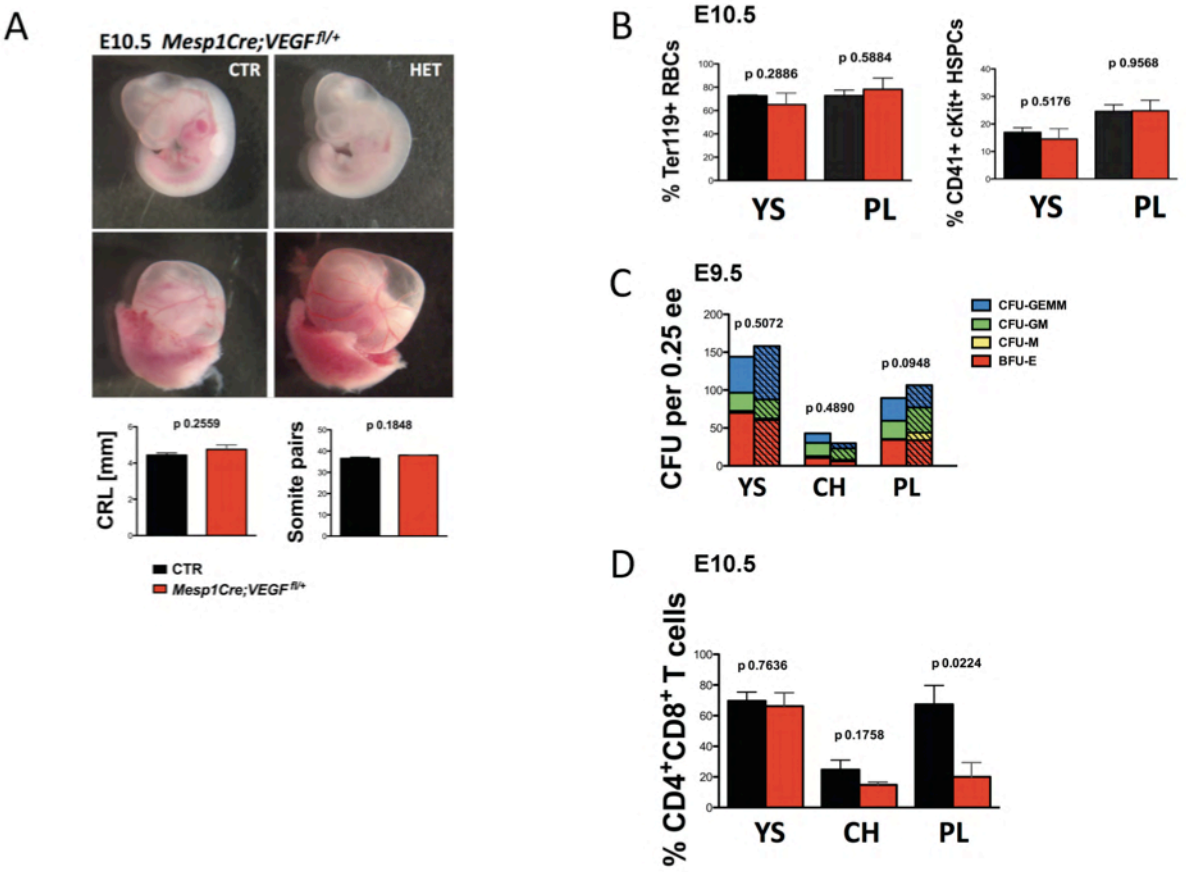

Figure 5. Mesoderm-specific VEGF-A haploinsufficiency
(A) Gross morphology of embryos and yolk sac. Embryonic size and developmental stage. (B) FACS plot and quantification of primitive erythroid cells in the yolk sac and placenta at E10.5. (C) Colony forming units from each hemogenic tissue at E9.5. (D) T lymphoid cells from OP9-DL1 co-culture.

Trophoblasts constitute a critical source of VEGF-A for not only the placenta but also distant organs

During the critical period of specification of hemogenic endothelium and HS/PCs, β-gal and VEGF-A immunostaining predominantly colored the trophoblasts. To dissect the exclusive contribution of trophoblasts in VEGF-A signaling, we used a novel lentiviral Cre-based technique of gene manipulation that inactivates a gene of interest specifically from the trophoblast compartment without disturbing other extra-embryonic tissues or any of the embryonic-derived tissues (Georgiades et al., 2007). We obtained trophoblast-specific *VEGF* heterozygous and null mutants by infecting the trophectoderm of E3.5 blastocysts from *VEGF* $^{fl/wt}$ intercrosses with the lentiviral vector encoding for *GFP-Cre* (referred as LV-Cre hereafter). Because the trophectoderm gives rise to trophoblasts only, lentiviral transduction resulted in green fluorescence protein (GFP) expression confined to trophoblast cell lineages. On the other hand, GFP was absent in all derivatives of the inner cell mass, namely, the yolk sac, the allantoic vasculature of the placenta, the HS/PCs and the embryo (Fig. 6A). Trophoblast-specific VEGF-A mutant embryos at E9.5 appeared growth-restricted and developmentally delayed compared to controls (Fig. 6B). No embryos with loss of either one or both *VEGF* alleles from trophoblasts survived beyond the 26 somite-pair stage. Whole mount of trophoblast-specific VEGF-A haploinsufficient yolk sacs using PECAM1 antibody demonstrated enlarged capillary plexus without remodeling (Fig. 6C). In brief, *LV-Cre;VEGF*$^{fl/wt}$ and *LV-Cre;VEGF*$^{fl/fl}$ recapitulated the

phenotypes of the Vasa-Cre mediated global VEGF-A inactivation. Altogether, these data identify the placental trophoblasts as a critical source for VEGF-A ligand that is essential for embryonic survival, and required for proper hemato-vascular development also in distant organs.

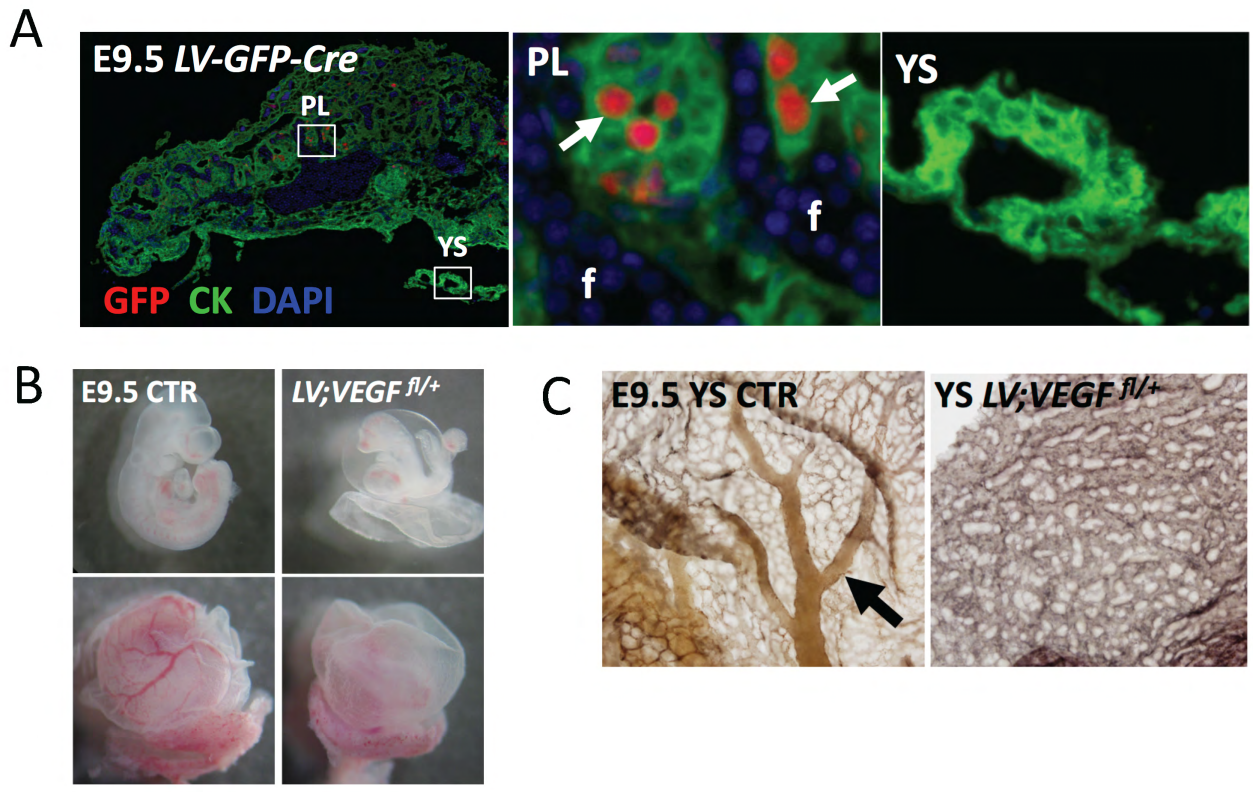

Figure 6. Trophoblast-derived VEGF-A
(A) IF staining of placenta and yolk sac against GFP (arrows). F, fetal circulation. (B) Gross morphology of embryo and yolk sac at E9.5. (C) Whole mount of yolk sac against PECAM1 vascular marker.

DISCUSSION

Despite the essential requirement of VEGF-A for embryonic survival, its role in development has been inferred mostly from *in vitro* or non-mammalian studies. Here, using the Cre/loxP recombination with a germline deleter mouse strain, we expand the scope of current understanding with *in vivo* observations.

First, we present evidence for VEGF-A dose dependent effects in regulating the different hematopoietic waves. To our surprise and contrasting previous reports, VEGF-A deficiency from the loss of one *VEGF-A* allele was sufficient to support the lineage-restricted primitive and transient-definitive waves. But deletion of both alleles resulted in the loss of all myeloerythroid colony-forming progenitors (Lee, Mikkola, unpublished data 2013), indicating that VEGF-A is indispensable for definitive hematopoiesis. On the other hand, the HS/PCs with lymphoid lineage potential were completely eliminated in the heterozygous tissues, suggesting that the tightly regulated VEGF-A dosage determines hematopoietic fate. Our findings thus far cannot ascertain whether the unequivocal eradication of the lymphoid potential has resulted because VEGF-A plays a pivotal role in lymphoid differentiation, HS/PC specification and/or survival, or hemogenic endothelial specification and/or survival. However, as evidence from zebrafish studies have indicated that VEGF-A up-regulates Notch signaling, which is important in determining arterial cell fate (Lawson and Weinstein, 2002), further studies to confirm that this molecular network is conserved in mice and directs the fate of arterial hemogenic endothelium are needed.

Fetal survival and hematopoies do not depend on or at least end an autocrine VEGF-A requirement in HSC or hemogenic endothelium by the time Tie2-Cre is activated. Then, if cell intrinsic VEGF-A is dispensable for hematopoiesis during development, the exogenous sources of VEGF-A from the hematopoietic niches must account for the lethal defects. In the yolk sac, VEGF-A is expressed in the extra-embryonic visceral endoderm and mesoderm in proximity with the hemogenic endothelium (Miquerol et al., 1999). When VEGF-A expression is depleted from all tissues except in the yolk sac visceral endoderm, the hematopoietic and vascular compartments near intact VEGF-A secretion can be adequately established but the embryo proper cannot be rescued (Damert et al., 2002). Consistent with the limited role of yolk sac derived ligand, the VEGF-A deficient embryo died at midgestation despite aggregation with wild-type embryos, which results in normal VEGF-A expression in not only yolk sac endoderm but also all trophoblast lineages (Ferrara et al., 1996). Hence, although the placenta was previously thought to be a minor source of VEGF-A, our findings from trophoblast-specific *VEGF-A* deletion reveal that the trophoblast compartment is a vital player and that the yolk sac and embryonic sources of VEGF-A are insufficient to support their local hemogenic niches and/or vascularization.

The precise trophoblast cell types that supply VEGF-A have not been well characterized. Previous published reports indicated that after gastrulation, VEGF-A is expressed in the parietal trophoblast giant cells that encircle the conceptus. During midgestation, the VEGF-A ligand was located in the trophoblast giant cells

that wraps around the yolk sac as well as those that reside in the spongiotrophoblast layer. The expression of VEGF-A as assessed by the transcription of *lacZ* under the control of *VEGF-A* promoter resides though in the trophoblasts of the labyrinthine region, which contains the niche for HS/PC proliferation. Since the placenta harbors 15-fold more HSCs than any other organ generating them (Gekas et al., 2005) and VEGF-A acts primarily in a paracrine fashion, we suspect that these trophoblasts comprise the immediate source of VEGF-A for HS/PC development in the placenta. Hence, further understanding of the unique properties of the trophoblasts and other niche cells in the placenta will be instrumental to produce transplantable HSCs in culture.

MATERIALS AND METHODS

Mouse models. *VasaCre* (Gallardo et al., 2007) heterozygous females were obtained from the Jackson laboratory and intercrossed with $VEGF^{fl/wt}$ males (Gerber et al., 1999). Similar breeding strategies were used for *Tie2Cre;* $VEGF^{fl/wt}$ concepti. *Ncx1* heterozygous mice for knockout experiments were obtained from (Koushik et al., 2001). Trophoblast-specific *VEGF-A* deletion was obtained by microinjecting a lentivirus vector expressing Cre-GFP under the zona pellucida of E3.5 blastocysts derived from $VEGF^{fl/wt}$ intercrosses. These blastocysts were transferred into wild-type pseudo-pregnant females. Timed matings were performed and the noon of the day of vaginal plug was recorded as embryonic day 0.5 (E0.5). Mice were maintained according to protocols of Animal Research Committee at the University of California, Los Angeles.

Preparation of tissue sections. After isoflurane-induced anesthesia, mice were sacrificed by cervical dislocation. Fetal hematopoietic organs were dissected and fixed in 4% paraformaldehyde at 4° C for 4-6 hours, followed by 30% sucrose in PBS solution overnight, 1:1 30% sucrose:OCT (Tissue-Tek, Electron Microscopy Sciences) for 1 hour at 4° C, and finally embedded and frozen in 100% OCT. Frozen sections were cut at 5-7 μm with a Leica CM3050 S cryostat. For paraffin-embedded blocks, tissues were fixed in 4% paraformaldehyde at 4° C overnight and processed by standard protocol at the Tissue Procurement and Histology Core Laboratory of the Pathology and Laboratory Medicine at UCLA. Paraffin sections were cut at 5 μm.

Immunostaining. Fixed frozen and paraffin-embedded sections were prepared and immunostained as described elsewhere (Rhodes et al., 2008) but using the following antibodies: VEGF (1:200; Abcam), Ter119 (1:500, BD Pharmingen), β-globin (1:100; gift from Palis lab), CD34 (1:200; eBiosciences), cytokeratin (1:1000; Dako). Biotinylated secondary antibodies (1:500; Vector) and Tyramide Signal Amplification kit (PerkinElmer) were used as directed by manufacturer's protocol. Immunofluorescent images were obtained on a Zeiss Axio Imager.A1 with a Zeiss Axiocam MRm camera or a Zeiss LSM 510 microscope equipped with 405 nm, 488 nm, 543 nm, and 633 nm lasers. Whole mount staining was performed using purified CD31 antibody (1:600; BD Pharmingen) and imaged using the confocal Zeiss LSM 510.

Flow cytometry. Tissues were dissociated with collagenase (Worthington), DNase (Qiagen) and dispase (Invitrogen) at 37° C for 20 minutes. Cells were stained with rat anti-mouse monoclonal antibodies against Ter119, CD71, CD41, cKit, Sca1, CD31, and flk1 (all from BD Biosciences or eBiosciences). Dead cells were excluded with DAPI. Cells were assayed on a Becton Dickinson Biosciences LSRII or Fortessa flow cytometer and data was analyzed with FlowJo software (Tree Star Inc.).

Clonogenic progenitor assay. Methylcellulose colony-forming assays were performed as described previously (Chhabra et al., 2012). Briefly, single cell suspension was plated in MethoCult 3434 (Stem Cell Technologies) supplemented with TPO (PeproTech) and colonies were enumerated in 5-7 days. Clustering of 30 or more cells were defined as one

colony. Colonies were imaged using a Canon PowerShot G6 camera connected to Zeiss Axiovert 40 CFL microscope.

Complete blood cell count. Peripheral blood from the tail was collected into heparinized tubes and submitted to the Division of Laboratory Animal Medicine at UCLA for analysis using Humavet Interface.

Lymphoid cultures. Fetal organ explants or their dissociated single cell suspensions were cocultured on mouse OP9 or OP9-DL1 stromal cells (Schmitt et al., 2004) in 24-well plates as previously described (Rhodes et al., 2008).

Statistical analysis. Mathematical analysis and statistics were performed using GraphPad Prism Software. P values and data reported as mean ± SEM were calculated using the Student's unpaired two-tailed t tests.

ACKNOWLEDGMENTS

We thank Akanksha Chhabra, Vincenzo Calvanese and Luisa Iruela-Arispe for scientific discussions. We thank James Palis for providing us with β-globin antibody, Juan Zúñiga-Pflücker for the OP9-DL1 stroma line, Andreas Nagy for the VEGF-lacZ knockin mouse, Felicia Codrea and Jessica Scholes at the Flow Cytometry Core Laboratory at the Broad Center of Regenerative Medicine and Stem Cell Research at UCLA for flow cytometry, UCLA Translational Pathology Core Laboratory for preparing the paraffin tissue sections,

Ying Wang and Meisheng Jiang at Molecular and Medical Pharmacology Department for trophoblast-specific gene targeting, and the UCLA Division of Laboratory Medicine for blood analysis.

This work was supported by the following funding sources: NIH R01 HL097766-01 and Eli and Edythe Broad Center of Regenerative Medicine and Stem Cell Research at UCLA Innovation Award to H.K.A.M and TG2-01169 CIRM Type I Training Grant, the American Association of Obstetricians and Gynecologists Foundation Scholarship and the Specialty Training and Advanced Research (STAR) Training Fellowship at UCLA to L.K.L.

REFERENCES

Alvarez-Silva, M., Belo-Diabangouaya, P., Salaun, J. and Dieterlen-Lievre, F. (2003). Mouse placenta is a major hematopoietic organ. *Development* **130**, 5437-44.

Barcena, A., Kapidzic, M., Muench, M. O., Gormley, M., Scott, M. A., Weier, J. F., Ferlatte, C. and Fisher, S. J. (2009). The human placenta is a hematopoietic organ during the embryonic and fetal periods of development. *Dev Biol* **327**, 24-33.

Bertrand, J. Y., Chi, N. C., Santoso, B., Teng, S., Stainier, D. Y. and Traver, D. (2010). Haematopoietic stem cells derive directly from aortic endothelium during development. *Nature* **464**, 108-11.

Carmeliet, P., Ferreira, V., Breier, G., Pollefeyt, S., Kieckens, L., Gertsenstein, M., Fahrig, M., Vandenhoeck, A., Harpal, K., Eberhardt, C. et al. (1996). Abnormal

blood vessel development and lethality in embryos lacking a single VEGF allele. *Nature* **380**, 435-9.

Chen, M. J., Yokomizo, T., Zeigler, B. M., Dzierzak, E. and Speck, N. A. (2009). Runx1 is required for the endothelial to haematopoietic cell transition but not thereafter. *Nature* **457**, 887-91.

Chhabra, A., Lechner, A. J., Ueno, M., Acharya, A., Van Handel, B., Wang, Y., Iruela-Arispe, M. L., Tallquist, M. D. and Mikkola, H. K. (2012). Trophoblasts regulate the placental hematopoietic niche through PDGF-B signaling. *Dev Cell* **22**, 651-9.

Damert, A., Miquerol, L., Gertsenstein, M., Risau, W. and Nagy, A. (2002). Insufficient VEGFA activity in yolk sac endoderm compromises haematopoietic and endothelial differentiation. *Development* **129**, 1881-92.

de Bruijn, M. F., Speck, N. A., Peeters, M. C. and Dzierzak, E. (2000). Definitive hematopoietic stem cells first develop within the major arterial regions of the mouse embryo. *EMBO J* **19**, 2465-74.

Eilken, H. M., Nishikawa, S. and Schroeder, T. (2009). Continuous single-cell imaging of blood generation from haemogenic endothelium. *Nature* **457**, 896-900.

Ferrara, N., Carver-Moore, K., Chen, H., Dowd, M., Lu, L., O'Shea, K. S., Powell-Braxton, L., Hillan, K. J. and Moore, M. W. (1996). Heterozygous embryonic lethality induced by targeted inactivation of the VEGF gene. *Nature* **380**, 439-42.

Ferrara, N., Gerber, H. P. and LeCouter, J. (2003). The biology of VEGF and its receptors. *Nat Med* **9**, 669-76.

Gallardo, T., Shirley, L., John, G. B. and Castrillon, D. H. (2007). Generation of a germ cell-specific mouse transgenic Cre line, Vasa-Cre. *Genesis* **45**, 413-7.

Gekas, C., Dieterlen-Lievre, F., Orkin, S. H. and Mikkola, H. K. (2005). The placenta is a niche for hematopoietic stem cells. *Dev Cell* **8**, 365-75.

Georgiades, P., Cox, B., Gertsenstein, M., Chawengsaksophak, K. and Rossant, J. (2007). Trophoblast-specific gene manipulation using lentivirus-based vectors. *Biotechniques* **42**, 317-8, 320, 322-5.

Gerber, H. P., Hillan, K. J., Ryan, A. M., Kowalski, J., Keller, G. A., Rangell, L., Wright, B. D., Radtke, F., Aguet, M. and Ferrara, N. (1999). VEGF is required for growth and survival in neonatal mice. *Development* **126**, 1149-59.

Haar, J. L. and Ackerman, G. A. (1971). A phase and electron microscopic study of vasculogenesis and erythropoiesis in the yolk sac of the mouse. *Anat Rec* **170**, 199-223.

Koushik, S. V., Wang, J., Rogers, R., Moskophidis, D., Lambert, N. A., Creazzo, T. L. and Conway, S. J. (2001). Targeted inactivation of the sodium-calcium exchanger (Ncx1) results in the lack of a heartbeat and abnormal myofibrillar organization. *FASEB J* **15**, 1209-11.

Lancrin, C., Sroczynska, P., Stephenson, C., Allen, T., Kouskoff, V. and Lacaud, G. (2009). The haemangioblast generates haematopoietic cells through a haemogenic endothelium stage. *Nature* **457**, 892-5.

Lawson, N. D. and Weinstein, B. M. (2002). Arteries and veins: making a difference with zebrafish. *Nat Rev Genet* **3**, 674-82.

Lee, S., Chen, T. T., Barber, C. L., Jordan, M. C., Murdock, J., Desai, S., Ferrara, N., Nagy, A., Roos, K. P. and Iruela-Arispe, M. L. (2007). Autocrine VEGF signaling is required for vascular homeostasis. *Cell* **130**, 691-703.

Medvinsky, A. and Dzierzak, E. (1996). Definitive hematopoiesis is autonomously initiated by the AGM region. *Cell* **86**, 897-906.

Mikkola, H. K. and Orkin, S. H. (2006). The journey of developing hematopoietic stem cells. *Development* **133**, 3733-44.

Miquerol, L., Gertsenstein, M., Harpal, K., Rossant, J. and Nagy, A. (1999). Multiple developmental roles of VEGF suggested by a LacZ-tagged allele. *Dev Biol* **212**, 307-22.

Palis, J. (2008). Ontogeny of erythropoiesis. *Curr Opin Hematol* **15**, 155-61.

Palis, J., Robertson, S., Kennedy, M., Wall, C. and Keller, G. (1999). Development of erythroid and myeloid progenitors in the yolk sac and embryo proper of the mouse. *Development* **126**, 5073-84.

Rhodes, K. E., Gekas, C., Wang, Y., Lux, C. T., Francis, C. S., Chan, D. N., Conway, S., Orkin, S. H., Yoder, M. C. and Mikkola, H. K. (2008). The emergence of hematopoietic stem cells is initiated in the placental vasculature in the absence of circulation. *Cell Stem Cell* **2**, 252-63.

Robin, C., Bollerot, K., Mendes, S., Haak, E., Crisan, M., Cerisoli, F., Lauw, I., Kaimakis, P., Jorna, R., Vermeulen, M. et al. (2009). Human placenta is a potent hematopoietic niche containing hematopoietic stem and progenitor cells throughout development. *Cell Stem Cell* **5**, 385-95.

Saga, Y., Miyagawa-Tomita, S., Takagi, A., Kitajima, S., Miyazaki, J. and Inoue, T. (1999). MesP1 is expressed in the heart precursor cells and required for the formation of a single heart tube. *Development* **126**, 3437-47.

Schmitt, T. M., de Pooter, R. F., Gronski, M. A., Cho, S. K., Ohashi, P. S. and Zuniga-Pflucker, J. C. (2004). Induction of T cell development and establishment of T cell competence from embryonic stem cells differentiated in vitro. *Nat Immunol* **5**, 410-7.

Van Handel, B., Montel-Hagen, A., Sasidharan, R., Nakano, H., Ferrari, R., Boogerd, C. J., Schredelseker, J., Wang, Y., Hunter, S., Org, T. et al. (2012). Scl represses cardiomyogenesis in prospective hemogenic endothelium and endocardium. *Cell* **150**, 590-605.

Zeigler, B. M., Sugiyama, D., Chen, M., Guo, Y., Downs, K. M. and Speck, N. A. (2006). The allantois and chorion, when isolated before circulation or chorio-allantoic fusion, have hematopoietic potential. *Development* **133**, 4183-92.

Zovein, A. C., Hofmann, J. J., Lynch, M., French, W. J., Turlo, K. A., Yang, Y., Becker, M. S., Zanetta, L., Dejana, E., Gasson, J. C. et al. (2008). Fate tracing reveals the endothelial origin of hematopoietic stem cells. *Cell Stem Cell* **3**, 625-36.

Developmental Cell
Article

c-Met-Dependent Multipotent Labyrinth Trophoblast Progenitors Establish Placental Exchange Interface

Masaya Ueno,[1] Lydia K. Lee,[1] Akanksha Chhabra,[1] Yeon Joo Kim,[1] Rajkumar Sasidharan,[1] Ben Van Handel,[1] Ying Wang,[5] Masakazu Kamata,[6] Paniz Kamran,[3,7] Konstantina-Ioanna Sereti,[3,7] Reza Ardehali,[3,7] Meisheng Jiang,[5] and Hanna K.A. Mikkola[1,2,3,4,*]

[1]Department of Molecular, Cell and Developmental Biology
[2]Department of Microbiology, Immunology and Molecular Genetics
[3]Eli and Edythe Broad Center for Regenerative Medicine and Stem Cell Research
[4]Jonsson Comprehensive Cancer Center
[5]Molecular and Medical Pharmacology, School of Medicine
[6]Department of Hematology and Oncology
[7]Department of Cardiology, David Geffen School of Medicine
University of California, Los Angeles, Los Angeles, CA 90095, USA
*Correspondence: hmikkola@mcdb.ucla.edu
http://dx.doi.org/10.1016/j.devcel.2013.10.019

SUMMARY

The placenta provides the interface for gas and nutrient exchange between the mother and the fetus. Despite its critical function in sustaining pregnancy, the stem/progenitor cell hierarchy and molecular mechanisms responsible for the development of the placental exchange interface are poorly understood. We identified an Epcam^{hi} labyrinth trophoblast progenitor (LaTP) in mouse placenta that at a clonal level generates all labyrinth trophoblast subtypes, syncytiotrophoblasts I and II, and sinusoidal trophoblast giant cells. Moreover, we discovered that hepatocyte growth factor/c-Met signaling is required for sustaining proliferation of LaTP during midgestation. Loss of trophoblast c-Met also disrupted terminal differentiation and polarization of syncytiotrophoblasts, leading to intrauterine fetal growth restriction, fetal liver hypocellularity, and demise. Identification of this c-Met-dependent multipotent LaTP provides a landmark in the poorly defined placental stem/progenitor cell hierarchy and may help us understand pregnancy complications caused by a defective placental exchange.

INTRODUCTION

The mammalian placenta serves as the interface for gas and nutrient exchange during development. The placenta also provides an immunological barrier between the fetus and the mother and secretes hormones that regulate pregnancy. Recent studies identified the placenta as a hematopoietic organ that generates hematopoietic stem/progenitor cells (HS/PC) and macrophages and provides a niche that protects definitive HS/PC from premature erythroid differentiation (Gekas et al., 2005; Rhodes et al., 2008; Van Handel et al., 2010; Chhabra et al., 2012). Dysfunctional placental development has been associated with maternal hypertension and preeclampsia (Young et al., 2010), while disruption of placental circulation and fetal-maternal exchange can lead to intrauterine fetal growth restriction (IUGR) and demise (Scifres and Nelson, 2009). Therefore, proper placental function is critical for a healthy pregnancy.

In the mouse placenta, substance exchange occurs in the labyrinth (La; analogous to chorionic villi in human), which is composed of highly branched fetal vasculature and trophoblast-lined maternal blood spaces (Figure S1A available online; Rossant and Cross, 2001; Watson and Cross, 2005; Maltepe et al., 2010). Trophoblasts are epithelial cells that develop from the trophectoderm (Te), the outermost layer of the blastocyst. Mitotic activity is limited to polar Te that differentiates into chorionic trophoblasts and the ectoplacental cone (EPC). Chorionic trophoblasts form the labyrinth, while the EPC gives rise to the junctional zone (JZ) consisting of spongiotrophoblasts (Sp) and trophoblast giant cells (TGC) that provide structural support and enable invasion to the uterus (Figure 1A; Figure S1A). Morphogenesis of the labyrinth occurs after fusion of the allantoic mesoderm with chorionic trophoblasts (embryonic day 8.5 [E8.5]), which undergo extensive branching (Figure 1A). The labyrinth consists of two layers of multinucleated syncytiotrophoblasts (SynT-I and -II) that control fetal-maternal transport, and sinusoidal trophoblast giant cells (sTGCs) that have endocrine functions and act as hematopoietic signaling centers (Chhabra et al., 2012). Fibroblast growth factor 4 (Fgf4)-dependent trophoblast stem (TS) cells that generate all trophoblast subtypes can be established from the blastocyst and early postimplantation embryos, and are the in vitro equivalents of Te (Tanaka et al., 1998). However, TS cell potential disappears after chorioallantoic fusion (Uy et al., 2002) suggesting that yet unidentified precursors downstream of TS cells form the placenta (Figure 1A; Simmons and Cross, 2005). Recent studies identified an EPC-derived Blimp1^{+} precursor that generates multiple types of TGC in the Sp layer (Mould et al., 2012). However, the precursors

that generate the exchange interface in the placental labyrinth are unknown.

Targeted mutagenesis in mice has provided clues to mechanisms regulating key stages of placental development (Rossant and Cross, 2001; Watson and Cross, 2005). c-Met receptor tyrosine kinase and its ligand, hepatocyte growth factor (Hgf), have been identified as regulators of labyrinth morphogenesis. *Hgf* and *c-Met* knockout (KO) embryos exhibit IUGR and a smaller placenta and die by E14.5; Bladt et al., 1995; Schmidt et al., 1995; Uehara et al., 1995). c-Met signaling governs various morphogenetic events in development, tissue repair, and cancer metastasis by regulating cell growth and motility and stem/progenitor cells in multiple tissues express c-Met (Boccaccio and Comoglio, 2006). Nevertheless, little is known about the cellular and molecular mechanisms of how c-Met signaling governs placental development, and the extent to which placental dysfunction underlies the defective development of c-Met-deficient embryos.

Here we identify an Hgf/c-Met signaling-dependent Epcam^{hi} multipotent labyrinth progenitor that gives rise to all labyrinth trophoblast subtypes. Trophoblast-specific loss of *c-Met* abrogated the proliferation of labyrinth trophoblast progenitors (LaTPs) and terminal differentiation and polarization of syncytiotrophoblasts, compromising both placental and fetal development. These discoveries advance our understanding of placental stem/progenitor cell hierarchy and provide an in vivo model for studying how dysfunctional placental exchange compromises pregnancy.

RESULTS

Epcam Marks Proliferative, Undifferentiated Trophoblasts in the Placental Labyrinth

To identify candidate trophoblast progenitor cells in the placental labyrinth, proliferative cells were labeled with bromodeoxyuridine (BrdU) 1 hr before dissection, and immunofluorescence (IF) was performed for BrdU and CD9 or Epcam (Trop1; Figure 1B; Figure S1A). CD9, a trophoblast marker upregulated at E10.5 during labyrinth morphogenesis (Wynne et al., 2006), was expressed broadly in syncytiotrophoblasts (SynT) in E12.5 labyrinth (Figure 1B; Figure S1A). In contrast, Epcam, a marker of many epithelial stem cells (McQualter et al., 2010), was expressed highly in a subset of labyrinth trophoblasts, while SynT showed low expression (Figure 1B; Figure S1A). Moreover, Epcam^{hi} cells were arranged in clusters and showed much higher frequency of BrdU incorporation than CD9^{+} cells (Figure 1B). To assess whether Epcam^{hi} cells are undifferentiated trophoblasts, sections were costained for monocarboxylate transporter (Mct) 4, which is expressed in the basal plasma membrane of SynT-II (Nagai et al., 2010) adjacent to fetal vasculature. Mct4 was undetectable by IF at E10.5 (data not shown), whereas by E12.5, Mct4 colocalized with Epcam in SynT-II (Epcam^{low}; Figure 1C). In contrast, Epcam^{hi} cells were devoid of Mct4 expression (Figure 1C). At E9.5, Epcam^{hi} cells resided at the site of chorioallantoic fusion (Figure 1D), and by E12.5, they formed clusters adjacent to laminin^{+} stromal cells in the labyrinth. No Epcam^{hi} cells were detectable after completion of labyrinth morphogenesis at E14.5 (Figure 1D). These data nominated Epcam^{hi} cells as candidate progenitor cells in the placental labyrinth.

To define the identity of Epcam^{hi} cells, magnetic bead selection was used to isolate them from E10.5 placenta (Figure 1E; Figure S1B). Fluorescence-activated cell sorting (FACS) analysis confirmed the enrichment of Epcam^{hi} cells without a significant contribution of Epcam^{low} CD9^{hi} SynT (Figure S1B). Results of quantitative RT-PCR (qRT-PCR) indicated that the expression of genes required for labyrinth trophoblast development, including transcription factors *Gcm1*, *Dlx3*, and *Ovol2* (Morasso et al., 1999; Anson-Cartwright et al., 2000; Unezaki et al., 2007), and orphan nuclear factor *Nr6a1* (Morasso et al., 1999), was enriched in Epcam^{hi} fraction in E10.5 placenta as compared to Epcam cells or TS cells (Figure 1F). Low expression of sTGC markers (*Ctsq* and *Prl3b*) was detected in both Epcam^{hi} and Epcam cells, but not in TS cells, whereas TGC (*Prl3d1*) and Sp (*Tpbpa*) markers were absent from both Epcam^{hi} and TS cells (Figure 1F). These data suggested that Epcam^{hi} cells are primed for differentiation to labyrinth trophoblasts.

Epcam^{hi} Cells Represent Multipotent Labyrinth Trophoblast Progenitors

To define the ability of Epcam^{hi} cells to differentiate into labyrinth trophoblasts, magnetic-activated cell-sorted Epcam^{hi} cells were cultured on OP9 stroma. OP9 cells highly express *Vcam1*, a ligand for integrin α4 (Itga4), which is expressed both in Epcam^{hi} cells (Figure 2A) and on the basal surface of the chorion at the time of chorioallantoic fusion (Stecca et al., 2002). The differentiation potential of Epcam^{hi} cells was compared to that of TS cells, which upregulate markers for the SynT, Sp, and TGC lineages after removal of Fgf4 (Tanaka et al., 1998). After 7 days of culture on OP9, Epcam^{hi} cells maintained the expression of SynT transcription factors *Dlx3* and *Ovol2* and upregulated the mature SynT markers *Mct1* (SynT-I) and *Mct4* (SynT-II; Nagai et al., 2010; Figure 2B) to greater levels than differentiated TS cells, confirming the ability of Epcam^{hi} cells to efficiently generate SynT. Moreover, after 7 days in culture, E-cadherin^{+} (Cdh1) cells with multiple nuclei (>20) were observed (Figure 2C), suggesting that SynT derived from Epcam^{hi} cells can form syncytia in vitro. Costaining with CD9 confirmed that the multinucleated cells were trophoblasts (Figure 2D). Interestingly, expression of sTGC markers *Ctsq* and *Prl3b1* also increased by 7 days of culture, suggesting that Epcam^{hi} cells also differentiate into labyrinth sTGC in vitro (Figure 2B). In contrast, cultured Epcam^{hi} cells evidenced minimal expression of TGC and Sp markers, implying that their differentiation potential is restricted to labyrinth trophoblasts. These data nominated Epcam^{hi} cells as labyrinth trophoblast progenitor cells (LaTP) that can give rise to SynT-I, II, and sTGC.

We next asked if Epcam^{hi} cells are clonally linked to SynT and sTGC in vivo. Tamoxifen-inducible *Rosa26-CreER^{T2}* mice were crossed with *Rosa26-Rainbow* reporter strain (Rinkevich et al., 2011), in which all cells express GFP until Cre-mediated recombination induces one of the three other fluorescent proteins (mCherry, mOrange, and mCerulean; Figures 2E and 2F). 4-OH tamoxifen was injected at E9.5 when labyrinth morphogenesis begins, and placentas were analyzed at E12.5 when Epcam^{hi} cells and differentiated SynT and sTGC are present. To facilitate clonal analysis, the dose of 4-OH tamoxifen was titrated to induce rare recombination in trophoblasts. While individual cells marked with mCherry, mOrange, or mCerulean were found in all

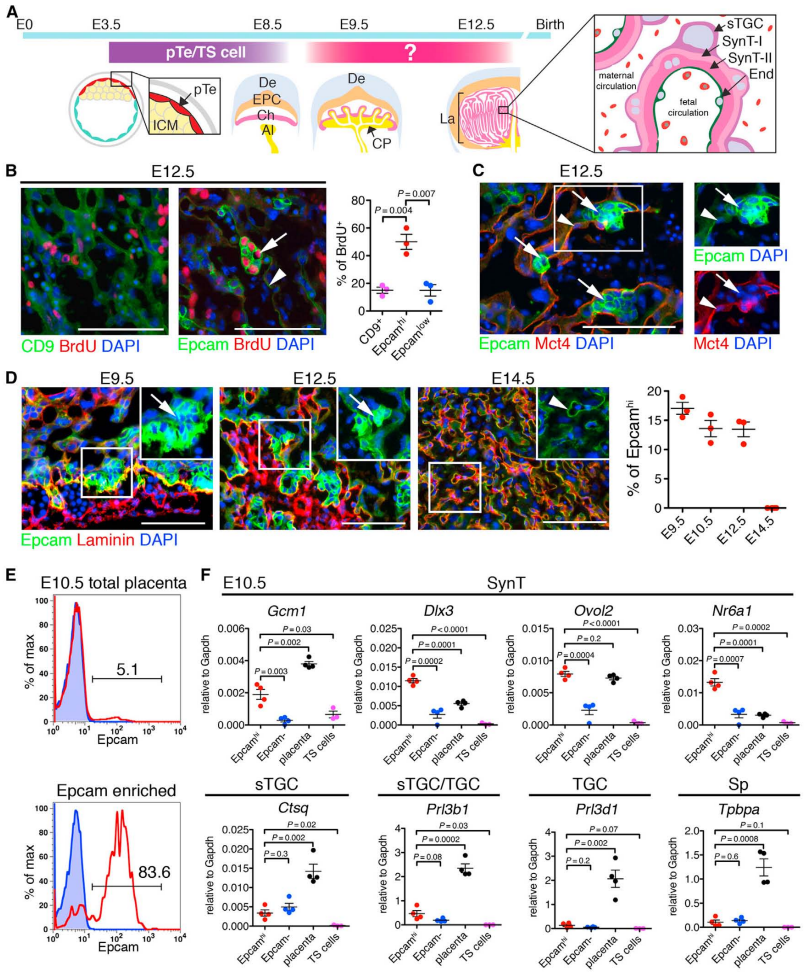

Figure 1. Epcam^{hi} Cells Are Candidate LaTP Cells

(A) Schematic depicting the development of the mouse placenta. Polar trophectoderm (pTe) develops into ectoplacental cone (EPC) and chorion (Ch). Trophoblast stem (TS) cells can established from trophoectoderm/placenta before E8.5, however, TS cells disappear after chorioallantoic fusion, suggesting that yet unidentified progenitors are responsible for labyrinth development. The labyrinth (La) contains three trophoblast cell types: SynT-I, SynT-II, and sinusoidal trophoblast giant cells (sTGCs). The SynT-II layer is facing fetal endothelium (End), and the sTGC is facing maternal blood. ICM, inner cell mass; De, decidua; Al, allantois; CP, chorionic plate.

(B) Identification of Epcam as a marker for proliferating trophoblasts. Sections from E12.5 placental labyrinth were stained with CD9 or Epcam. DNA synthesis was visualized by BrdU incorporation. Arrow, Epcam^{hi} cluster. Arrowhead, SynT. Scale bar, 100 μm.

(C) Correlation of SynT-II differentiation marker, Mct4, with low Epcam expression in SynT-II (arrowhead). Arrow, Epcam^{hi} cluster. Scale bar, 100 μm.

(D) Kinetic analysis of the frequency of Epcam^{hi} cells in midgestation placentas. Scale bar, 100 μm.

(E) Enrichment of Epcam^{hi} cells from E10.5 placenta using magnetic bead separation.

(F) Quantitative analysis of the expression of trophoblast subtype-specific genes in Epcam^{hi}-enriched cells.

All error bars indicate SEM. See also Figure S1.

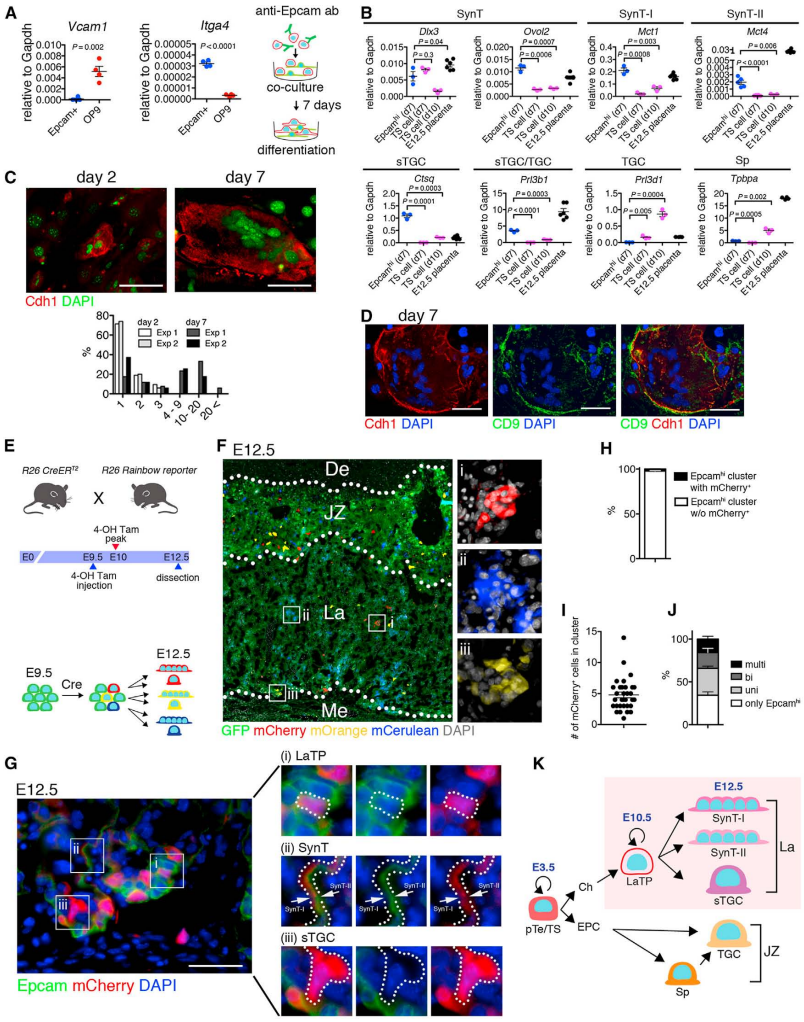

Figure 2. Epcam^{hi} Cells Represent Multipotent LaTPs

(A) Schematic for analysis of the developmental potential of Epcam^{hi} cells in vitro. Epcam^{hi} cells from E10.5 placenta were enriched using magnetic beads and cocultured with OP9 for 7 days. qRT-PCR documents the expression of *Itga4* in Epcam^{hi} cells and *Vcam1* in OP9.

(B) qRT-PCR showing the maintenance of SynT-specific genes and upregulation of markers for differentiated SynT-I and -II and sTGC in Epcam^{hi} cultures after 7 days.

(C) Documentation of increased frequency of Cdh1^{+} SynT with multiple nuclei after 7 days in culture.

(D) Documentation that Cdh1^{+} multinucleated cells coexpress trophoblast marker CD9.

(E) Schematic for in vivo clonality analysis. *Rosa26 (R26) Rainbow* reporter mice were mated with *R26 CreER^{T2}* mice. At E9.5, Cre-mediated gene deletion was induced by injection with 4OH-tamoxifen, and embryos were dissected at E12.5.

(F) Fluorescence image indicating that Cre-mediated gene recombination induces multi-color labeling and establishment of clones of labeled cells in the labyrinth. JZ, junctional zone; La, labyrinth; Me, mesenchyme.

(legend continued on next page)

parts of the fetal placenta, the labyrinth contained several clusters of cells marked with the same color (Figure 2F). To investigate differentiation potential of cells in individual clones, mCherry-labeled clusters were chosen for further analysis (Figure 2G). Of all Epcam^{hi} cell clusters, 2.2% (± 0.4) harbored mCherry^{+} Epcam^{hi} cells (Figure 2H), with each cluster containing on average 4.8 (± 2.6) mCherry-labeled trophoblasts (Figure 2I). Quantitative analysis indicated that 15.8% (± 4.1) of mCherry-labeled clusters were multipotent and contained labeled clones with Epcam^{hi} LaTP, Epcam$^{low/neg}$ SynT, and Epcam^{neg} sTGC (Figures 2G and 2J). Comparable results of clonal association of Epcam^{hi} LaTP with SynT and sTGC were obtained using *Rosa26-YFP* reporter mice (Figures S2A–S2F). Costaining for Epcam, Cytokeratin, and Mct4 further confirmed labeling of all labyrinth trophoblast subtypes within YFP^{+}-labeled Epcam^{hi} LaTP clusters (Figure S2G). Together, these data suggest that Epcam^{hi} cells are LaTPs that generate all labyrinth trophoblast subtypes in vivo (Figure 2K).

c-Met Signaling Directly Regulates Labyrinth Trophoblast Development

To identify regulators for LaTP, we searched for mouse models with labyrinth defects; the Hgf receptor c-Met was identified as a candidate. We first analyzed the placental defect in *c-Met* KO embryos generated by deleting the conditionally targeted *c-Met* locus (Huh et al., 2004) in the germline (g-KO). Lethality of *c-Met* g-KO embryos occurred by E14.5, as reported for *Hgf* and *c-Met* KO embryos (Bladt et al., 1995; Schmidt et al., 1995; Uehara et al., 1995). No macroscopic defects were observed in placentas or embryos until E12.5, when *c-Met* g-KO placentas and embryos exhibited decreased size and hypocellular fetal liver (FL; Figures S3A–S3D). *c-Met* g-KO placentas had a thinner labyrinth (La) while the JZ composed of Sp and TGC was unaffected (Figure 3A), confirming that placental defects were limited to the labyrinth.

To assess whether loss of Hgf/c-Met signaling in placental trophoblasts alone is sufficient to cause the defects in the placenta and the fetus, we generated trophoblast-specific *c-Met* KO (t-KO) embryos by deleting the *c-Met* gene in trophoblasts using a lentiviral Cre (Figure 3B; Chhabra et al., 2012). *UbiC-Cre-GFP* lentiviral vector was injected under the zona pellucida (ZP) of *c-Met*$^{fl/fl}$ blastocysts, while *c-Met*$^{fl/+}$ blastocysts and untransduced *c-Met*$^{fl/fl}$ blastocysts served as controls. Strikingly, trophoblast-specific *c-Met* deletion mimicked the phenotype of *c-Met* g-KO mutants, resulting in reduced placental labyrinth size and poorly developed branching structure (Figure S3E), IUGR of the embryo (Figures 3C and 3D), and lethality by E14.5 (data not shown). Moreover, loss of *c-Met* in placental trophoblasts alone was sufficient to cause hypocellularity of the FL (Figure S3F). Importantly, transduction of *c-Met*$^{fl/+}$ blastocysts did not show any phenotype in the embryo or the placenta (data not shown). These findings indicate that trophoblast-specific loss of c-Met causes both labyrinth and FL hypoplasia and IUGR of the embryo.

To examine how c-Met regulates labyrinth development, we conducted Affymetrix microarray analysis on wild-type (WT) and *c-Met* g-KO CD9^{+} labyrinth trophoblasts. We identified 1,294 genes as downregulated and 1,221 genes as upregulated in *c-Met*-deficient trophoblasts (> 2-fold, $p < 0.05$; Tables S1 and S2; Figure S3G). The GO category "placenta development" included genes regulating labyrinth development (Figure 3E; Figure S3G). qRT-PCR confirmed reduced expression of SynT genes (*Gcm1*, *Dlx3*, *Ovol2*, *Cebpa*, and *Tead3*; Natale et al., 2006) in *c-Met* g-KO labyrinth trophoblasts (Figure 3F). qRT-PCR of all E12.5 placentas showed that there was no reduction in labyrinth sTGC- (*Ctsq* and *Prl3b1*), TGC- (*Prl3b1*, *Limk1*, *Limk2*, and *Hand1*), or Sp-specific genes (*Tpbpa* and *Nodal*; Figure 3G; (Watson and Cross, 2005; Natale et al., 2006). These data further indicated that c-Met signaling specifically regulates labyrinth trophoblast development.

c-Met Sustains Proliferation of LaTP in Midgestation Placenta

The selective suppression of SynT genes and the morphological defects in the placental labyrinth raised the hypothesis that c-Met signaling regulates the emergence, maintenance, and/or differentiation of LaTP. qRT-PCR documented the expression of *c-Met* in both Epcam^{hi} LaTP and CD9^{hi} Epcam$^{low/neg}$ SynT, whereas the mature SynT marker *Mct4* was expressed at a higher level in SynT (Figure 4A). The frequency of Epcam^{hi} cells in *c-Met* g-KO placenta was comparable to that of WT at E9.5, but dramatically decreased from E10.5 onward (Figure 4B). These data suggested that c-Met signaling is not required for specification of LaTP, but rather for their maintenance through midgestation.

The most highly enriched GO categories among genes downregulated in *c-Met*-deficient placentas were related to "cell cycle" (Figures S3G and S4A). qRT-PCR confirmed downregulation of several genes required for cell division, including *Ccna2, Ccne1*, *Ccne2*, *Chek1*, and *Cdc45* (Figure 4C). BrdU incorporation assay verified significant reduction in actively proliferating Cytokeratin^{+} trophoblasts in both *c-Met* g-KO and t-KO placentas at E12.5 (Figure S4B), whereas no difference in DNA fragmentation was observed (Figure S4C), suggesting that defective proliferation rather than apoptosis underlies labyrinth hypoplasia in *c-Met*-deficient placentas. Costaining for phospho-Histone H3 (PH3), a marker of mitosis, and Epcam showed no significant difference in mitotic activity between WT and *c-Met* g-KO Epcam^{hi} LaTP at E9.5, whereas their proliferation was dramatically decreased E10.5 onward (Figure 4D). These data implied that c-Met signaling is required to sustain the proliferation of LaTP in midgestation.

To verify that reduced proliferation of c-Met-deficient LaTP is not caused by indirect effects from other tissues, c-Met signaling

(G) Documentation of multilineage differentiation in a cluster of mCherry-labeled trophoblasts. (i) Epcam^{hi} (LaTP), (ii) SynT (Epcam$^{low/neg}$), and (iii) sTGC (Epcam^{neg} with large nuclei).
(H) Analysis of the frequency of clusters containing mCherry-labeled Epcam^{hi} cells documenting infrequent labeling of clusters with the same fluorescent color.
(I) Average number of mCherry^{+} cells in a labeled cluster documenting the establishment of multicellular, labeled clones.
(J) Differentiation potential of mCherry-labeled cells documenting the presence of clones with Epcam^{hi} LaTP and all labyrinth trophoblast subtypes.
(K) Schematic representing the hierarchy of trophoblast lineage differentiation. LaTP gives rise to all types of labyrinth trophoblasts, but not Sp or TGC.
All error bars indicate SEM. See also Figure S2.

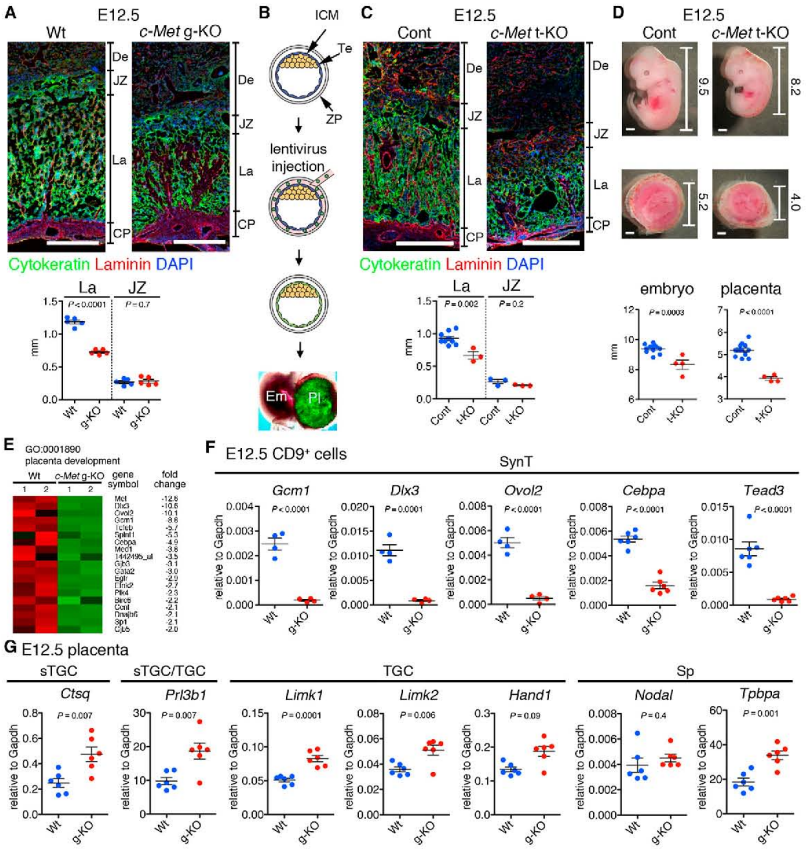

Figure 3. Loss of c-Met Signaling in Trophoblasts Induces Placental Labyrinth Hypoplasia and IUGR

(A) IF for Cytokeratin (green, trophoblast), Laminin (red, mesenchymal cell), and DAPI (blue, nuclei) on WT and *c-Met* germline KO (g-KO) placenta at E12.5 showing La-specific hypoplasia in *c-Met* g-KO placenta. Scale bar, 500 μm.

(B) Generation of trophoblast-specific *c-Met* KO (t-KO) embryos. Injection of *Cre-GFP* lentivirus under the zona pellucida (ZP) induces Te-specific gene deletion. ICM, inner cell mass; Te, trophectoderm.

(C) Trophoblast-specific *c-Met* gene deletion induces placental labyrinth hypoplasia.

(D) Representative images of *c-Met*$^{fl/fl}$ and *c-Met* trophoblast-specific KO (t-KO) embryos and placentas. Numbers indicate size (in millimeters) of each embryo and placenta. Scale bar, 1 mm.

(E) Heatmap representing differential expression of genes related to placental development (>2.0-fold, $p < 0.05$) in WT versus *c-Met* g-KO CD9$^+$ trophoblasts.

(F) qRT-PCR for SynT-specific genes on E12.5 WT and *c-Met* g-KO CD9$^+$ trophoblasts. The mean of biological replicates normalized to *Gapdh* is shown.

(G) qRT-PCR for sTGC, TGC, and Sp-specific genes in E12.5 placenta.

All error bars indicate SEM. See also Figure S3 and Tables S1 and S2.

was blocked in LaTP culture using c-Met inhibitor PHA-665752 (Christensen et al., 2003). Inhibition of c-Met signaling impaired the proliferation of Epcam$^+$ cells in culture without increasing apoptosis (Figures 4E and 4F), demonstrating a cell autonomous role for c-Met in sustaining the proliferation of LaTP and/or their progeny.

c-Met Signaling Is Essential for the Establishment of Labyrinth Exchange Interface

Because the expression analysis of *c-Met*-deficient placentas had indicated a dramatic reduction of labyrinth trophoblast-specific transcription factors, we investigated whether c-Met signaling is required for the differentiation of LaTP into SynT

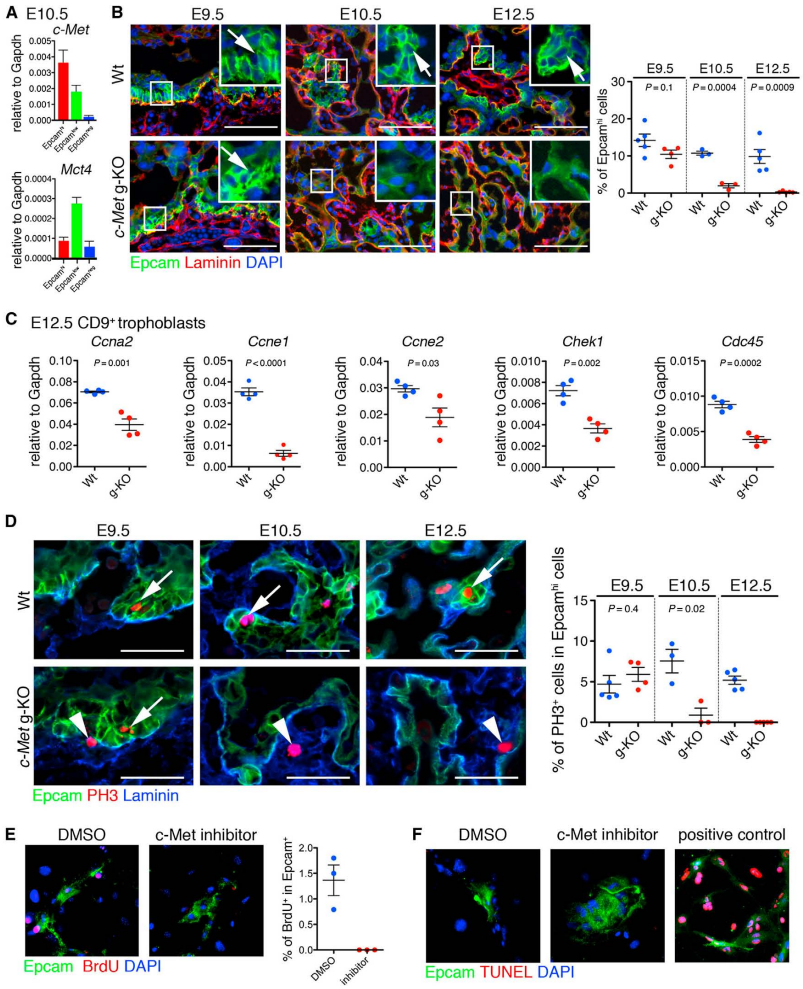

Figure 4. c-Met Signaling Regulates the Maintenance of LaTP

(A) qRT-PCR documenting the expression of *c-Met* in both Epcam^{hi} LaTP and Epcam^{low} SynT.

(B) IF for Epcam (green) and Laminin (red) on WT and *c-Met* g-KO placenta at E9.5, E10.5, and E12.5 documenting loss of Epcam^{hi} cells in c-Met-deficient placenta after E9.5. Arrows, Epcam^{hi} cells adjacent to laminin^{+} mesenchymal cells. Scale bar, 100 μm.

(C) qRT-PCR analysis of gene expression in CD9^{+} trophoblast from WT and *c-Met* g-KO placentas verifying downregulation of cell cycle regulators.

(D) IF for Epcam (green), phospho-Histone-H3 (PH3, red) and laminin (blue) on WT and *c-Met* g-KO placenta at E9.5, E10.5, and E12.5 documenting premature loss of proliferative LaTP in c-Met-deficient placenta. Arrows, PH3^{+} Epcam^{hi} cells. Arrowheads, PH3^{+} Epcam^{-} cells. Scale bar, 50 μm.

(E) Treatment of cultured LaTP with c-Met inhibitor documents reduced BrdU incorporation in Epcam^{+} cells. Epcam (green), BrdU (red), DAPI (blue).

(F) Treatment of cultured LaTP with c-Met inhibitor documenting no difference in cell death of Epcam^{+} cells. Epcam (green), TUNEL (red), DAPI (blue). Positive control, cells treated with DNase I.

All error bars indicate SEM. See also Figure S4.

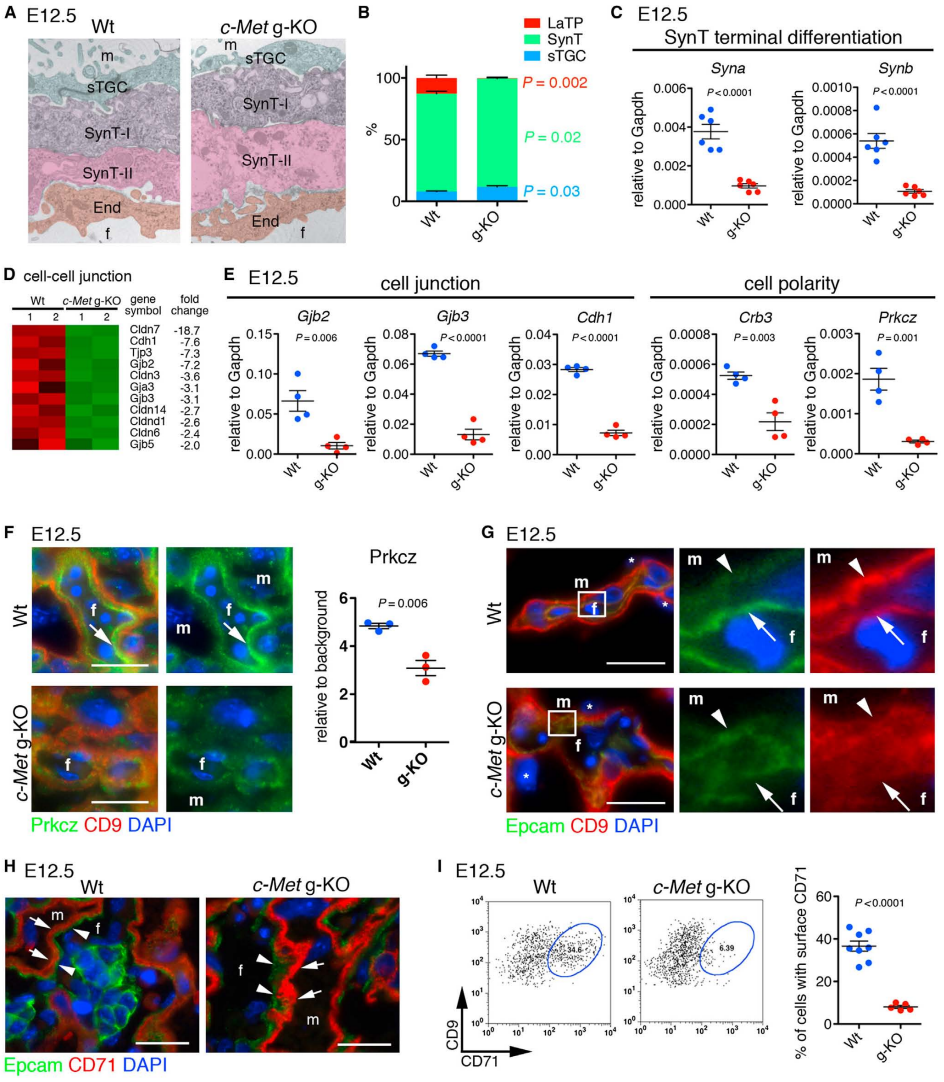

Figure 5. c-Met Signaling Is Dispensable for SynT and sTGC Specification but Essential for SynT Terminal Differentiation and Cell Polarity

(A) Electron microscopy showing trilaminar structure of labyrinth trophoblasts (SynT-I, SynT-II, and sTGC) in WT and *c-Met* g-KO placentas.

(B) Quantitative analysis for trophoblast subtypes.

(C) qRT-PCR showing decreased expression of *Syna* and *Synb* in E12.5 *c-Met* KO CD9$^+$ trophoblasts.

(D) Heatmap of cell-cell junction genes differentially expressed between WT and *c-Met* g-KO CD9$^+$ trophoblasts.

(E) qRT-PCR showing reduced expression of cell-cell junction and cell polarity genes in *c-Met* g-KO trophoblasts.

(legend continued on next page)

and/or sTGC. Electron microscopy indicated that the trilaminar trophoblast structure consisting of SynT-II, SynT-I, and sTGC was established in *c-Met* g-KO placenta (Figure 5A). Costaining for Mct4 (SynT-II) and CD9 (both SynT subtypes) confirmed the presence of both SynT-I and -II in *c-Met* g-KO placentas (Figure S5A). Quantification of the relative frequencies of labyrinth trophoblasts in *c-Met* g-KO placentas at E12.5 revealed a slight decrease of SynT and increase of sTGC, while Epcam^{hi} cells were nearly undetectable (Figure 5B). Nevertheless, despite the presence of both SynT-I and SynT-II in *c-Met* g-KO placentas, the expression of *Syncytin-a* (*Syna*) and *-b* (*Synb*) that mark terminally differentiated SynT-I and SynT-II, respectively, was dramatically reduced, suggesting a defect in terminal differentiation (Figure 5C). Microarray analysis and qRT-PCR revealed reduced expression of genes encoding tight junction proteins *Cldn3*, *6*, *7*, and *14*, and *Tjp3*, adherence junction proteins (*Cdh1* [*E-cadherin*]), and gap junction proteins *Gjb2* (*Cx26*) and *Gjb3* (*Cx31*), which are highly expressed in differentiated SynT and critical for labyrinth development (Gabriel et al., 1998; Plum et al., 2001; Figures 5D and 5E).

Epithelial cells exhibit apical-basolateral polarity that is essential for organ development and function (Martin-Belmonte and Perez-Moreno, 2012). Closer examination of the CD9 staining pattern in c-Met-deficient trophoblasts revealed that although CD9 was localized on both the fetal side of SynT-II and maternal (apical) side of SynT-I in WT placentas (Figure S5A), it was diffusely localized in *c-Met* g-KO SynT, suggesting that c-Met signaling regulates SynT cell polarity. Microarray analysis and qRT-PCR revealed downregulation of polarity genes *Crb3* and *aPKCζ* (*Prkcz*) in *c-Met* g-KO trophoblasts (Figure 5E). No statistically significant reduction was observed by qRT-PCR for *Pard3* and *Pard6b* (data not shown), which form a complex with Prkcz to establish cell polarity in many cell types (Martin-Belmonte and Perez-Moreno, 2012). Quantitative IF analysis documented reduction of Prkcz protein in *c-Met* KO placenta (Figure 5F). Moreover, while Prkcz was expressed at the fetal side of SynT-II in WT placenta (Figure 5F), a more diffuse expression of the residual Prkcz protein was observed in *c-Met* g-KO SynT-II. Likewise, although Epcam expression in SynT in WT placenta was confined to the membrane of the fetal (basal) side of SynT-II (Figure 5G), in *c-Met* g-KO placenta, Epcam was diffusely expressed. In the yolk sac, Epcam was distributed on the basolateral membrane and CD9 was abundantly expressed at the apical surface in both WT and *c-Met* g-KO (Figure S5B), indicating that cell polarity was disrupted only in the placenta. These data demonstrated a pivotal role for c-Met signaling in the establishment of apical-basolateral cell polarity during SynT differentiation.

Transplacental iron transport from the mother is critical for normal fetal development. Serum iron is bound to transferrin (Trf), and is taken up by transferrin receptor (CD71) via endocytosis. After iron dissociation, Trf-CD71 complex is recycled to the cell surface (Grant and Donaldson, 2009). CD71 is necessary for fetal development (Levy et al., 1999), and the endocytic recycling of CD71 is tightly regulated by cell polarity machinery (Golachowska et al., 2010). IF and FACS analysis showed that in WT placenta, CD71 is expressed in both the cytoplasm and cell surface of SynT-I (Figures 5H and 5I). However, although IF demonstrated abundant cytoplasmic expression of CD71 in *c-Met*-deficient SynT-I (Figure 5H), FACS analysis revealed drastic reduction of surface CD71 (Figure 5I). These data suggested that impaired cell polarity in the *c-Met* KO placenta causes abnormal subcellular distribution of CD71 and other proteins required for fetal-maternal transport.

c-Met Signaling Is Required for the Maintenance of *Gcm1* Expression in Midgestation Placenta

Expression analysis of c-Met-deficient trophoblasts had indicated a dramatic reduction of transcription factors regulating SynT development; the analysis of trophoblast subtypes in the labyrinth indicated that both SynT-I and SynT-II were specified in the absence of c-Met, but their terminal differentiation was compromised. To investigate whether c-Met signaling in trophoblasts is directly required for the expression of transcription factors regulating labyrinth morphogenesis, cultured Epcam^{hi} cells were treated with c-Met inhibitor. qRT-PCR revealed that blocking c-Met signaling in vitro in LaTP and their progeny resulted in a drastically reduced expression of *Gcm1*, but not *Ovol2, Dlx3*, or *Tead3* (Figure 6A). IF verified the reduction of Gcm1 LaTP cultures treated with the c-Met inhibitor (Figure 6B).

Gcm1 is a transcription factor essential for labyrinth morphogenesis and SynT differentiation (Anson-Cartwright et al., 2000; Simmons et al., 2008). While *Gcm1* is highly expressed in differentiated, postmitotic SynT-II, *Gcm1* expression has also been reported in the chorion at E8.5 and in putative precursors of the labyrinth trophoblasts at E9.5 (Basyuk et al., 1999; Hunter et al., 1999; Stecca et al., 2002). qRT-PCR analysis of FACS-sorted Epcam^{hi} LaTP and Epcam^{low} CD9^{hi} SynT cells from E10.5 placenta documented *Gcm1* expression in both fractions (Figure S6A). In situ hybridization evidenced the expression of *Gcm1* also in Epcam^{hi} LaTP at E10.5 (Figure S6B), whereas by E14.5, *Gcm1* expression was largely confined to SynT-II (Figure S6C). IF suggested that Gcm1 is expressed in some Epcam^{hi} LaTP that are undergoing mitosis (Figure S6D). These data imply that *Gcm1* expression is not restricted to differentiated, postmitotic SynT but begins already at the level of LaTP.

To investigate whether Gcm1 expression is required for the emergence and/or differentiation of LaTP, the expression of

(F) IF for Prkcz (green) and CD9 (red) showing polarized localization of Prkcz protein in fetal side of SynT-II in WT placenta (arrow), and diffuse and decreased expression of Prkcz in *c-Met* g-KO placenta. DAPI (blue, nuclei).
(G) IF for Epcam (green), CD9 (red), and DAPI (blue) on WT and *c-Met* g-KO placenta at E12.5. Arrows indicate fetal side of SynT-II and arrowheads indicate apical membrane of SynT-I. m, maternal blood space; f, fetal vascular lumen.
(H) IF for Epcam (green), CD71 (red), and DAPI (blue) on placental section at E12.5. Expression of cytoplasmic CD71 in SynT-I (arrowheads) is observed in both WT and *c-Met* g-KO placenta.
(I) FACS analysis indicating reduced surface expression of CD71 on SynT in *c-Met* g-KO placentas.
All error bars indicate SEM. See also Figure S5.

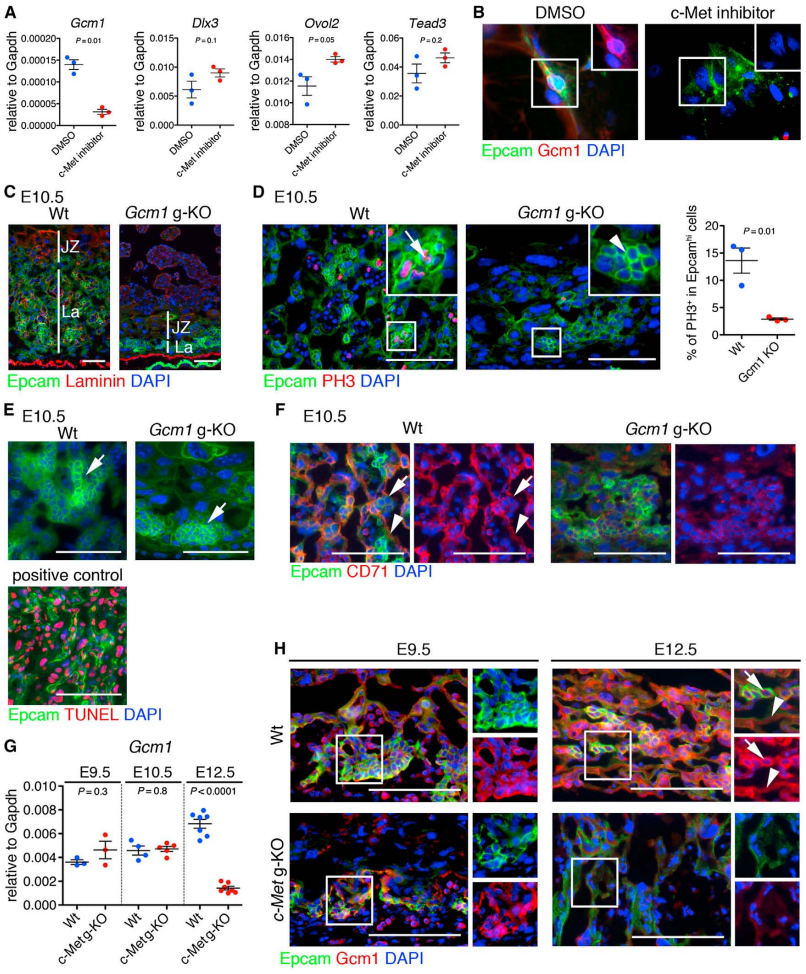

Figure 6. c-Met Signaling Is Required to Maintain Gcm1 Expression in Midgestation Placenta

(A) qRT-PCR demonstrating loss of *Gcm1* expression upon treatment of cultured LaTP with c-Met inhibitor.

(B) IF documenting loss of Gcm1 in Epcam^{+} cells upon treatment with c-Met inhibitor. Epcam (green), Gcm1 (red), DAPI (blue).

(C) IF documenting reduced labyrinth size in *Gcm1* g-KO placenta. Scale bar, 100 μm. Epcam (green), laminin (red), DAPI (blue).

(D) Phospho-Histone H3 staining documenting reduction of mitotic Epcam^{hi} cells (arrow) in *Gcm1* KO placentas. Arrowheads, PH3 negative Epcam^{hi} cluster. Epcam (green), PH3 (red), DAPI (blue). Scale bar, 100 μm.

(E) TUNEL staining indicating apoptosis is not induced in *Gcm1* g-KO placenta at E10.5. Positive control for Tunel staining is shown below. Epcam (green), TUNEL (red), DAPI (blue). Scale bar, 100 μm.

(F) IF showing absence of CD71^{+} SynT in *Gcm1* g-KO placenta. Epcam (green), CD71 (red), DAPI (blue). Scale bar, 100 μm.

(G) qRT-PCR and (H) IF documenting loss of Gcm1 expression by E12.5 in *c-Met* g-KO placentas. Epcam (green), Gcm1 (red) DAPI (blue). Scale bar 100 μm. All error bars indicate SEM. See also Figure S6.

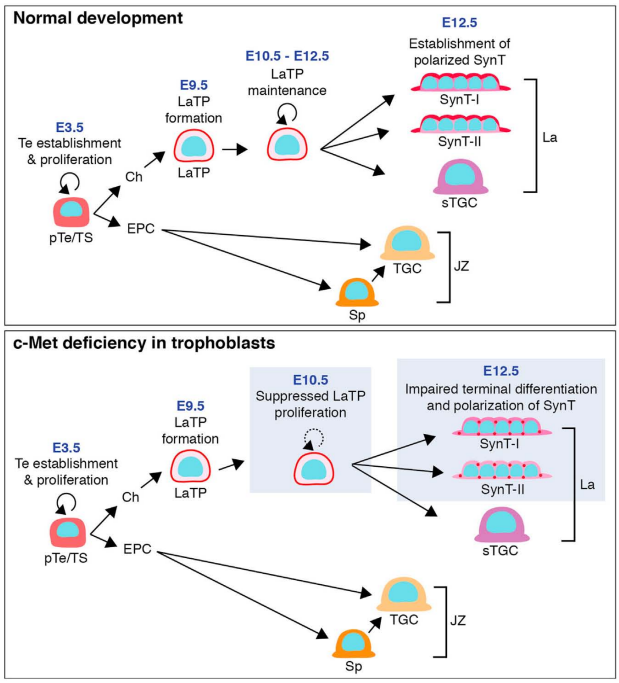

Figure 7. Model for Function of Hgf/c-Met Signaling in the Development of Placental Exchange Interface

LaTPs are responsible for the generation of SynT I and II and sTGC that compose the placental exchange interface. While LaTP can be specified independently of c-Met signaling, c-Met is essential for sustained proliferation of LaTP. c-Met signaling is also required for the establishment of SynT cell polarity. Loss of c-Met signaling results in placental hypoplasia, a compromised exchange interface, and defective fetal development.

Epcam was assessed in *Gcm1* KO placentas at E10.5, before embryonic death. As reported previously (Anson-Cartwright et al., 2000), the labyrinth layer was much thinner, and no branching morphogenesis was observed (Figure 6C). Notably, *Gcm1* KO placentas harbored Epcam^{hi} cells; however, the frequency of PH3^{+} mitotic Epcam^{hi} cells was drastically reduced (Figure 6D), while no increase in apoptosis was revealed by TUNEL assay (Figure 6E). Moreover, no CD71^{+} differentiating SynT were found in *Gcm1* KO placentas (Figure 6F). These data suggested that complete lack of Gcm1 expression compromises both the proliferation and differentiation of Epcam^{hi} LaTP in vivo.

Because the placental phenotype in *Gcm1* KO embryos was much more severe than that in *c-Met* KO embryos, we investigated the kinetics of *Gcm1* expression in c-Met-deficient placentas. At E9.5, there was no difference in the expression of *Gcm1* between *c-Met* deficient and WT placentas, whereas by E12.5, *Gcm1* expression in the mutant trophoblasts was nearly undetectable with IF and qRT-PCR (Figures 6G and 6H). These data suggested that c-Met is not essential for inducing *Gcm1* expression, but rather for maintaining its expression in LaTP and SynT through midgestation. Altogether, these findings identify Gcm1 as a key downstream effector of c-Met signaling, and suggest that its continued expression in LaTP and/or SynT in the midgestation placenta is required for the establishment of a functional placental exchange interface.

DISCUSSION

The stem/progenitor cell hierarchy of the trophoblasts responsible for placental labyrinth morphogenesis and exchange function has been unknown. We discovered that the midgestation mouse placenta harbors Epcam^{hi} multipotent labyrinth trophoblast progenitors (LaTP) that differentiate into all labyrinth trophoblast subtypes, SynT-I, SynT-II, and sTGC, in vitro and in vivo. We discovered that c-Met signaling is required for sustained proliferation of LaTP during midgestation and for terminal differentiation and polarization of SynT, which is a prerequisite for a functional placental exchange interface and healthy fetal development (Figure 7).

Clonal analysis using multicolor Rainbow reporter mouse (Rinkevich et al., 2011) revealed that marking individual cells in the placenta results in the generation of multicellular clusters that contain Epcam^{hi} LaTP, SynT-I, SynT-II, and sTGC. Although 15.8% of the labeled trophoblast clusters identified at E12.5 (labeled at around E9.5) were multipotent, 34.5% of all labeled the clusters contained only undifferentiated Epcam^{hi} LaTP, indicating that they had not started to differentiate at this stage, while the remaining labeled clones were composed of Epcam^{hi} LaTP and SynT or sTGC only. Future studies using marking at different time points will reveal whether the differentiation potential of LaTP changes during development. Thus, studies should focus on creating a Cre line that confers LaTP-specific labeling to lineage trace the progeny of LaTP throughout development.

Our data show that both LaTP and SynT express c-Met, while mesenchymal cells derived from the allantois secrete Hgf (Uehara et al., 1995), suggesting paracrine signaling. Abrogation of c-Met signaling disrupted the proliferation of Epcam^{hi} cells both in vivo and in vitro. Nevertheless, our data suggest that Hgf/c-Met signaling is necessary, but not sufficient to support LaTP proliferation and/or SynT differentiation without other niche factors; culture of Epcam^{hi} cells in TS cell conditions or on Matrigel with Hgf failed to support SynT differentiation and maintain Gcm1 expression. However, culture of Epcam^{hi} cells on OP9 mesenchymal stroma, which secretes Hgf and expresses Vcam1 (Malhotra and Kincade, 2009) that is essential

for maintaining *Gcm1* expression in placental explant cultures (Stecca et al., 2002), facilitated the maintenance/induction of SynT genes and formation of multinucleated syncytia. Cultured Epcam^{hi} LaTP also induced genes specific for labyrinth sTGC, which have been implicated as key hematopoietic niche cells (Chhabra et al., 2012). These data imply that the Epcam^{hi} cell culture may be used to study the trophoblast subtypes that establish the exchange interface and the hematopoietic niche in the placental labyrinth. Future work will be needed to define distinct niche components to direct the differentiation of LaTP to specific labyrinth trophoblast subtypes and to investigate whether LaTP can be sustained in an undifferentiated state in culture.

Although previous studies had associated defective c-Met signaling with disrupted labyrinth development, the underlying mechanisms were unknown. Our data revealed a critical role for c-Met in the maintenance of *Gcm1* expression in midgestation placenta whereas the initial induction of *Gcm1* occurs independently of c-Met. This finding helps explain the less drastic placental defect in *c-Met* KO embryos than in *Gcm1* KO embryos, because a complete lack of *Gcm1* disrupted labyrinth morphogenesis and SynT differentiation entirely, causing embryonic death by E10.5 (Anson-Cartwright et al., 2000). Analysis of *Gcm1* KO placentas suggested that Epcam^{hi} LaTP can be specified in the absence of *Gcm1*, but their proliferation and differentiation is disturbed. In contrast, loss of *c-Met* did not abolish the expression of *Gcm1* or cause macroscopic defects in *c-Met* KO labyrinth until E12.5, when LaTP were extinguished and *Gcm1* expression dropped to undetectable levels. Altogether, these data suggest that the specification of LaTP is induced by a c-Met- and Gcm1-independent mechanism; however, c-Met is required for SynT terminal differentiation and establishment of the placental exchange interface, which may at least in part be linked to the requirement of c-Met signaling to maintain Gcm1 expression.

Previous studies have shown that Gcm1 is highly expressed in postmitotic cells in the labyrinth and that overexpression of Gcm1 induces cell cycle arrest (Hughes et al., 2004). Our data also confirmed high expression of Gcm1 in differentiated SynT-II. In addition, the ability to distinguish undifferentiated LaTP in the labyrinth by Epcam^{hi} staining identified a small population of proliferative LaTP that also express Gcm1. Because TS cells do not express Gcm1, it is plausible that expression of Gcm1 is important for LaTP commitment to the SynT lineage. To verify if Gcm1 governs the differentiation of LaTP to SynT, and/or is directly involved in maintaining LaTP proliferation, further studies deleting Gcm1 in a cell-type-specific and temporal manner will be required.

As with mouse placenta, little is known about the stem/progenitor cell hierarchy in the human placenta. Despite similarities in molecular regulation, the mouse and human placentas are macroscopically distinct (Georgiades et al., 2002). Thus, the direct relevance of the findings of mouse LaTP to human placental progenitor biology needs to be explored separately. Recent studies documented that the chorionic membrane of the first trimester human placenta can serve as a source of trophoblast progenitor cell lines that highly express *GCM1* and upregulate *SYNCYTIN* after differentiation in vitro (Genbacev et al., 2011), raising the hypothesis that they originate from a precursor that has a parallel function in establishing the placental exchange interface as the mouse LaTP.

Differentiated SynT form a "placental barrier" that tightly regulates the passage of substances between the maternal and fetal circulations (Kokkinos et al., 2010). We showed that while c-Met-deficient LaTP can form all labyrinth trophoblast subtypes, c-Met is necessary for terminal differentiation into polarized SynT. Trophoblast cell lines have provided a useful tool to study cell polarity in vitro (Sivasubramaniyam et al., 2013); however, little is known about the direct functional consequences of disrupted SynT cell polarity in vivo. In addition to the low expression of key cell polarity molecules and the inability to achieve polarized localization of SynT surface proteins in *c-Met* KO placentas, the surface localization of transferrin receptor (CD71), required for transplacental iron transfer, on SynT-I was impaired. Future studies are needed to define the mechanisms as to how the disturbed placental exchange *c-Met*-deficient embryos causes fetal liver hypocellularity, IUGR, and death of the fetus. Thus, c-Met-deficient placentas not only offer a unique in vivo model to investigate how the apical-basolateral polarity and bidirectional transport in SynT is established, but may also help uncover the etiology of pregnancy complications related to placental transport function.

Reduced expression of Hgf has been observed in human placentas from preeclampsia and IUGR pregnancies (Furugori et al., 1997; Somerset et al., 1998), and in vitro studies demonstrated that Hgf activates invasion of human trophoblasts (Kauma et al., 1999; Nasu et al., 2000), providing evidence for MET signaling in placental development and disease in human. Moreover, similar to many human placenta-related disorders such as spontaneous abortion, premature delivery, IUGR, and preeclampsia that are accompanied by placental inflammation (Young et al., 2010), *c-Met* deficiency in trophoblasts induced inflammation and macrophage infiltration in the placenta (unpublished data). Although the mechanisms that trigger inflammation in c-Met-deficient trophoblasts are still unknown, this may be related to downregulation of cell-cell junction molecules and/or defective cell polarity in SynT that compromise fetal-maternal barrier function. Moreover, c-Met is constitutively activated in human choriocarcinoma, and Hgf stimulates the proliferation of choriocarcinoma cells (Saito et al., 1995; Takayanagi et al., 2000). *c-Met* also regulates the proliferation and migration of various other cancer cells and stem cells (Boccaccio and Comoglio, 2006). Thus, defining how Hgf/c-Met signaling governs the proliferation of stem/progenitor cells such as LaTP and the establishment of cell polarity in their differentiated progeny may have implications to understanding the pathophysiology of other common diseases.

EXPERIMENTAL PROCEDURES

Animals

All procedures with animals were conducted according to the guidelines of the UCLA Animal Research Committee. For LaTP culture, E10.5 pregnant mice (ICR, Taconic) were used. For the in vivo clonality experiments, *Rosa26-Rainbow* reporter or *Rosa26-YFP* reporter mice were mated with *Rosa26-Cre-ER^{T2}* mice. Pregnant females were injected with 0.5 mg 4-OH tamoxifen at E9.5, and tissues were collected at E12.5. *c-Met$^{fl/fl}$* mice were provided by Dr. Snorri S. Thorgeirsson (NIH, Bethesda, MD, USA; Huh et al., 2004). To generate trophoblast-specific *c-Met* KO embryos, lentiviral

vector-expressing *Cre-Gfp* was microinjected under the ZP of the blastocyst and embryos were transplanted into pseudopregnant females, as shown earlier (Chhabra et al., 2012). For details, see the Supplemental Experimental Procedures. Sections of *Gcm1* KO placentas were provided by Dr. James C. Cross (University of Calgary, Calgary, Canada).

LaTP and TS Cell Culture

E10.5 placenta was digested with 1 mg/ml collagenase and 1 mg/ml dispase. $Epcam^{hi}$ cells were enriched using anti-Epcam antibody and anti-rat IgG magnetic beads. $Epcam^{hi}$ cells were cocultured with mitomycin C-treated OP9 stroma cell with TS medium (RPMI 1640; Invitrogen) containing 20% fetal calf serum (HyClone), 2 mM L-glutamine, 100 U/ml penicillin, 100 μg/ml streptomycin, 1 mM sodium pyruvate, and 100 μM β-mercaptoethanol) with or without c-Met inhibitor, PHA665752 (4 μM, Sigma-Aldrich) for 7 days. TS cells were maintained as described (Tanaka et al., 1998). TS cell differentiation was induced by removing mouse embryonic fibroblast-conditioned medium, Fgf4, and heparin for 7 and 10 days.

Immunofluorescence and In Situ Hybridization

Histology, BrdU incorporation assay, electron microscopy, qRT-PCR, and immunofluorescence were performed as described (Chhabra et al., 2012). For details of the antibodies, see the Supplemental Experimental Procedures. For demonstration of vascular branching, thick placental sections (3 mm) were prepared by vibratome and three-dimensional images were constructed using confocal microscopy. In situ hybridization was performed using digoxigenin (DIG)-labeled RNA antisense or sense probes for *Gcm1* and the alkaline phosphatase reaction (Simmons et al., 2008).

Gene Expression Analysis

For microarray analysis of *c-Met*-deficient trophoblasts, a single cell suspension of E12.5 placentas was stained with PE-conjugated anti-CD9 antibody and $CD9^+$ trophoblasts were enriched using anti-PE antibody-magnetic microbeads. Affymetrix MOE430_2.0 microarrays were performed on two independent WT and two *c-Met* g-KO $CD9^+$ trophoblasts. Details about microarray analysis and primer sequences (Table S3) are available in the Supplemental Experimental Procedures.

Statistical Analysis

For statistical analysis, Student's unpaired two-tailed t test was used for all comparisons.

ACCESSION NUMBERS

The Gene Expression Omnibus accession number for the microarray data reported in the paper is GSE38342.

SUPPLEMENTAL INFORMATION

Supplemental Information includes Supplemental Experimental Procedures, six figures, and three tables can be found with this article online at http://dx.doi.org/10.1016/j.devcel.2013.10.019.

AUTHOR CONTRIBUTIONS

M.U. conceived the hypothesis, designed and performed the experiments, and analyzed the data. L.K.L., A.C., Y.J.K., Y.W., B.V.H., M.K., P.K., K-I.S., R.A., and M.J. carried out experiments, and R.S. carried out bioinformatics analyses. H.K.A.M. conceived the hypothesis and directed the project. M.U. and H.K.A.M. prepared the manuscript, which all authors edited and approved.

ACKNOWLEDGMENTS

We thank Yanling Wang and Hirohito Shimizu for technical assistance, UCLA Vector Core for preparation of *Cre-Gfp* lentiviral vector, Marianne Cilluffo and Sirus A. Kohan for electron microscopy, and UCLA Clinical Microarray Core for microarray analysis. We thank Dr. James Cross at University of Calgary for *Gcm1* KO tissues. This work was supported by RO1 HL097766 (to H.K.A.M.) and Eli and Edythe Broad Center of Regenerative Medicine and Stem Cell Research at UCLA. M.U. was supported by the Japan Society for the Promotion of Science Postdoctoral Fellowships for Research Abroad, and L.L. was supported by the American Association of Obstetricians and Gynecologists Foundation Scholarship and a Fellowship from CIRM. A.C. was supported by JCCF at UCLA. B.V.H. was supported by the Ruth L. Kirschstein National Research Service Award NIH/NHLBI T32 HL69766.

Received: January 24, 2013
Revised: June 28, 2013
Accepted: October 24, 2013
Published: November 25, 2013

REFERENCES

Anson-Cartwright, L., Dawson, K., Holmyard, D., Fisher, S.J., Lazzarini, R.A., and Cross, J.C. (2000). The glial cells missing-1 protein is essential for branching morphogenesis in the chorioallantoic placenta. Nat. Genet. *25*, 311–314.

Basyuk, E., Cross, J.C., Corbin, J., Nakayama, H., Hunter, P., Nait-Oumesmar, B., and Lazzarini, R.A. (1999). Murine Gcm1 gene is expressed in a subset of placental trophoblast cells. Dev. Dyn. *214*, 303–311.

Bladt, F., Riethmacher, D., Isenmann, S., Aguzzi, A., and Birchmeier, C. (1995). Essential role for the c-met receptor in the migration of myogenic precursor cells into the limb bud. Nature *376*, 768–771.

Boccaccio, C., and Comoglio, P.M. (2006). Invasive growth: a MET-driven genetic programme for cancer and stem cells. Nat. Rev. Cancer *6*, 637–645.

Chhabra, A., Lechner, A.J., Ueno, M., Acharya, A., Van Handel, B., Wang, Y., Iruela-Arispe, M.L., Tallquist, M.D., and Mikkola, H.K.A. (2012). Trophoblasts regulate the placental hematopoietic niche through PDGF-B signaling. Dev. Cell *22*, 651–659.

Christensen, J.G., Schreck, R., Burrows, J., Kuruganti, P., Chan, E., Le, P., Chen, J., Wang, X., Ruslim, L., Blake, R., et al. (2003). A selective small molecule inhibitor of c-Met kinase inhibits c-Met-dependent phenotypes in vitro and exhibits cytoreductive antitumor activity in vivo. Cancer Res. *63*, 7345–7355.

Furugori, K., Kurauchi, O., Itakura, A., Kanou, Y., Murata, Y., Mizutani, S., Seo, H., Tomoda, Y., and Nakamura, T. (1997). Levels of hepatocyte growth factor and its messenger ribonucleic acid in uncomplicated pregnancies and those complicated by preeclampsia. J. Clin. Endocrinol. Metab. *82*, 2726–2730.

Gabriel, H.D., Jung, D., Bützler, C., Temme, A., Traub, O., Winterhager, E., and Willecke, K. (1998). Transplacental uptake of glucose is decreased in embryonic lethal connexin26-deficient mice. J. Cell Biol. *140*, 1453–1461.

Gekas, C., Dieterlen-Lièvre, F., Orkin, S.H., and Mikkola, H.K.A. (2005). The placenta is a niche for hematopoietic stem cells. Dev. Cell *8*, 365–375.

Genbacev, O., Donne, M., Kapidzic, M., Gormley, M., Lamb, J., Gilmore, J., Larocque, N., Goldfien, G., Zdravkovic, T., McMaster, M.T., and Fisher, S.J. (2011). Establishment of human trophoblast progenitor cell lines from the chorion. Stem Cells *29*, 1427–1436.

Georgiades, P., Ferguson-Smith, A.C., and Burton, G.J. (2002). Comparative developmental anatomy of the murine and human definitive placentae. Placenta *23*, 3–19.

Golachowska, M.R., Hoekstra, D., and van IJzendoorn, S.C. (2010). Recycling endosomes in apical plasma membrane domain formation and epithelial cell polarity. Trends Cell Biol. *20*, 618–626.

Grant, B.D., and Donaldson, J.G. (2009). Pathways and mechanisms of endocytic recycling. Nat. Rev. Mol. Cell Biol. *10*, 597–608.

Hughes, M., Dobric, N., Scott, I.C., Su, L., Starovic, M., St-Pierre, B., Egan, S.E., Kingdom, J.C., and Cross, J.C. (2004). The Hand1, Stra13 and Gcm1 transcription factors override FGF signaling to promote terminal differentiation of trophoblast stem cells. Dev. Biol. *271*, 26–37.

Hunter, P.J., Swanson, B.J., Haendel, M.A., Lyons, G.E., and Cross, J.C. (1999). Mrj encodes a DnaJ-related co-chaperone that is essential for murine placental development. Development *126*, 1247–1258.

Huh, C.G., Factor, V.M., Sánchez, A., Uchida, K., Conner, E.A., and Thorgeirsson, S.S. (2004). Hepatocyte growth factor/c-met signaling pathway

is required for efficient liver regeneration and repair. Proc. Natl. Acad. Sci. USA *101*, 4477–4482.

Kauma, S.W., Bae-Jump, V., and Walsh, S.W. (1999). Hepatocyte growth factor stimulates trophoblast invasion: a potential mechanism for abnormal placentation in preeclampsia. J. Clin. Endocrinol. Metab. *84*, 4092–4096.

Kokkinos, M.I., Murthi, P., Wafai, R., Thompson, E.W., and Newgreen, D.F. (2010). Cadherins in the human placenta—epithelial-mesenchymal transition (EMT) and placental development. Placenta *31*, 747–755.

Levy, J.E., Jin, O., Fujiwara, Y., Kuo, F., and Andrews, N.C. (1999). Transferrin receptor is necessary for development of erythrocytes and the nervous system. Nat. Genet. *21*, 396–399.

Malhotra, S., and Kincade, P.W. (2009). Canonical Wnt pathway signaling suppresses VCAM-1 expression by marrow stromal and hematopoietic cells. Exp. Hematol. *37*, 19–30.

Maltepe, E., Bakardjiev, A.I., and Fisher, S.J. (2010). The placenta: transcriptional, epigenetic, and physiological integration during development. J. Clin. Invest. *120*, 1016–1025.

Martin-Belmonte, F., and Perez-Moreno, M. (2012). Epithelial cell polarity, stem cells and cancer. Nat. Rev. Cancer *12*, 23–38.

McQualter, J.L., Yuen, K., Williams, B., and Bertoncello, I. (2010). Evidence of an epithelial stem/progenitor cell hierarchy in the adult mouse lung. Proc. Natl. Acad. Sci. USA *107*, 1414–1419.

Morasso, M.I., Grinberg, A., Robinson, G., Sargent, T.D., and Mahon, K.A. (1999). Placental failure in mice lacking the homeobox gene Dlx3. Proc. Natl. Acad. Sci. USA *96*, 162–167.

Mould, A., Morgan, M.A., Li, L., Bikoff, E.K., and Robertson, E.J. (2012). Blimp1/Prdm1 governs terminal differentiation of endovascular trophoblast giant cells and defines multipotent progenitors in the developing placenta. Genes Dev. *26*, 2063–2074.

Nagai, A., Takebe, K., Nio-Kobayashi, J., Takahashi-Iwanaga, H., and Iwanaga, T. (2010). Cellular expression of the monocarboxylate transporter (MCT) family in the placenta of mice. Placenta *31*, 126–133.

Nasu, K., Zhou, Y., McMaster, M.T., and Fisher, S.J. (2000). Upregulation of human cytotrophoblast invasion by hepatocyte growth factor. J. Reprod. Fertil. Suppl. *55*, 73–80.

Natale, D.R.C., Starovic, M., and Cross, J.C. (2006). Phenotypic analysis of the mouse placenta. Methods Mol. Med. *121*, 275–293.

Plum, A., Winterhager, E., Pesch, J., Lautermann, J., Hallas, G., Rosentreter, B., Traub, O., Herberhold, C., and Willecke, K. (2001). Connexin31-deficiency in mice causes transient placental dysmorphogenesis but does not impair hearing and skin differentiation. Dev. Biol. *231*, 334–347.

Rhodes, K.E., Gekas, C., Wang, Y., Lux, C.T., Francis, C.S., Chan, D.N., Conway, S., Orkin, S.H., Yoder, M.C., and Mikkola, H.K.A. (2008). The emergence of hematopoietic stem cells is initiated in the placental vasculature in the absence of circulation. Cell Stem Cell *2*, 252–263.

Rinkevich, Y., Lindau, P., Ueno, H., Longaker, M.T., and Weissman, I.L. (2011). Germ-layer and lineage-restricted stem/progenitors regenerate the mouse digit tip. Nature *476*, 409–413.

Rossant, J., and Cross, J.C. (2001). Placental development: lessons from mouse mutants. Nat. Rev. Genet. *2*, 538–548.

Saito, S., Sakakura, S., Enomoto, M., Ichijo, M., Matsumoto, K., and Nakamura, T. (1995). Hepatocyte growth factor promotes the growth of cytotrophoblasts by the paracrine mechanism. J. Biochem. *117*, 671–676.

Schmidt, C., Bladt, F., Goedecke, S., Brinkmann, V., Zschiesche, W., Sharpe, M., Gherardi, E., and Birchmeier, C. (1995). Scatter factor/hepatocyte growth factor is essential for liver development. Nature *373*, 699–702.

Scifres, C.M., and Nelson, D.M. (2009). Intrauterine growth restriction, human placental development and trophoblast cell death. J. Physiol. *587*, 3453–3458.

Simmons, D.G., and Cross, J.C. (2005). Determinants of trophoblast lineage and cell subtype specification in the mouse placenta. Dev. Biol. *284*, 12–24.

Simmons, D.G., Natale, D.R.C., Begay, V., Hughes, M., Leutz, A., and Cross, J.C. (2008). Early patterning of the chorion leads to the trilaminar trophoblast cell structure in the placental labyrinth. Development *135*, 2083–2091.

Sivasubramaniyam, T., Garcia, J., Tagliaferro, A., Melland-Smith, M., Chauvin, S., Post, M., Todros, T., and Caniggia, I. (2013). Where polarity meets fusion: role of Par6 in trophoblast differentiation during placental development and preeclampsia. Endocrinology *154*, 1296–1309.

Somerset, D.A., Li, X.F., Afford, S., Strain, A.J., Ahmed, A., Sangha, R.K., Whittle, M.J., and Kilby, M.D. (1998). Ontogeny of hepatocyte growth factor (HGF) and its receptor (c-met) in human placenta: reduced HGF expression in intrauterine growth restriction. Am. J. Pathol. *153*, 1139–1147.

Stecca, B., Nait-Oumesmar, B., Kelley, K.A., Voss, A.K., Thomas, T., and Lazzarini, R.A. (2002). Gcm1 expression defines three stages of chorio-allantoic interaction during placental development. Mech. Dev. *115*, 27–34.

Takayanagi, T., Aoki, Y., and Tanaka, K. (2000). Expression of constitutively active c-MET receptor in human choriocarcinoma. Gynecol. Obstet. Invest. *50*, 198–202.

Tanaka, S., Kunath, T., Hadjantonakis, A.K., Nagy, A., and Rossant, J. (1998). Promotion of trophoblast stem cell proliferation by FGF4. Science *282*, 2072–2075.

Uehara, Y., Minowa, O., Mori, C., Shiota, K., Kuno, J., Noda, T., and Kitamura, N. (1995). Placental defect and embryonic lethality in mice lacking hepatocyte growth factor/scatter factor. Nature *373*, 702–705.

Unezaki, S., Horai, R., Sudo, K., Iwakura, Y., and Ito, S. (2007). Ovol2/Movo, a homologue of Drosophila ovo, is required for angiogenesis, heart formation and placental development in mice. Genes Cells *12*, 773–785.

Uy, G.D., Downs, K.M., and Gardner, R.L. (2002). Inhibition of trophoblast stem cell potential in chorionic ectoderm coincides with occlusion of the ectoplacental cavity in the mouse. Development *129*, 3913–3924.

Van Handel, B., Prashad, S.L., Hassanzadeh-Kiabi, N., Huang, A., Magnusson, M., Atanassova, B., Chen, A., Hamalainen, E.I., and Mikkola, H.K. (2010). The first trimester human placenta is a site for terminal maturation of primitive erythroid cells. Blood *116*, 3321–3330.

Watson, E.D., and Cross, J.C. (2005). Development of structures and transport functions in the mouse placenta. Physiology (Bethesda) *20*, 180–193.

Wynne, F., Ball, M., McLellan, A.S., Dockery, P., Zimmermann, W., and Moore, T. (2006). Mouse pregnancy-specific glycoproteins: tissue-specific expression and evidence of association with maternal vasculature. Reproduction *131*, 721–732.

Young, B.C., Levine, R.J., and Karumanchi, S.A. (2010). Pathogenesis of preeclampsia. Annu. Rev. Pathol. *5*, 173–192.

Developmental Cell, Volume 27

Supplemental Information

c-Met-Dependent Multipotent Labyrinth Trophoblast Progenitors Establish Placental Exchange Interface

Masaya Ueno, Lydia K. Lee, Akanksha Chhabra, Yeon Joo Kim, Rajkumar Sasidharan, Ben Van Handel, Ying Wang, Masakazu Kamata, Paniz Kamran, Konstantina-Ioanna Sereti, Reza Ardehali, Meisheng Jiang, and Hanna K.A. Mikkola

Inventory of Supplemental Items

Related to Figure 1:

- Figure S1

Related to Figure 2:

- Figure S2

Related to Figure 3:

- Figure S3
- Table S1
- Table S2

Related to Figure 4:

- Figure S4

Related to Figure 5:

- Figure S5

Related to Figure 6:

- Figure S6

Related to Supplemental Extended Experimental Procedures:

- Table S3

Supplemental Figures

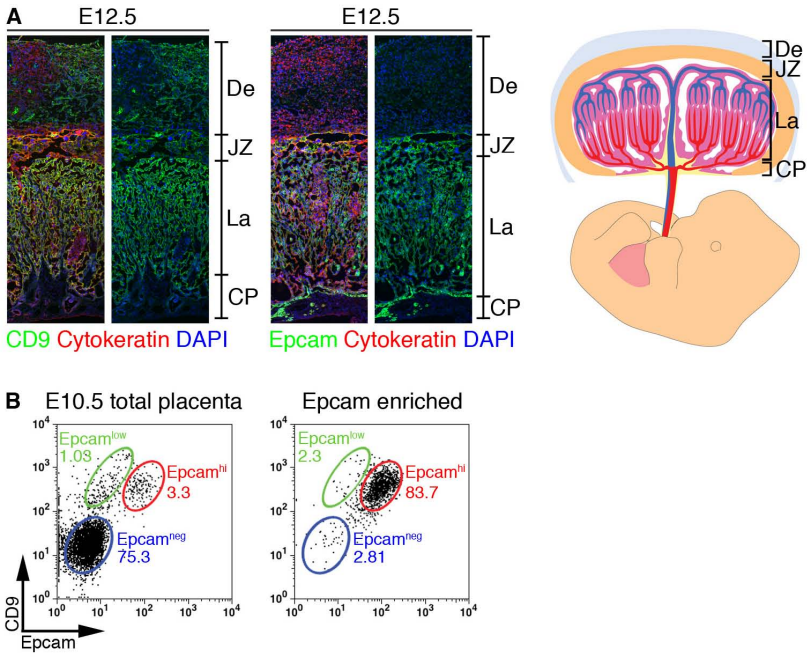

Figure S1. Labyrinth trophoblasts express CD9 and Epcam. Related to Figure 1.
(A) Immunofluorescence and schematic representation of mouse placental structure. Sections from E12.5 placenta were stained with antibodies for CD9 or Epcam (green), and Cytokeratin (red, trophoblasts). DAPI (blue) indicates nuclei. The fully developed placenta is composed of three major layers: a decidual layer (De), which includes decidual cells of the uterus; a junctional zone (JZ) which attaches the fetal placenta to the decidua and contains trophoblast giant cells (TGC) and spongiotrophoblasts (Sp); and a labyrinth layer (La), composed of fetal endothelial cells and labyrinth trophoblasts (SynT-I and -II, and sinusoidal trophoblast giant cells (sTGC)) that establish the substance exchange interface between fetal and maternal circulations. CP, chorionic plate.
(B) FACS analysis of cells enriched by anti-Epcam antibody documents effective isolation of Epcam^{hi} cells without significant contamination of differentiated Epcam^{low} cells.

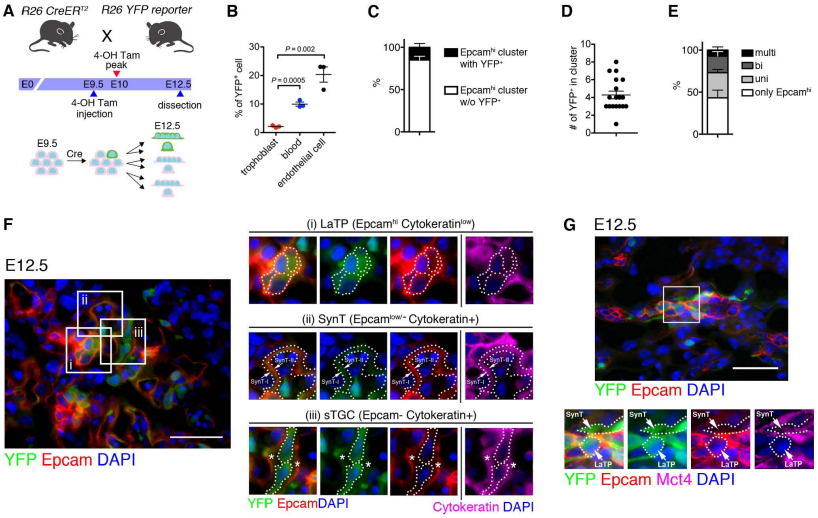

Figure S2. Epcam^{hi} LaTP cells are clonally linked to terminally differentiated SynT. Related to Figure 2.

(A) Schematic for *in vivo* clonality experiment. *Rosa26 (R26) YFP* reporter mice were mated with *R26 CreER^{T2}* mice. At E9.5 Cre-mediated gene deletion was induced by injection with 4OH-tamoxifen and embryos were dissected at E12.5.

(B) Frequency of Cre-mediated gene-recombination in different cell types in the placenta documenting rare marking of trophoblasts. (C) Frequency of Epcam^{hi} clusters containing YFP-labeled cells.

(D) Average number of YFP^{+} cells in a labeled Epcam^{hi} cell cluster.

(E) Differentiation potential of YFP labeled cells in individual clusters. Multi, Epcam^{hi} LaTP with SynT-I, SynT-II and sTGC; bi, Epcam^{hi} with SynT-I and SynT-II; uni, Epcam^{hi} with sTGC, SynT-I or SynT-II.

(F) Documentation of multi-lineage differentiation in a cluster of YFP^{+} labeled trophoblasts. (i) Epcam^{hi} Cytokeratin^{low} (LaTP), (ii) SynT-I (Epcam^{-} Cytokeratin^{+}) and SynT-II (Epcam^{low} Cytokeratin^{+}) and sTGC (iii) (Epcam^{-} Cytokeratin^{+}), *, SynT layer.

(G) Documentation of terminally differentiated SynT cells (Epcam^{low} Mct4^{+}) in the same YFP^{+} marked clusters as Epcam^{hi} LaTP. Epcam (red), YFP (green), DAPI (blue), Mct4 (purple). Scale bar 100 μm.

All error bars indicate SEM (Standard error of mean).

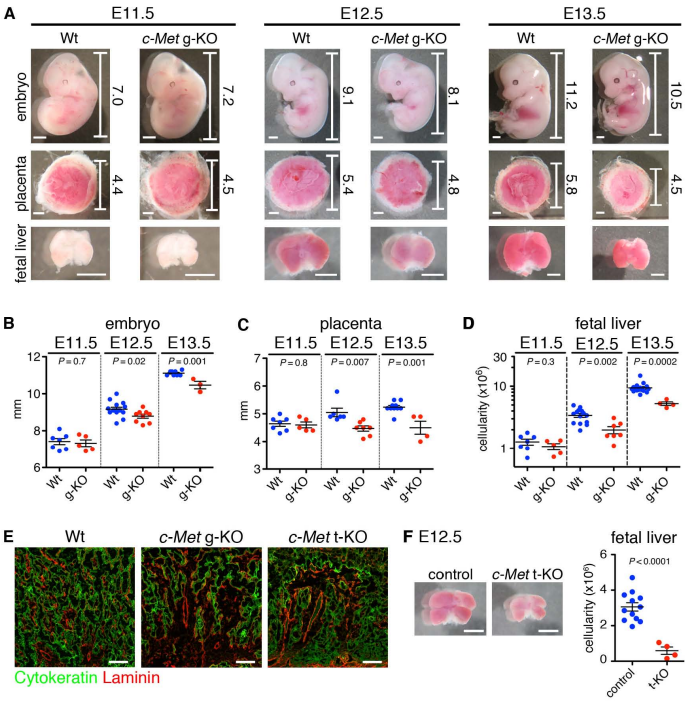

G

GO terms of 1,294 downregulated genes in *c-Met* g-KO CD9⁺ placental cells

rank	GO term	gene count	P value
1	cell cycle phase	89	5.80E-22
2	cell cycle	130	1.99E-21
4	DNA metabolic process	100	4.67E-20
5	M phase	78	9.39E-20
6	RNA processing	101	2.35E-19
24	transcription	219	1.76E-07
25	one-carbon metabolic process	29	9.88E-07
26	cellular macromolecule catabolic process	91	1.02E-06
27	methylation	22	3.73E-06
62	placenta development	18	0.00157

GO terms of 1,221 upregulated genes in *c-Met* g-KO CD9⁺ placental cells

rank	GO term	gene count	P value
1	response to wounding	128	6.78E-33
2	immune response	148	2.99E-29
3	cell adhesion	159	6.15E-26
8	vasculature development	79	6.99E-16
12	coagulation	36	9.61E-15
14	regulation of cell proliferation	129	1.42E-14
19	chemotaxis	41	3.22E-11
16	positive regulation of response to stimulus	61	3.07E-13
22	regulation of cytokine production	47	6.77E-11
23	positive regulation of cell activation	38	1.86E-10

Figure S3. c-Met regulates both placental and embryonic development. Related to Figure 3.

(A, B, C and D) Kinetic analysis documenting growth retardation of *c-Met* deficient embryos, fetal livers and placentas after E12.5. Scale bar 1 mm.

(E) IF for trophoblast specific marker (Cytokeratin) and ECM marker that marks blood vessels (Laminin) documenting poorly developed branching structure in *c-Met* g-and t-KO placenta.

(F) *c-Met* t-KO fetal livers show smaller size and low cellularity.

(G) Selected GO (gene ontology) categories representing genes down- or up-regulated in placental CD9$^+$ cells in the absence of c-Met signaling.

All error bars indicate SEM (Standard error of mean).

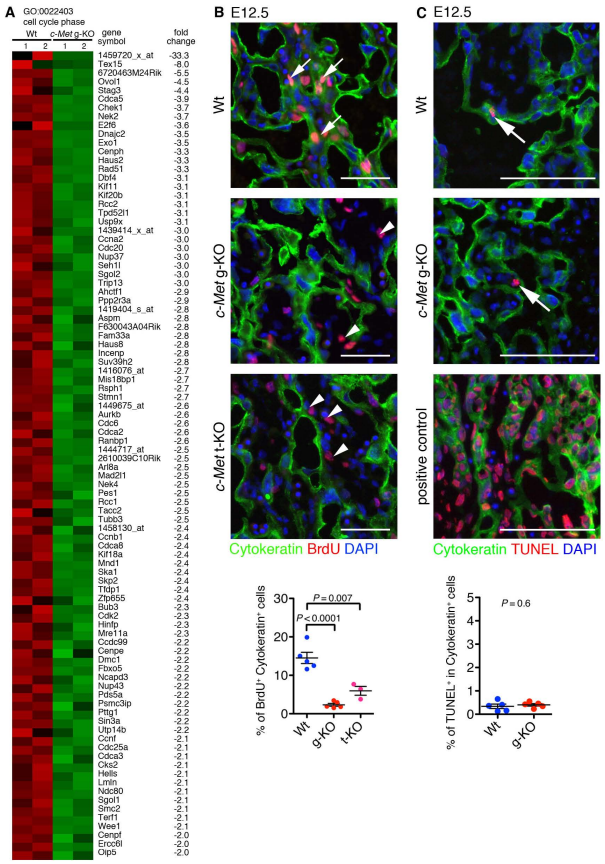

Figure S4. c-Met directly regulates trophoblast proliferation. Related to Figure 4.
(A) Microarray analysis of $CD9^+$ trophoblasts from Wt *vs. c-Met* g-KO placenta. The heat map presents expression of various genes that related to GO category "cell cycle phase" that are suppressed in $CD9^+$ trophoblasts of *c-Met* g-KO placenta.
(B) BrdU incorporation assay. Sections from E12.5 Wt, *c-Met* g-KO and t-KO placentas were stained for Cytokeratin (green), BrdU (red), and DAPI (blue). Although $BrdU^+$ $Cytokeratin^+$ trophoblasts (arrows) were observed in Wt placenta, only $Cytokeratin^-$ cells (arrowheads) showed mitotic activity in *c-Met* g- and t-KO placenta. Scale bar 100 μm.
(C) Sections from Wt and *c-Met* g-KO placentas were stained for TUNEL (red), Cytokeratin (green) and DAPI (blue). Arrows indicate TUNEL and Cytokeratin double-positive cells. No significant difference was observed in apoptosis between Wt and *c-Met* g-KO trophoblasts. Scale bar 100 μm.
All error bars indicate SEM (Standard error of mean).

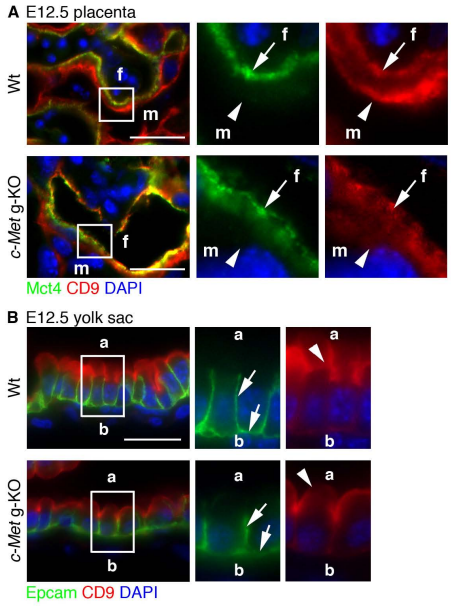

Figure S5. Loss of *c-Met* compromises cell polarity specifically in the placenta. Related to Figure 5.

(A) IF for Mct4 (green), CD9 (red) and DAPI (blue) in Wt and *c-Met* g-KO placentas at E12.5. Presence of both $Mct4^{-}$ $CD9^{+}$ cells and $Mct4^{+}$ $CD9^{+}$ cells indicates that both SynT-I and II are present in Wt and *c-Met* g-KO placentas. Notably, in Wt placenta, Mct4 is specifically expressed on the fetal side in SynT-II and CD9 is expressed on both apical side of SynT-I and fetal side of SynT-II. However diffused localization of both CD9 and Mct4 was observed in *c-Met* g-KO placenta. Arrows indicate fetal side of SynT-II and arrowheads indicate apical membrane of SynT-I. f, fetal side. m, maternal side. Scale bar 25 μm.

(B) IF for Epcam (green), CD9 (red), and DAPI (blue) on Wt and *c-Met* g-KO yolk sac. No abnormal localization of Epcam or CD9 and was observed in *c-Met* g-KO yolk sac. Arrows indicate basolateral localization of Epcam and arrowheads indicate apical staining of CD9; a, apical; b, basal. Scale bar 25 μm.

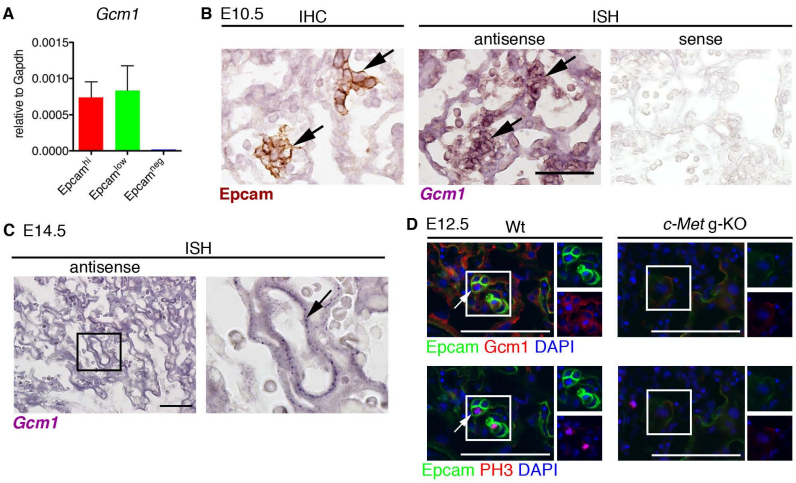

Figure S6. Gcm1 is expressed in LaTP and SynT in the placenta. Related to Figure 6.

(A) QRT-PCR documenting the enriched expression of *Gcm1* in both Epcam^{hi} LaTP and Epcam^{low} SynT in E 10.5 placenta. Error bars indicate SEM (Standard error of mean)

(B) IHC with anti-Epcam antibody and *in situ* hybridization (ISH) with *Gcm1* antisense probe indicates high expression of *Gcm1* in Epcam^{hi} LaTP (arrows) in E10.5 placenta. Scale bar 100 µm.

(C) ISH analysis showing high expression of *Gcm1* in SynT-II layer (arrow in the inset) adjacent to maternal blood spaces in E14.5 placenta. Scale bar 100 µm.

(D) Sections from Wt and *c-Met* g-KO placentas at E12.5 were stained for Epcam, Gcm1, PH3, and DAPI. Arrows indicate Epcam^{hi} and PH3^{+} cells that also express *Gcm1*. Scale bar 100 µm.

Supplemental Table Legends

Table S1. Genes induced by c-Met signaling in placental trophoblasts. 1,294 genes down-regulated in *c-Met* g-KO $CD9^+$ placental cells with p value <0.05 and fold change cutoff ≥2.0. Related to Figure 3.

Table S2. Genes suppressed by c-Met signaling in placental trophoblasts. 1,221 genes up-regulated in *c-Met* g-KO $CD9^+$ placental cells with p value <0.05 and fold change cutoff ≥2.0. Related to Figure 3.

Supplemental Extended Experimental Procedures

Generation of germline *c-Met* KO and trophoblast specific *c-Met* KO embryos

The *c-Met* germline KO (g-KO) mice were generated by breeding *c-Met*$^{fl/wt}$ mice with *VavCre* transgenic mouse (kindly provided by Dr Thomas Graf, Center for Genomic Regulation, Barcelona, Spain), which occasionally results in Cre mediated gene deletion in germ cells. Subsequent breeding was carried out with germline deleted heterozygous animals.

To generate trophoblast specific *c-Met* KO (t-KO) mice, lentiviral Cre was used to delete conditionally targeted c-Met floxed alleles in the trophoblasts. FU-CreGFP-W (lentiviral vector expressing *Cre-Gfp* under the *UbiC* promoter) vector was kindly provided by Dr. Guoping Fan (UCLA, Los Angeles, CA, USA). *c-Met*$^{fl/fl}$ or *c-Met*$^{fl/w}$ female mice were superovulated by treatment with pregnant mare's serum gonadotropin followed by human chorionic gonadotropin 48 h later, and then mated with *c-Met*$^{fl/fl}$ male mice. Blastocysts were collected from uterus at 3.5 day after copulation. Embryos were maintained in M2 media (Sigma-Aldrich) during microinjection process. Lentiviral vector (titer 1-5 x 10^8/ml) was injected using a Fematotips II glass needle and FematoJet microinjector (Eppendorf) with an injection pressure Pi=120 and constant flow pressure Pc=20. After lentiviral vector injection, embryos were transplanted into the uterus of 2.5-day

pseudopregnant recipients. After 10 days of transplantation, embryos (E12.5) were dissected and analyzed.

Immunofluorescence Staining

IF was performed as previously reported (Rhodes et al., 2008). Briefly, for IHC and IF, tissues were fixed in 4% para-formaldehyde at 4°C overnight, and frozen in O.C.T. Compound (Sakura Finetek). For Bromodeoxyuridine (BrdU) incorporation assay, BrdU (Sigma-Aldrich, 100 µl of 10 mg/ml) was injected intraperitoneally into pregnant females. The females were sacrificed 1 hr after injection, and placentas were fixed and processed for IF (see below). For detection of Cytokeratin or Epcam, antigen retrieval was performed with Proteinase K treatment. For detection of incorporated BrdU, section was treated with 1 mg/ml DNase (Sigma-Aldrich) for 20 min. For amplification signal, Tyramide Signal Amplification kit (Invitrogen) was used for detection of Cre-Gfp and BrdU antigen. Following antibodies were used: FITC-conjugated anti-BrdU, Anti-CD31 (PECAM), FITC-conjugated and PE-conjugated anti-CD9, FITC-conjugated anti-CD71, and anti-Epcam antibody (CD326), (all from BD Pharmingen); Anti-phospho-histone H3 and anti-Mct4 antibody (Millipore); Biotinylated anti-FITC, Cy3-conjugated anti-Rat IgG , and biotinylated anti-rabbit IgG antibody (Jackson ImmunoResearch); Anti-Prkcz and anti-Gcm1 antibody (Santa Cruz Biotechnology); anti-Uvomorulin/ E-cadherin antibody (Sigma-Aldrich), anti-Cytokeratin antibody (Dako). For detection of YFP, Alexa Fluor 488 conjugated anti-GFP antibody (Invitrogen) was used. TUNEL assay was

performed using *in situ* cell death detection kit (Roche). End-labeled DNA with fluorescein-dUTP was detected by anti-FITC antibody. To stain cultured LaTP and their progeny, Epcam^{hi} cells were first cultured on cover glass and then fixed with 4% PFA for 5 min. All stainings were performed as indicated for IF sections. For detection of BrdU, fixed cells were treated with 2N HCl for 5min before staining with anti-BrdU antbody. For detection of cell-cell boundaries, anti-uvomolulin/E-cadherin antibody (Sigma) was used. Contrast and levels of images were adjusted for display with Adobe Photoshop.

Microarray analysis

To isolate trophoblasts for microarray analysis, single cell suspension of E12.5 placentas was stained with PE-conjugated anti-CD9 antibody, followed by coating with anti-PE antibody-microbeads (Miltenyi Biotec) and separation of CD9 positive cells with MACS LS column (Miltenyi Biotec) according to the manufacture's instructions. RNA from CD9$^+$ cells was purified by RNeasy mini kit (Qiagen). For comparison of gene expression in Wt and *c-Met* germline KO (g-KO) CD9$^+$ trophoblasts, Affymetrix MOE430_2.0 microarrays (Affymetrix) were performed on CD9$^+$ cells from two Wt and two *c-Met* g-KO placentas. Raw data are available at GEO with accession numbers GSE38342. Differential expression assessment was performed using the LIMMA package (Smyth, 2004). Probes with a p value less than 0.05 and absolute fold change threshold of two were called as differentially expressed. Functional annotation (gene ontology terms

and pathway terms enrichment analysis) was performed using the online software DAVID (http://david.abcc.ncifcrf.gov/) on the list of differentially expressed genes for both up-regulated and down-regulated genes. The normalized expression values derived using RMA method (Irizarry et al., 2003) were converted to z-scores for drawing heatmaps.

Quantitative RT-PCR (QRT-PCR)

$CD9^+$ cells from placenta were isolated and total RNA was extracted (see above). cDNA synthesis was carried out according to the manufacturer's protocol of Quantitect Reverse transcription kit (QIAGEN), and QRT-PCR was performed using a LightCycler 480 (Roche) with LightCycler 480 SYBR Green I Master (Roche). Primer sequences are shown in Table S3.

Table S3. List of primers used for QRT-PCR. Related to Figures 1-6.

gene name	forward primer sequence	reverse primer sequence
Ccna2	TGATAGATGCTGACCCGTACCTT	CTCTGGTGGGTTGAGAAGAGAAA
Ccne1	TTGAATTGGGGCAATAGAGAAGA	AGTCCTGTGCCAAGTAGAACGTC
Ccne2	GTGCATTCTAGCCATCGACTCTT	AGGCACCATCCAGTCTACACATT
Cdc45	CCTGAAGCAAGTCAAGCAGAAAT	AGTCTGTACACGCATGTCCTTCA
Cdh1	AGAGAACTCATTTACAGTGGCATTC	GTTTCTCTCCTTTTCTCTCCTCTGT
Cebpa	GCAGTGTGCACGTCTATGCT	AAGTCTTAGCCGGAGGAAGC
Chek1	CGCTTACTGAACAAGATGTGTGG	TTTATGAAGCAAAGCCAGAGGAG
Crb3	CCTTTCACAAATAGCACAACTCAAC	AGAAACAGTCCCACTGCTATAAGG
Ctsq	TGGAAAGAGTGGATGGGAAG	CAAGTGCACGTTTCCAGAGA
Dlx3	AGTCACTGACCTGGGCTATTACA	CCTATAGGATCCCCCGTAGGTAT
Gapdh	GGAGAAACCTGCCAAGTATGATG	AAGAGTGGGAGTTGCTGTTGAAG
Gcm1	GCCTTACGAAGAGAAAGTATCTGTG	AGAACAGAAGTTTAGGAGCATCTCA
Gjb2	AAACTTCTAGACTCCCAATCCTGTT	TATTGTTACAAAATGGCTTTCCAAT
Gjb3	CTCCCACTTTGAATTCACTAAGCTA	AGTTCTTTTTGCTGTTGCTATGTCT
Hand1	GTTCCCATTCGTTGCTGAAT	CTGCGAGTGGTCACACTGAT
Limk1	CATGTCTTCACTCCGCTTCA	GTGGGGAGCACAGAATTGAT
Limk2	GTGGGCTCAGTCAAAAGCTC	CCACAAGGGTGCAAAGAAAT
Mct1	TTGCCCCTTTGTCTACAACC	CAGCATTCCACAATGGTCAC
Mct4	GGATGGTCGTGCTTCATTTT	AATGGATCCAATCCAACCAA
Nodal	ACTTTGCTTTGGGAAGCTGA	ACCTGGAACTTGACCCTCCT
Nr6a1	CTGTTTCCGTCCCAGATGAT	TGTTGCAAATGCTCCTCTTG
Ovol2	AACTCCAGAGCTTCACGACG	CTGGGTGAAGGCCTTGTTAC
Prkcz	GAACACTGAAGACTACCTTTTCCAA	TGGGATCCTTATTTAAAAATCCTTT
Prl3b1	CCACACTGCTGCAATCCTTA	CTGACCATGCAGACCAGAAA
Prl3d1	GGGAGAATGTGTCCTCCAAA	ATCTGCGGCCAAGATAAATG
Syna	TACCCTGTCTGTGGACACCA	ACCAGAGGAGTTGAGGCAGA
Synb	ATCCCCATAAGGACCGTTTC	AGGCAGAGAGGTTGCCTACA
Tead3	CGAACGCTTTCTTCCTTGTC	TACTTCTCGGGCAGATGCTT
Tpbpa	AAGTTAGGCAACGAGCGAAA	AGTGCAGGATCCCACTTGTC

Placenta as a newly identified source of hematopoietic stem cells

Lydia K. Lee[a,b], Masaya Ueno[b], Ben Van Handel[b] and Hanna K.A. Mikkola[b,c]

[a]Department of Obstetrics and Gynecology, [b]Department of Molecular, Cell and Developmental Biology and [c]Eli and Edythe Broad Center of Regenerative Medicine and Stem Cell Research, University of California, Los Angeles, Los Angeles, California, USA

Correspondence to Hanna K.A. Mikkola, Department of Molecular, Cell and Developmental Biology, Eli and Edythe Broad Center of Regenerative Medicine and Stem Cell Research, University of California, Los Angeles, 615 Charles E Young Drive South, BSRB, Room 451B, Los Angeles, CA 90095, USA
Tel: +1 310 825 2565; fax: +1 310 206 5553;
e-mail: hmikkola@mcdb.ucla.edu

Current Opinion in Hematology 2010, 17:313–318

Purpose of review

The lifelong stream of all blood cells originates from the pool of hematopoietic stem cells (HSCs) generated during embryogenesis. Given that the placenta has been recently unveiled as a major hematopoietic organ that supports HSC development, the purpose of this review is to present current advances in defining the origin and regulation of placental HSCs.

Recent findings

The mouse placenta has been shown to have the potential to generate multipotential myelo-lymphoid hematopoietic stem/progenitor cells *de novo*. The cellular origin of HSCs generated in the placenta and other sites has been tracked to the hemogenic endothelium by using novel genetic and imaging-based cell-tracing approaches. Transplantable, myelo-lymphoid hematopoietic stem/progenitor cells have also been recovered from the human placenta throughout gestation.

Summary

The discovery of the placenta as a major organ that generates HSCs and maintains them in an undifferentiated state provides a valuable model to further elucidate regulatory mechanisms governing HSC emergence and expansion during mouse and human development. Concurrent efforts to optimize protocols for placental banking and HSC harvesting may increase the therapeutic utility of the human placenta as a source of transplantable HSCs.

Keywords

blood flow, hematopoietic stem cell, hemogenic endothelium, lineage tracing, placenta

Curr Opin Hematol 17:313–318

1065-6251

Introduction

Lifelong production of all blood cell types is sustained by the multipotent hematopoietic stem cells (HSCs). HSCs are formed only during a narrow time window in embryonic development, after which their pool is maintained by self-renewing cell divisions. However, HSCs are not the first hematopoietic cells to appear during development, as early embryonic survival depends on the immediate production of mature blood cells. The challenge of rapidly generating the differentiated blood cells while concomitantly protecting developing HSCs from premature differentiation is met by segregating embryonic hematopoiesis into multiple waves that occur in different anatomical compartments.

The first, transient populations of blood progenitors giving rise to the primitive erythroblasts and definitive myelo-erythroid cells – required to ensure fetal oxygen delivery, tissue remodeling and defense – are produced in the blood islands of the extra-embryonic yolk sac [1,2]. As the conceptus develops, other vascular tissues are recruited for HSC production. Once generated, HSCs are sequestered into the fetal liver for their expansion and maturation before establishing lifelong residence in the bone marrow [3]. The aorta–gonad–mesonephros (AGM) region and the umbilical and vitelline arteries have been regarded as the sites of HSC emergence [4,5]. However, as the fetal liver cannot generate HSCs *in situ* and the number of HSCs found in the liver far exceeds the quantity formed in the AGM, the question was raised whether the yolk sac could also contribute to the pool of fetal liver HSCs, or whether another yet unidentified organ could participate in this process. Recent studies have revealed that the placenta is a major hematopoietic organ contributing to both generation and expansion of multipotential hematopoietic stem/progenitor cells. Here, we review how hematopoietic activity in the placenta was discovered in mice and humans, and discuss the recent findings on the cellular origin and regulation of placental HSCs.

Discovery of hematopoietic stem cells in the mouse placenta

Evidence of hematopoietic activity in the placenta was introduced by early reports documenting that the mouse placenta contains clonogenic hematopoietic precursors capable of rescuing anemia or triggering graft-versus-host disease after transplantation [6–8]. Although the placenta

was overlooked as a potential hematopoietic organ for decades, newfound interest in its role in blood formation has awakened in light of recent findings confirming that the placenta possesses intrinsic hematopoietic properties.

The hypothesis that the placenta could bear *de novo* hematopoietic activity stemmed from chick-to-quail grafting experiments, which revealed the presence of multipotent hematopoietic cells in the avian allantois [9]. The allantois is a mesodermal appendage that functions in oxygen and nutrient exchange in avian embryos, analogous to the mammalian placenta. As the mammalian allantois gives rise to the umbilical cord and placental vasculature, it was hypothesized that these tissues could be engaged in hematopoiesis. A screen for hematopoietic activity across extraembryonic and intraembryonic sites in mid-gestation embryos revealed multipotent progenitors in the placenta at the 20 somite-pair stage (approximately E9.0), that is, after similar progenitors were detectable in the yolk sac and the caudal half of the embryo but before the fetal liver [10]. Subsequent studies confirmed that the placenta harbors bona fide HSCs that are able to generate all blood cell types upon serial transplantation into lethally irradiated adult mice [11,12]. Transplantation assays detected the first HSCs in the placenta at E10.5–11.0, concurrently with the AGM. Placental HSC activity increased rapidly by E12.5–13.5. At this time, the placenta harbored 15-fold more HSCs than the AGM or the yolk sac, whose repopulating units remained low. The number of HSCs in the liver increased concomitantly with the placenta [11], rising through late gestation even while the placental HSC pool declined. As the placenta is directly upstream of the liver in fetal circulation, these findings pointed to the placenta as a major contributor of HSCs seeding the liver.

Transplantation of cells from the placenta, purified by fluorescence-activated cell sorting, confirmed that its HSCs at E12.5 displayed the classical surface phenotype of actively cycling fetal HSCs, expressing CD34 and c-Kit [11]. Interestingly, another study presented E12.0 placental cells that were able to engraft in *Rag-2*$^{-/-}\gamma C^{-/-}$ recipients and lacked the expression of CD150 and CD48 surface antigens [13]. This finding implies that although these CD150^{-}CD48^{-} HSCs are capable of multilineage engraftment, they may be phenotypically more immature than the CD150^{+}CD48^{-} HSCs found in the fetal liver later in development. Phenotypic maturation also occurs with respect to vascular endothelial cadherin (VEC), which is expressed on endothelium and nascent HSCs [14], but this cell-surface protein is rapidly downregulated upon HSC colonization of the fetal liver and is absent from bone marrow HSCs [15,16]. These results suggest that in addition to changes in anatomic localization of HSCs, the dynamic process of HSC development also involves transitions in cell surface phenotype.

Hematopoietic activity in the human placenta

Because hematopoiesis is highly conserved in vertebrates, the discovery of HSCs in the mouse placenta attracted interest in the hematopoietic potential of the human placenta. Recent studies have provided evidence that the human placenta harbors hematopoietic activity throughout gestation [17•,18•,19]. It is important to note that two different systems are used to denote the age of a human conceptus: the developmental age [18•] calculated as the number of weeks from conception, and the clinical gestational age [17•,19], which is 2 weeks more than the developmental age. One group reported that CD34^{++}CD45^{low} placental cells could generate myeloid cells with some erythroid derivatives in methylcellulose assays, as well as natural killer and B cells in liquid cultures. Although the total number of CD34^{++}CD45^{low} cells increases with placental mass as gestational age advances, the frequency of these cells peaks at 5–8 weeks and declines sharply at 9 weeks of gestation (i.e. 3–6 weeks and 7 weeks of developmental age, respectively) [17•,19]. This was reminiscent of the kinetics of HSCs in the mouse placenta [11]. Residence of long-term reconstituting HSCs in human placentas was demonstrated in another study by performing transplantation assays of sorted CD34^{+} cells into irradiated nonobese diabetic-severe combined immunodeficiency or *Rag* $\gamma C^{-/-}$ mice [18•]. Multilineage reconstitution was observed from 9 weeks after conception until full-term delivery, whereas engraftment of human cells could be detected by PCR as early as 6 developmental weeks (11 and 8 weeks of gestational age, respectively). Although more work needs to be done to define the origin of HSCs in the human placenta, these studies have uncovered the human placenta as a robust and more accessible hematopoietic organ that can be used to investigate HSC ontogeny and regulation during human development.

Furthermore, the placenta may provide an additional source of HSCs for transplantation. Since the pioneering clinical studies that established the umbilical cord blood as a source of transplantable HSCs two decades ago, there have been continuous efforts to enhance the methods for the collection, cryopreservation and recovery of viable cells [20,21]. It is possible that in combination with the HSCs harvested from the cord blood, HSCs obtained from the placenta proper may provide sufficient HSCs to transplant adult patients.

Origin of hematopoietic stem cells in the placenta

Although functional assays suggested that the placenta provides a supportive niche for HSCs, these assays alone could not determine definitively whether placental HSCs emerge *in situ* or migrate from other hematopoietic sites.

Because fetal blood circulation is directed from the dorsal aorta through the placenta to the fetal liver, most HSCs generated in the AGM traverse the placenta along their journey towards the liver and may pause in placental niches for expansion, thereby contributing to the total placental HSC count.

In order to evaluate the capacity of the placenta to generate HSCs *de novo*, it is important to understand its ontogeny and structure [22,23]. The placenta is composed of two main tissues, the trophoblast and the mesoderm. The trophoblast lineage (trophectoderm) segregates from the embryonic lineage (inner cell mass) before implantation at the blastocyst stage (E3.5 in mice). Trophoblasts comprise the most abundant cell type in the placenta and line the maternal blood spaces, whereas the mesoderm-derived allantois generates the feto-placental vasculature. The allantois grows from the posterior primitive streak into the exocoelomic cavity and fuses with the chorion, inducing the extensive branching of the fetal vasculature into the trophoblast layer. This chorioallantoic patterning results in the formation of the labyrinthine region in the murine placenta and the chorionic villi in the human placenta, which are homologous sites of fetal–maternal exchange (See Fig. 1).

To investigate whether the placental mesodermal tissues possess endogenous hematopoietic potential, mouse allantois and chorion were isolated prior to the establishment of circulation and subjected to explant or stroma co-culture assays. Two independent studies reported the capacity of these mesodermal tissues to generate myeloid and definitive erythroid cells in culture, providing evidence that placental tissues devoid of any circulating cells indeed had intrinsic hematopoietic potential [24,25]. Further evidence that the placenta is an autonomous site of origin of multipotential hematopoietic stem/progenitor cells was provided by studies using *Ncx1*$^{-/-}$ mouse embryos, which do not have blood flow owing to the lack of heartbeat [26]. Even in the absence of circulating contributors, cells expressing CD41 (a marker of nascent hematopoietic cells) were found to emerge from the lumen of large fetal blood vessels in the placenta at E10.0. Most importantly, placental tissues possessed the ability to generate both myelo-erythroid as well as B and T lymphoid cells, documenting the broad differentiation potential that is characteristic of HSCs. The results were comparable to the observed multilineage hematopoietic potential in the caudal half of the embryo proper (which contains the developing AGM) as well as in the yolk sac. Because the *Ncx1*$^{-/-}$ embryos become developmentally retarded and die before

Figure 1 The placenta is a hematopoietic organ that supports generation and proliferation of hematopoietic stem cells

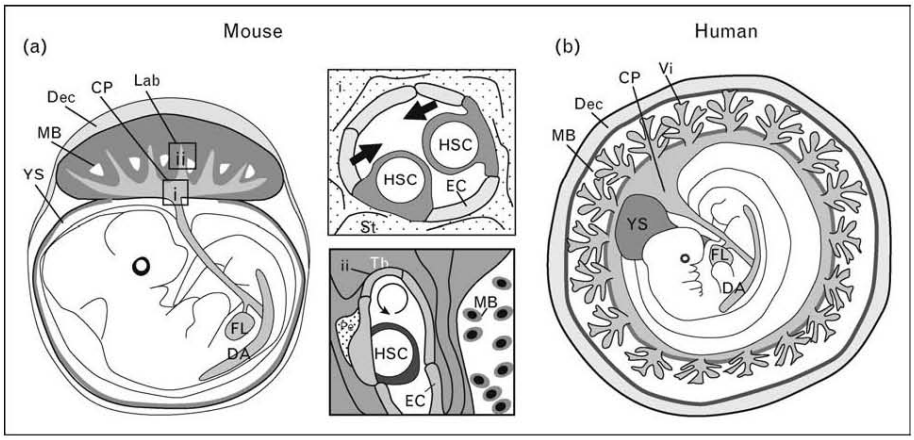

(a) The mouse placenta consists of two distinct vascular regions that function as putative niches for HSC development. The chorionic plate harbors large fetal blood vessels that are contiguous with the umbilical cord vessels and connect with the fetus. These blood vessels are potential sites of HSC generation (i). The labyrinth region contains an extensive network of small fetal blood vessels that are surrounded by trophoblasts lining the maternal blood spaces. The labyrinth is the site of fetal–maternal exchange, and may serve as a niche for HSC expansion (ii). (b) The human placenta also contains two vascularized regions, the chorionic plate and the villi. The villi are physiologically analogous with the labyrinth of the mouse placenta and contain hematopoietic stem/progenitor cells in the vascular and perivascular locations. It is hypothesized that the large vessels of the chorionic plate in the human placenta also have *de novo* hematopoietic potential. Although the macroscopic organization of the placenta and other extra-embryonic tissues differ between humans and mice, it is likely that similar cellular and molecular mechanisms coordinate placental hematopoiesis in both species. CP, chorionic plate; DA, dorsal aorta; Dec, decidua; EC, endothelial cell; FL, fetal liver; HSC, hematopoietic stem cell; Lab, labyrinth; MB, maternal blood space; Pe, pericyte; St, stroma; Tb, trophoblast; Vi, villi; YS, yolk sac.

E10.5, it was not possible to assess the engraftment and self-renewal potential of these cells by transplantation into adult recipients. Nevertheless, these studies provide strong evidence that the placenta parallels the AGM and the yolk sac in its intrinsic capacity to generate multipotential hematopoietic stem/progenitor cells *de novo*.

Not only the anatomical source but also the cellular origin of HSCs has been a controversial topic. It has been postulated that the HSCs derive from a bipotent hemato-endothelial precursor (the hemangioblast) or a specialized endothelial cell (the hemogenic endothelium). One opposing theory has suggested that HSCs are specified within the tissue encapsulating the vascular endothelium and migrate through the vessel wall to be released into the bloodstream [27]. Recent studies using imaging techniques and conditionally targeted mouse models for lineage tracing suggest a unifying pathway whereby the hemangioblast first gives rise to hemogenic endothelium, which in turn generates hematopoietic stem/progenitor cells. One study used time-lapse imaging of embryonic stem cell in-vitro differentiation to document the development of hematopoietic progenitors from blast colonies, the in-vitro equivalents of the hemangioblasts [28•]. The cellular morphology and immunophenotype suggested that hemangioblasts first undergo *Scl*-dependent establishment of hemogenic endothelial intermediates before giving rise to committed blood cells. Another study confirmed the transition of individual embryonic stem cell-derived hemangioblasts to hematopoietic cells via an endothelial intermediate using an imaging-based fate tracing approach that allowed monitoring of single cells and their progeny [29•]. The role of the hemogenic endothelium as a source of HSCs was verified *in vivo* using a conditional deletion of *Runx1* (a transcriptional factor essential for HSC formation) from cells expressing VEC [30••]. At E9.5, *VEC* is expressed in the vasculature throughout the conceptus, including the developing placental labyrinth. Although excision of *Runx1* from VEC^+ cells impaired hematopoietic stem/progenitor cells development, its excision from VAV^+ hematopoietic cells no longer caused this defect. This indicated that *Runx1* is essential for hematopoietic stem/progenitor cell development during a short developmental window (the time between the onset of *VEC* and *Vav* expression), providing evidence of the hemogenic endothelium as the HSC precursor. Likewise, when the vasculature and the perivascular mesenchyme were labeled with the inducible *VEC Cre* line and the *myocardin Cre* line, respectively, it was shown that HSCs in the AGM, placenta and yolk sac were traced to the VEC^+ endothelial fraction [31]. Although these studies strongly suggest that a crucial commitment step to HSC fate occurs during the hemogenic endothelial stage, they do not exclude the possibility that the hemogenic endothelium could develop from a mesenchymal precursor that does not express myocardin.

Hematopoietic microenvironment in the placenta

In addition to the progress made in understanding the cellular origin of HSCs, current reports provide novel insights into signals regulating HSC development in the microenvironment. Recent studies demonstrate that blood flow and shear stress are critical for efficient HSC formation in the placenta. $Ncx1^{-/-}$ embryos, which lack a heartbeat, show reduced numbers of nascent $CD41^+$ hematopoietic cells in the placental vasculature [26]. Although the lack of circulating hematopoietic stem/progenitor cells could result in decreased hematopoietic progenitors, prominent clusters of round cells expressing the endothelial marker CD31, and occasionally the hematopoietic marker CD41, were observed in the lumens of the large vessels in the $Ncx1^{-/-}$ placenta. It was hypothesized that these endothelial cell clusters represent hemogenic intermediates, which are unable to emerge in the absence of blood flow and thus accumulate in the placental vessels. The relationship between blood flow and shear stress was shown mechanistically in the zebrafish system. In *Sih* (silent heart) mutant zebrafish embryos, which also lack a heartbeat, the absence of blood flow impaired arterial identity and HSC formation in the AGM owing to defective nitric oxide signaling [32••]. A similar phenotype was found in wild-type embryos where blood vessel tone was altered with small molecules. The induction of shear forces has also been shown to enhance *Runx1* expression and hematopoietic potential in cells derived from mouse embryonic stem cells and embryos [33•]. These results implicate hemodynamic forces as a conserved modulator of HSC development.

Although the molecular cues that regulate hematopoiesis in the placenta remain largely undefined, many cell types likely contribute to this supportive microenvironment. In mice, $Runx1^+$ hematopoietic stem/progenitor cells undergoing mitosis localized to small vessels in the labyrinthine region, suggesting that local signals support hematopoietic stem/progenitor cell proliferation [26] (see Fig. 1). In human tissues, $CD34^+$ hematopoietic stem/progenitor cells were found in the stroma and vasculature of the chorionic villi, the region analogous to the murine labyrinth [17•,18•,26]. The ability of trophoblasts to secrete mitogens and angiogenic factors, in addition to their proximity to placental blood vessels, makes them intriguing candidates for niche cells [34]. Trophoblast-derived signals may affect HSCs by direct contact, or indirectly by establishing a vascular/perivascular niche, where HSCs reside. Perivascular cells and/or mesenchymal stem cells (MSCs) in other hematopoietic organs have been associated with HSC supportive activity [35]. Cells with pericyte characteristics capable of expanding colony forming unit-granulocyte monocyte (CFU-GM)

and CFU-Mix progenitors during coculture were identified as putative niche cells in the human placenta [18•]. One study detected cells containing MSC properties with perivascular cells in the villi of second and third trimester human placentas [36]. Beyond identifying the cellular composition of the placental microenvironment, it is also important to understand the physiological changes that occur in the placenta during development. For example, changes in local oxygen levels are also likely to impact HSC fate during embryogenesis. It is known that hypoxia during early gestation promotes not only vasculogenesis and establishment of arterial endothelium [37], but also trophoblast proliferation [38]. These data highlight the dynamic and multifaceted composition of the placental hematopoietic microenvironment, and provide new avenues to explore the complex regulation of HSC emergence and expansion.

Conclusion

The limited supply of HSCs for therapeutic use remains as one of the most pressing challenges in treating patients with hematopoietic malignancies and inherited blood disorders. The placenta provides another source of HSCs that can be harvested to supplement the circulating HSCs obtained from umbilical cord blood. The term placenta is an attractive source for HSCs because its procurement is noninvasive and it is routinely discarded. Furthermore, the first trimester placenta provides an accessible model for studying the earliest stages of HSC development. Improved understanding of the molecular and cellular mechanisms that govern HSC development in the placenta at different stages may ultimately provide effective tools to enhance protocols for HSC harvesting, ex-vivo expansion, and generation from pluripotent cells.

Acknowledgements

This work was supported in part by grants from the National Institutes of Health (NIH HL097766-01) and California Institute for Regenerative Medicine (CIRM RN1-00557-1 and RS1-00420-1) for H.K.A.M, California Institute for Regenerative Medicine Training Grant (CIRM TG2-01169) for L.K.L, the Ruth Kirschstein National Research Service Award (GM007185) for B.V.H and JSPS Postdoctoral Fellowship for M.U.

References and recommended reading

Papers of particular interest, published within the annual period of review, have been highlighted as:

- • of special interest
- •• of outstanding interest

Additional references related to this topic can also be found in the Current World Literature section in this issue (p. 376).

1 Lux CT, Yoshimoto M, McGrath K, *et al.* All primitive and definitive hematopoietic progenitor cells emerging before E10 in the mouse embryo are products of the yolk sac. Blood 2008; 111:3435–3438.

2 Palis J. Ontogeny of erythropoiesis. Curr Opin Hematol 2008; 15:155–161.

3 Mikkola HK, Orkin SH. The journey of developing hematopoietic stem cells. Development 2006; 133:3733–3744.

4 de Bruijn MF, Speck NA, Peeters MC, Dzierzak E. Definitive hematopoietic stem cells first develop within the major arterial regions of the mouse embryo. EMBO J 2000; 19:2465–2474.

5 Medvinsky A, Dzierzak E. Definitive hematopoiesis is autonomously initiated by the AGM region. Cell 1996; 86:897–906.

6 Dancis J, Samuels BD, Douglas GW. Immunological competence of placenta. Science 1962; 136:382–383.

7 Dancis J, Jansen V, Brown GF, *et al.* Treatment of hypoplastic anemia in mice with placental transplants. Blood 1977; 50:663–670.

8 Melchers F. Murine embryonic B lymphocyte development in the placenta. Nature 1979; 277:219–221.

9 Caprioli A, Jaffredo T, Gautier R, *et al.* Blood-borne seeding by hematopoietic and endothelial precursors from the allantois. Proc Natl Acad Sci U S A 1998; 95:1641–1646.

10 Alvarez-Silva M, Belo-Diabangouaya P, Salaun J, Dieterlen-Lievre F. Mouse placenta is a major hematopoietic organ. Development 2003; 130:5437–5444.

11 Gekas C, Dieterlen-Lievre F, Orkin SH, Mikkola HK. The placenta is a niche for hematopoietic stem cells. Dev Cell 2005; 8:365–375.

12 Ottersbach K, Dzierzak E. The murine placenta contains hematopoietic stem cells within the vascular labyrinth region. Dev Cell 2005; 8:377–387.

13 McKinney-Freeman SL, Naveiras O, Yates F, *et al.* Surface antigen phenotypes of hematopoietic stem cells from embryos and murine embryonic stem cells. Blood 2009; 114:268–278.

14 Kim I, Yilmaz OH, Morrison SJ. CD144 (VE-cadherin) is transiently expressed by fetal liver hematopoietic stem cells. Blood 2005; 106:903–905.

15 Taoudi S, Gonneau C, Moore K, *et al.* Extensive hematopoietic stem cell generation in the AGM region via maturation of VE-cadherin+CD45+ pre-definitive HSCs. Cell Stem Cell 2008; 3:99–108.

16 Taoudi S, Morrison AM, Inoue H, *et al.* Progressive divergence of definitive haematopoietic stem cells from the endothelial compartment does not depend on contact with the foetal liver. Development 2005; 132:4179–4191.

17 • Barcena A, Kapidzic M, Muench MO, *et al.* The human placenta is a hematopoietic organ during the embryonic and fetal periods of development. Dev Biol 2009; 327:24–33.
This study reports that the human placenta contains multipotent hematopoietic progenitors with myelo-erythroid and lymphoid potential and localizes placental hematopoietic stem/progenitor cells in the chorionic villi.

18 • Robin C, Bollerot K, Mendes S, *et al.* Human placenta is a potent hematopoietic niche containing hematopoietic stem and progenitor cells throughout development. Cell Stem Cell 2009; 5:385–395.
Human placental CD34+ cells were transplanted into immunocompromised mice and evidence of multilineage engraftment of human cells was demonstrated from 9 weeks of development onwards.

19 Barcena A, Muench MO, Kapidzic M, Fisher SJ. A new role for the human placenta as a hematopoietic site throughout gestation. Reprod Sci 2009; 16:178–187.

20 Broxmeyer HE, Cooper S, Hass DM, *et al.* Experimental basis of cord blood transplantation. Bone Marrow Transplant 2009; 44:627–633.

21 Serikov V, Hounshell C, Larkin S, *et al.* Human term placenta as a source of hematopoietic cells. Exp Biol Med (Maywood) 2009; 234:813–823.

22 Rossant J, Cross JC. Placental development: lessons from mouse mutants. Nat Rev Genet 2001; 2:538–548.

23 Georgiades P, Ferguson-Smith AC, Burton GJ. Comparative developmental anatomy of the murine and human definitive placentae. Placenta 2002; 23:3–19.

24 Zeigler BM, Sugiyama D, Chen M, *et al.* The allantois and chorion, when isolated before circulation or chorio-allantoic fusion, have hematopoietic potential. Development 2006; 133:4183–4192.

25 Corbel C, Salaun J, Belo-Diabangouaya P, Dieterlen-Lievre F. Hematopoietic potential of the prefusion allantois. Dev Biol 2007; 301:478–488.

26 Rhodes KE, Gekas C, Wang Y, *et al.* The emergence of hematopoietic stem cells is initiated in the placental vasculature in the absence of circulation. Cell Stem Cell 2008; 2:252–263.

27 Bertrand JY, Giroux S, Golub R, *et al.* Characterization of purified intraembryonic hematopoietic stem cells as a tool to define their site of origin. Proc Natl Acad Sci U S A 2005; 102:134–139.

28 • Lancrin C, Sroczynska P, Stephenson C, *et al.* The haemangioblast generates haematopoietic cells through a haemogenic endothelium stage. Nature 2009; 457:892–895.
Time-lapse imaging of differentiating mouse embryonic stem cells was used to delineate the developmental progression from the hemangioblast to hemogenic endothelium to hematopoietic cells.

29 Eilken HM, Nishikawa S, Schroeder T. Continuous single-cell imaging of blood • generation from haemogenic endothelium. Nature 2009; 457:896–900.
Using continuous imaging of embryonic stem cells at the single-cell level, this study documented that hematopoietic cells arise from the hemangioblast via a hemogenic endothelial intermediate.

30 Chen MJ, Yokomizo T, Zeigler BM, *et al.* Runx1 is required for the endothelial to •• haematopoietic cell transition but not thereafter. Nature 2009; 457:887–891.
Conditional deletion of *Runx1* from cells expressing vascular endothelial-cadherin was used to verify *in vivo* that HSCs originate from the endothelial cells in hematopoietic organs, including the placenta.

31 Zovein AC, Hofmann JJ, Lynch M, *et al.* Fate tracing reveals the endothelial origin of hematopoietic stem cells. Cell Stem Cell 2008; 3:625–636.

32 North TE, Goessling W, Peeters M, *et al.* Hematopoietic stem cell develop- •• ment is dependent on blood flow. Cell 2009; 137:736–748.
Using heartbeat deficient *sih* zebrafish embryos and a zebrafish chemical genetic screen, it was shown that blood flow is required for HSC formation. Nitric oxide signaling emerged as a novel regulator of HSC development in both zebrafish and mouse embryos.

33 Adamo L, Naveiras O, Wenzel PL, *et al.* Biomechanical forces promote • embryonic haematopoiesis. Nature 2009; 459:1131–1135.
This study presented *in vitro* and *in vivo* evidence that shear forces upregulate *Runx1* expression and stimulate hematopoiesis during development in cells derived from mouse embryonic stem cells and embryos.

34 Burton GJ, Charnock-Jones DS, Jauniaux E. Regulation of vascular growth and function in the human placenta. Reproduction 2009; 138: 895–902.

35 Chateauvieux S, Ichante JL, Delorme B, *et al.* Molecular profile of mouse stromal mesenchymal stem cells. Physiol Genomics 2007; 29:128–138.

36 Crisan M, Yap S, Casteilla L, *et al.* A perivascular origin for mesenchymal stem cells in multiple human organs. Cell Stem Cell 2008; 3:301–313.

37 Diez H, Fischer A, Winkler A, *et al.* Hypoxia-mediated activation of Dll4-Notch-Hey2 signaling in endothelial progenitor cells and adoption of arterial cell fate. Exp Cell Res 2007; 313:1–9.

38 Genbacev O, Zhou Y, Ludlow JW, Fisher SJ. Regulation of human placental development by oxygen tension. Science 1997; 277:1669–1672.

Have you seen?

THE EMBO JOURNAL

Sex hormone drives blood stem cell reproduction

Vincenzo Calvanese[1], Lydia K Lee[1,2] & Hanna K A Mikkola[1,3]

Stem cells ensure the maintenance of tissue homeostasis throughout life by tightly regulating their self-renewal and differentiation. In a recent study published in *Nature*, Nakada *et al*, 2014 unveil an unexpected endocrine mechanism that regulates hematopoietic stem cell (HSC) self-renewal.

See also: **D Nakada *et al*** (January 2014)

In the hematopoietic system, stem cells are largely quiescent and divide only rarely to protect genomic integrity of the hematopoietic stem cell (HSC) pool; however, this behavior can be altered to adapt to physiological needs and changes in the microenvironment (Wilson *et al*, 2008). The stem cell niche has been largely viewed as a support system that protects the stem cell pool via cell–cell contact and paracrine signals. There has been a significant progress in defining the niche cells and molecular cues that constitute the immediate HSC niche in the bone marrow (Morrison & Scadden, 2014). However, little has been known about possible long-range signals that govern HSC behavior.

Nakada *et al* (2014) discovered that the replicative activity of the HSC pool is augmented in female versus male mice, an observation that led them to study the role of sex hormones in HSC regulation. They showed that estradiol (E2) promotes cycling of HSC and multipotent progenitors (MPP) and increases their differentiation into megakaryocyte–erythroid progenitors (MEP). As the number of HSC did not alter upon stimulation by estradiol despite increased HSC proliferation and red cell and platelet production, the authors propose that estradiol largely promotes asymmetric rather than symmetric self-renewal in the bone marrow.

Estradiol function is mediated by nuclear hormone receptors, estrogen receptor-α and -β (encoded by *Esr1* and *Esr2*, respectively), which are transcription factors that dimerize and bind to regulatory sequences of target genes in response to the ligand (Heldring *et al*, 2007). The authors narrowed down the observed effect of estradiol on HSC self-renewal to estrogen receptor-α (ER-α) and activation of cell cycle-related genes to increase the proliferation of HSC. They further showed that HSCs in male mice also express ER-α and are capable of increasing their cycling in response to estradiol, identifying estradiol production as the defining factor that underlies the sex specificity of this HSC regulatory mechanism (Fig 1). This work thus uncovers an unanticipated role for a female sex hormone in a trait that has not been previously considered as sexually dimorphic, such as HSC self-renewal.

These findings raise the question as to why a female-specific mechanism to increase HSC proliferation and blood cell production would have evolved. From menarche to the onset of menopause, estradiol is cyclically secreted from the ovary. During pregnancy, its level increases 1,000-fold as its production is overtaken by placental trophoblasts (Gruber *et al*, 2002). Connecting these observations, one can hypothesize that such estrogen-mediated mechanism of HSC asymmetric self-renewal would enable the maternal adaptation to the increased blood cell demand associated with physiological blood loss during childbirth. On the other hand, during gestation, HSCs in both female and male fetuses are equally exposed to estrogens as the placental trophoblasts release them also into the fetal circulation (Kaludjerovic & Ward, 2012). Further studies are needed to define whether estrogens also play a role in the rapid cycling and symmetric self-renewal of the fetal HSC, which is critical for establishing the HSC pool during development.

For decades, exogenous estrogen has been used in the clinic due to the observed effects on breast epithelium, uterine endometrium, vasculature, and bone (Gruber *et al*, 2002; Practice Committee of ASRM, 2008). Furthermore, selective ER modulators have proven useful in the treatment for specific subsets of breast and ovarian cancers (Riggs & Hartmann, 2003). Nakada *et al* (2014) show that the estrogen-mediated HSC proliferative effect can be modulated *in vivo* by the administration of pharmacologic agonists and antagonists of the pathway. Hence, this work identifies HSC as yet another target tissue to be considered when assessing the therapeutic or secondary effects of estrogen or anti-estrogen treatments.

One tempting clinical application of estrogens might be to stimulate ER-α signaling to accelerate the recovery from chemotherapy and HSC transplantation by increasing HSC self-renewal and platelet production. On the other hand, potential implications of the increased cell cycle activity of HSC exposed to higher level of estrogens could include higher risk for mutations during cell divisions, susceptibility to genotoxic agents, and/or accelerated aging. Moreover, as leukemic

1 Department of Molecular, Cell and Developmental Biology, University of California Los Angeles, Los Angeles, CA, USA
2 Department of Obstetrics and Gynecology, University of California Los Angeles, Los Angeles, CA, USA
3 Eli and Edythe Broad Center for Regenerative Medicine and Stem Cell Research, University of California Los Angeles, Los Angeles, CA, USA. E-mail: hmikkola@mcdb.ucla.edu
DOI 10.1002/embj.201487976 | Published online 21 February 2014

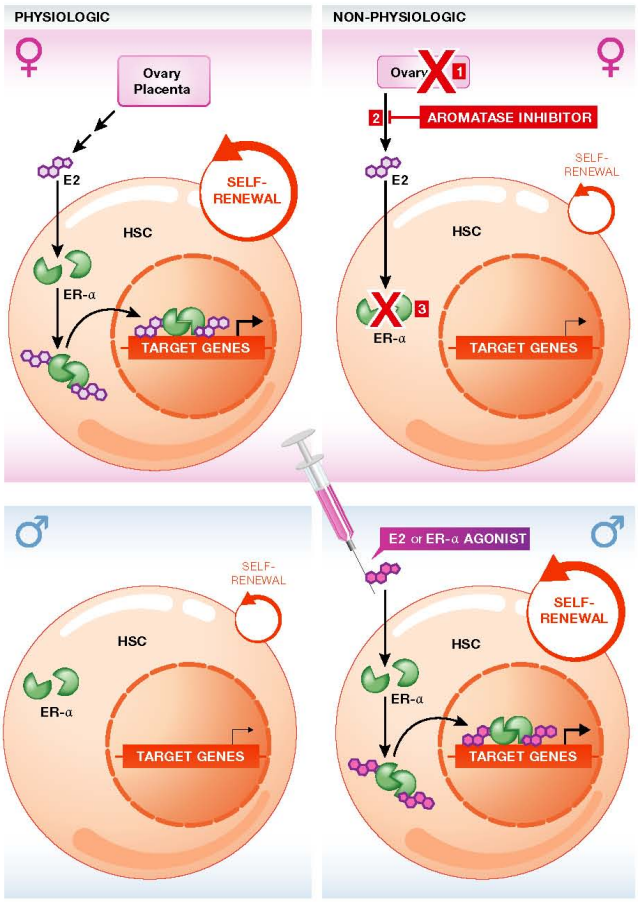

Figure 1. Estradiol promotes hematopoietic stem cell (HSC) self-renewal.
In female mice, HSC proliferation is augmented by circulating estradiol (E2), which is produced from the ovaries during reproductive years, and at higher levels from the placenta during pregnancy. E2 binds to the estrogen receptor-α (ER-α, green), which upon dimerization is translocated to the nucleus and enhances the expression of target genes involved in HSC proliferation (top left panel). Interrupting this pathway by ovariectomy (1), by the administration of an aromatase inhibitor that blocks the production of estradiol from its precursors (2), or by genetic disruption of *Esr1*, the gene encoding for ER-α (3), leads to reduced basal proliferation rate of HSC in females (top right panel). In males, despite the expression of ER-α in HSC, paucity of estradiol determines a lower basal HSC proliferation rate (bottom right panel). However, exogenous administration of E2 or ER-α agonists can induce an increase in HSC self-renewal also in males as well (bottom right panel).

stem cells (LSC) exploit many of the same mechanisms as HSC for sustaining self-renewal (Heidel *et al*, 2011), future studies investigating ER-α signaling as a potential mechanism that promotes LSC self-renewal, or as a therapeutic target to increase the cycling and drug sensitivity of otherwise quiescent LSC, will be of clinical interest. Thus, in addition to challenging the way we think of the extent of the HSC microenvironment and the endocrine system as a modulator of stem cell activity, this work opens new unexplored avenues to assess the physiological, pathological, and developmental functions of sex hormones.

Conflict of interest

The authors declare that they have no conflict of interest.

References

Gruber CJ, Tschugguel W, Schneeberger C, Huber JC (2002) Production and actions of estrogens. *New Engl J Med* 346: 340 352

Heidel FH, Mar BG, Armstrong SA (2011) Self-renewal related signaling in myeloid leukemia stem cells. *Int J Hematol* 94: 109 117

Heldring N, Pike A, Andersson S, Matthews J, Cheng G, Hartman J, Tujague M, Strom A, Treuter E, Warner M, Gustafsson JA (2007) Estrogen receptors: how do they signal and what are their targets. *Physiol Rev* 87: 905 931

Kaludjerovic J, Ward WE (2012) The interplay between estrogen and fetal adrenal cortex. *J Nutr Metab* 2012: 837901

Morrison SJ, Scadden DT (2014) The bone marrow niche for haematopoietic stem cells. *Nature* 505: 327 334

Nakada D, Oguro H, Levi BP, Ryan N, Kitano A, Saitoh Y, Takeichi M, Wendt GR, Morrison SJ (2014) Oestrogen increases haematopoietic stem cell self-renewal in females and during pregnancy. *Nature* 505: 555 558.

Practice Committee of ASRM (2008) Estrogen and progestogen therapy in postmenopausal women. *Fertil Steril* 90: S88 S102

Riggs BL, Hartmann LC (2003) Selective estrogen-receptor modulators mechanisms of action and application to clinical practice. *New Engl J Med* 348: 618 629

Wilson A, Laurenti E, Oser G, van der Wath RC, Blanco-Bose W, Jaworski M, Offner S, Dunant CF, Eshkind L, Bockamp E, Lio P, Macdonald HR, Trumpp A (2008) Hematopoietic stem cells reversibly switch from dormancy to self-renewal during homeostasis and repair. *Cell* 135: 1118 1129